

NASA-CR-192022

NASW-4435

1N-05-0R

141639

D. 116

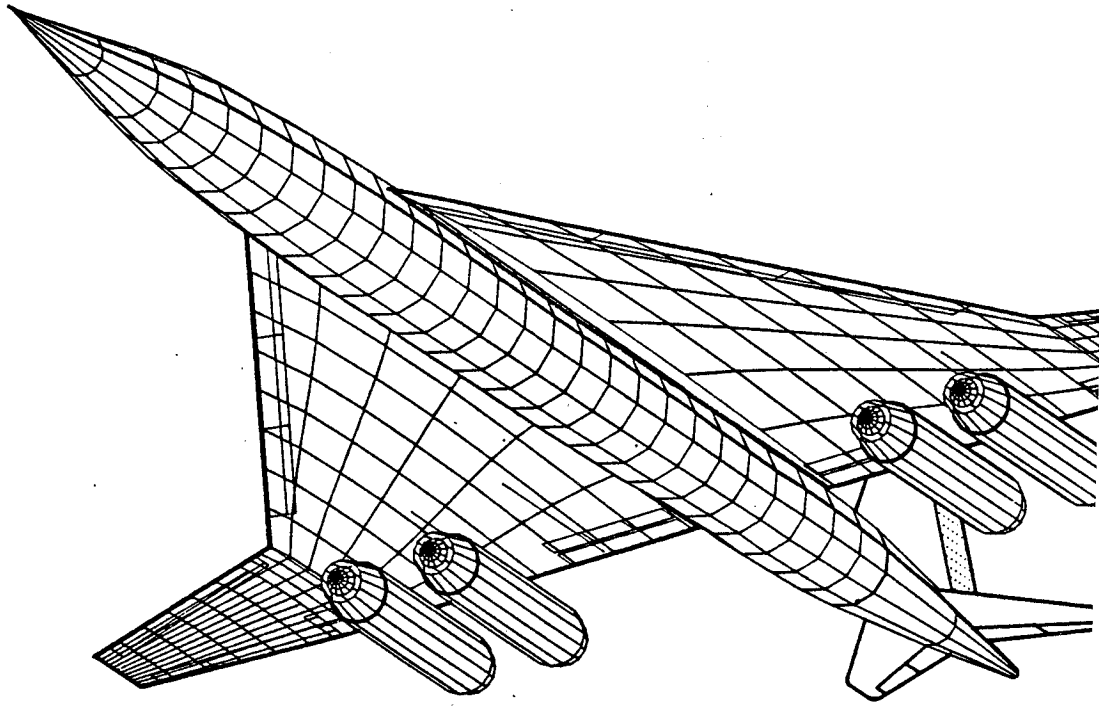
# A SECOND-GENERATION HIGH SPEED CIVIL TRANSPORT

## STINGRAY

N93-18059

Unclas

63/05 0141639



(NASA-CR-192022) A  
SECOND-GENERATION HIGH SPEED CIVIL  
TRANSPORT: STINGRAY (California  
polytechnic State Univ.) 116 p

PRESENTED TO:  
AERONAUTICAL ENGINEERING DEPARTMENT  
CALIFORNIA POLYTECHNIC STATE UNIVERSITY, SAN LUIS OBISPO  
SPRING, 1992

Team Members:

- Sean Engdahl
- Kevin Lopes
- Angelen Ngan
- Joseph Perrin
- Marcus Phipps
- Blake Westman
- Urn Yeo

## **ABSTRACT**

The Stingray is the second-generation High Speed Civil Transport (HSCT) designed for the 21st Century. This aircraft is designed to be economically viable and environmentally sound transportation competitive in markets currently dominated by subsonic aircraft such as the Boeing 747 and upcoming McDonnell Douglas MD-12. With the Stingray coming into service in 2005, a ticket price of 21% over current subsonic airlines will cover operational costs with a 10% return on investment. The cost per aircraft will be \$202 million with the Direct Operating Cost equal to \$0.072 per mile per seat.

This aircraft has been designed to be a realistic aircraft that can be built within the next ten to fifteen years. There was only one main technological improvement factor used in this design, that being for the engine specific fuel consumption. The Stingray, therefore, does not rely on technology that does not exist.

The Stingray will be powered by four mixed flow turbofans that meet both nitrous oxide emissions and FAR 36 Stage III noise regulations. It will carry 250 passengers a distance of 5200 nautical miles at a speed of Mach 2.4. The shape of the Stingray, while optimized for supersonic flight, is compatible with all current airline facilities in airports around the world. As the demand for economical, high-speed flight increases, the Stingray will be ready and able to meet those demands.

## TABLE OF CONTENTS

	TABLE OF CONTENTS	
	LIST OF FIGURES	
	LIST OF TABLES	
	LIST OF SYMBOLS AND ABBREVIATIONS	
1.0	INTRODUCTION	1
2.0	MISSION DESCRIPTION	5
3.0	PRELIMINARY SIZING	8
3.1	Preliminary Weight Estimates	8
3.2	Sensitivity Study	9
3.3	Design Point	9
4.0	AIRCRAFT CONFIGURATION	12
4.1	Wing Design	17
4.1.1	Wing Configuration	17
4.1.2	Wing Planform	17
4.1.3	Airfoil Selection	19
4.1.4	High Lift Devices	20
4.1.4	Fuel Volume	23
4.2	Fuselage Design	25
4.2.1	Interior Layout	25
4.2.2	Cross Sectional Layout	29
4.2.3	Cockpit Layout	30
4.3	Empennage Design	33
4.3.1	Horizontal Stabilizer	33
4.3.2	Vertical Stabilizer	34
5.0	PROPULSION SYSTEMS	36
5.1	Engine Selection	36
5.2	Engine Sizing and Location	37
5.3	Inlet Design	39
5.4	Environmental Concerns	40
6.0	LANDING GEAR	42
6.1	Landing Gear Overview	42
6.2	Nose Gear	44
6.3	Main Gear	46
7.0	MATERIALS AND STRUCTURES	49
7.1	Materials	49
7.2	V-n Diagram	53
7.3	Structural Layout	55
8.0	AERODYNAMICS	60
8.1	Lift Prediction	60

8.2	Drag Prediction	61
9.0	PERFORMANCE	65
9.1	Takeoff and Landing Performance	65
9.2	Climb Performance	65
9.3	Range-Payload	66
9.4	Fuel Consumption	68
10.0	STABILITY AND CONTROL	69
10.1	Weight and Balance	69
10.2	CG Excursion	70
10.3	Mass Moments of Inertia	74
10.4	Longitudinal Stability and Control	75
10.5	Lateral Stability and Control	75
10.6	Handling Qualities and Augmentation	77
11.0	SYSTEMS LAYOUT	78
11.1	Avionics	78
11.2	Electrical Systems	79
11.3.1	Pneumatic Systems-High Pressure Systems	80
11.3.2	Air Conditioning System	82
11.4	Fuel System	86
11.5	Escape System	87
11.6	Optical Signaling System	89
11.7	Oxygen System	89
11.8	Potable Water System	91
11.9	Waste System	91
12.0	AIRPORT OPERATION AND MAINTENANCE	92
13.0	MANUFACTURING	94
14.0	COST ANALYSIS	96
15.0	CONCLUSIONS AND RECOMMENDATIONS	99
16.0	REFERENCES	100

## LIST OF FIGURES

1.1	Stingray Isometric	3
1.2	Stingray Three-View	4
2.1	Stingray Mission Profile	7
3.1	Stingray Design Point	11
4.1	Boeing 747-400 Box	15
4.2	Stingray Wing Planform	17
4.3	Stingray Airfoil Section	20
4.4	Stingray Control Surface Placement	22
4.5	Stingray Fuel Tank Location	24
4.6	Stingray First Class Cross-sectional Layout	25
4.7	Stingray Breakdown of Cabin Layout	26
4.8	Stingray Business Class Cross-sectional Layout	27
4.9	Stingray Economy Class Cross-sectional Layout	28
4.10	Stingray Flight Deck Layout	31
4.11	Stingray Visual System	32
4.12	Stingray Pilot Visibility	32
4.13	Horizontal Empennage	34
4.14	Vertical Empennage	35
5.1	NASA Lewis Engine Cutaway	36
5.2	Stingray Noise Suppressor-Mixed Flow Ejector	40
6.1	Stingray Landing Gear Layout	43
6.2	Stingray Nose Gear Configuration	45
6.3	Main Gear Configurations	46
6.4	Stingray Landing Gear Leveling System (Ref. 18)	48

7.1	Stingray Materials Layout	52
7.2	V-n Diagram	54
7.3	Stingray Structural Layout	59
7.4	Stingray Shear Diagram	58
7.5	Stingray Moment Diagram	58
8.1	Variation Aircraft Lift Coefficient vs. Angle of Attack with Flaps up and Flaps Down	61
8.2	Stingray Drag Breakdown	63
8.3	Stingray Takeoff and Landing Drag Polars	63
8.4	Stingray Cruise Drag Polars	64
9.1	Stingray Flight Ceiling	66
9.2	Stingray Range-Payload Diagram	67
10.1	Stingray Weight Breakdown	69
10.2	Stingray CG Excursion Diagram	73
11.1	Stingray Conduit Layout Through a Fuselage Cross Section	78
11.2	Stingray Electrical Schematic	79
11.3	Stingray High Pressure System	81
11.4	Air Conditioning System	84
11.5	Stingray Cabin Air Circulation	85
11.6	Stingray Fuel System Layout	86
11.7	Stingray Emergency Escape System	88
11.8	Raft/Slide System (Ref. 4)	88
11.9	Schematic of Stingray Oxygen System	90
11.10	Stingray Passenger Cabin Oxygen System	91
12.1	Airport Ground Handling	93

13.1	Final Assembly of the Stingray	95
14.1	Stingray LCC Breakdown	96
14.2	Stingray Direct Operating Cost Breakdown	97

**LIST OF TABLES**

2.1	Cruise Flight Time Comparison	6
2.2	Mission Breakdown	6
3.1	Initial Sizing by Weight Fraction	8
3.2	Sensitivity Study	9
4.1	Wing Planform Characteristics	18
4.2	Fuel Tanks	24
5.1	Engine Parameters with All Engines Operational	37
5.2	Stingray Critical Engine Requirements	38
5.3	Engine Dimensions	39
6.1	Landing Gear Load Distribution	42
8.1	Lift Prediction for Different Flight Conditions	61
10.1	Aircraft Weights	70
10.2	Lateral Stability and Control Derivatives	77
14.1	Comparison of revenue for Selected Existing Aircraft	98



# LIST OF SYMBOLS AND ABBREVIATIONS

v

## Symbols

a	speed of sound
a.c.	aerodynamic center
AR	Aspect Ratio
b	span
c	chord
C	cost
$C_D$	total drag coefficient
$C_d$	section drag coefficient
CG	center of gravity
$C_L$	lift coefficient
$C_l$	section lift coefficient
$C_M$	moment coefficient
$C_m$	section moment coefficient
d	diameter
e	Oswald efficiency factor
f	equivalent parasitic area
g	acceleration due to gravity
I	mass moment of inertia
L	lift
l	length
L/D	lift to drag ratio
M	Mach number
m	mass
n	load factor
p	roll rate
q	dynamic pressure
q	pitch rate
r	yaw rate
S	surface area
$S_{ref}$	reference surface area
T	thrust
t/c	thickness ratio
T/W	thrust to weight ratio
U	freestream velocity
V	velocity
W	weight
W/S	wing loading
X	location on x axis
Y	location on y axis
Z	location on z axis

## Greek Symbols

$\alpha$	angle of attack
$\beta$	angle of sideslip
$\delta$	deflection
$\gamma$	kinematic viscosity
$\eta$	efficiency factor
$\rho$	density
$\omega$	natural frequency
$\zeta$	damping ratio
$\Lambda$	sweep angle
$\lambda$	taper ratio

## Subscripts

0	steady state
a	aileron
avail	available
e	elevator
f	flap
f	fuselage
h	horizontal tail
r	rudder
ref	reference
req	required
to	takeoff
v	vertical tail
w	wing
xx	about the x axis
yy	about the y axis
zz	about the z axis
cr	cruise

## Derivatives

$C_{D\alpha}$	drag coefficient due to angle of attack
$C_{D\beta}$	drag coefficient due to sideslip
$C_{D\delta e}$	drag coefficient due to elevator deflection
$C_{Di h}$	drag coefficient due to tail incidence
$C_{Dq}$	drag coefficient due to pitch rate
$C_{Du}$	drag due to velocity
$C_{L\alpha}$	lift coefficient due to angle of attack
$C_{L\beta}$	lift coefficient due to sideslip
$C_{L\delta e}$	lift coefficient due to elevator deflection
$C_{Li h}$	lift coefficient due to tail incidence

$C_{L\delta f}$	lift coefficient due to flap deflection
$C_{l\delta a}$	rolling moment due to aileron deflection
$C_{lp}$	rolling moment due to roll rate
$C_{Lq}$	lift coefficient due to pitch rate
$C_{lr}$	rolling moment due to yaw rate
$C_{Lu}$	lift due to velocity
$C_{M\alpha}$	moment coefficient due to angle of attack
$C_{M\beta}$	moment coefficient due to sideslip
$C_{M\delta e}$	moment coefficient due to elevator deflection
$C_{Mih}$	moment coefficient due to tail incidence
$C_{Mq}$	moment coefficient due to pitch rate
$C_{Mu}$	moment due to velocity
$C_{np}$	yawing moment due to roll rate
$C_{nr}$	yawing moment due to yaw rate
$C_{yp}$	sideforce due to roll rate
$C_{yr}$	sideforce due to yaw rate

### Acronyms

APU	auxiliary power unit
GWTO	takeoff gross weight
OEW	operational empty weight
DOC	direct operating cost
EW	empty weight
FAA	Federal Aviation Administration
FAR	Federal Aviation Regulations
FOD	foreign object damage
PAX	passengers and baggage
HUD	heads up display
HSCT	high speed civil transport
IFPC	integrated flight and propulsion computer
LCC	life cycle cost
LCD	liquid crystal display
LCN	load classification number
MAC	mean aerodynamic center
NACA	National Advisory Committee for Aeronautics
NASA	National Aeronautics and Space Association
NOx	nitrous oxide
EPNdB	Estimated Perceived Noise Decibel
RFP	request for proposal
SFC	specific fuel consumption
SM	static margin
TSFC	thrust specific fuel consumption

## 1.0 INTRODUCTION

With the increasing demands for transoceanic commercial transport, many believe that a supersonic transport is an inevitable necessity. The forecast shows that by the year 2010, international air traffic will represent 60% of the total world traffic (Ref. 16). In order to meet this anticipated demand, a supersonic transport must be an economical, environmentally sound aircraft that, besides creating its own market, must be competitive with the Boeing 747 fleet as well as other Boeing and McDonnell Douglas long-range subsonic fleets.

The first and only currently operational supersonic commercial transport was a British and French collaborated aircraft named the Concorde. This Mach 2.2 aircraft entered service in 1974 to a storm of environmental protests. Sonic boom prevented overland supersonic flight and the noise from the Rolls-Royce Olympus engines gained the Concorde the reputation of being a noisy airplane. For this reason, the Concorde was banned from most airports around the world.

Although it was a revolutionary airplane for its time, only fourteen Concorde airplanes were built. For this reason, the cost per airplane skyrocketed, causing the airframer to lose money. Concorde was limited to first-class only, driving the cost up to \$0.76 per passenger mile (1974 U.S.D), a 38% increase over current subsonic first class fare. In addition, unexpectedly high fuel costs coupled with the fact that the Concorde was not fuel-efficient drove the cost further up (Ref. 16).

Over the past twenty years, many designs for supersonic transports have been evaluated and discarded. Only in the past few years, with NASA sponsoring different programs (Ref. 22), has interest in the HSCT been rekindled. With many lessons learned from the Concorde's mistakes, it is believed that a next-generation HSCT is imminent.

The Stingray is designed to be an economically viable and environmentally sound supersonic transport that will utilize the long range oceanic routes. It is a Mach 2.4 aircraft that will carry 250 passengers a range of 5,200 nautical miles. This will meet one of the fastest growing markets, the Trans-Pacific route as well as servicing the Trans Atlantic, Europe to Asia, and Intra-Asian markets. The potential route study yielded more than twenty city pairs in an attempt to link up the major international airports across the oceans to complete the Great Circle (Ref. 23). The projected minimum ticket price is \$0.11 per passenger mile with a return on investment of 10%. Its three-class configuration will provide a faster alternative to the subsonic Boeing 747 while providing the same level of comfort. Its cruise altitude will be at 60,000 ft, in order to minimize the ozone breakdown due to nitrous oxide emission.

This report will discuss many of the preliminary steps taken in the design of the Stingray as well as the trade studies that yielded the final configuration of the aircraft. Also to be discussed will be engine specifications, performance capability, structures and stability and control; all of which provided interesting challenges that must be overcome in order for this airplane to move into a detailed design.

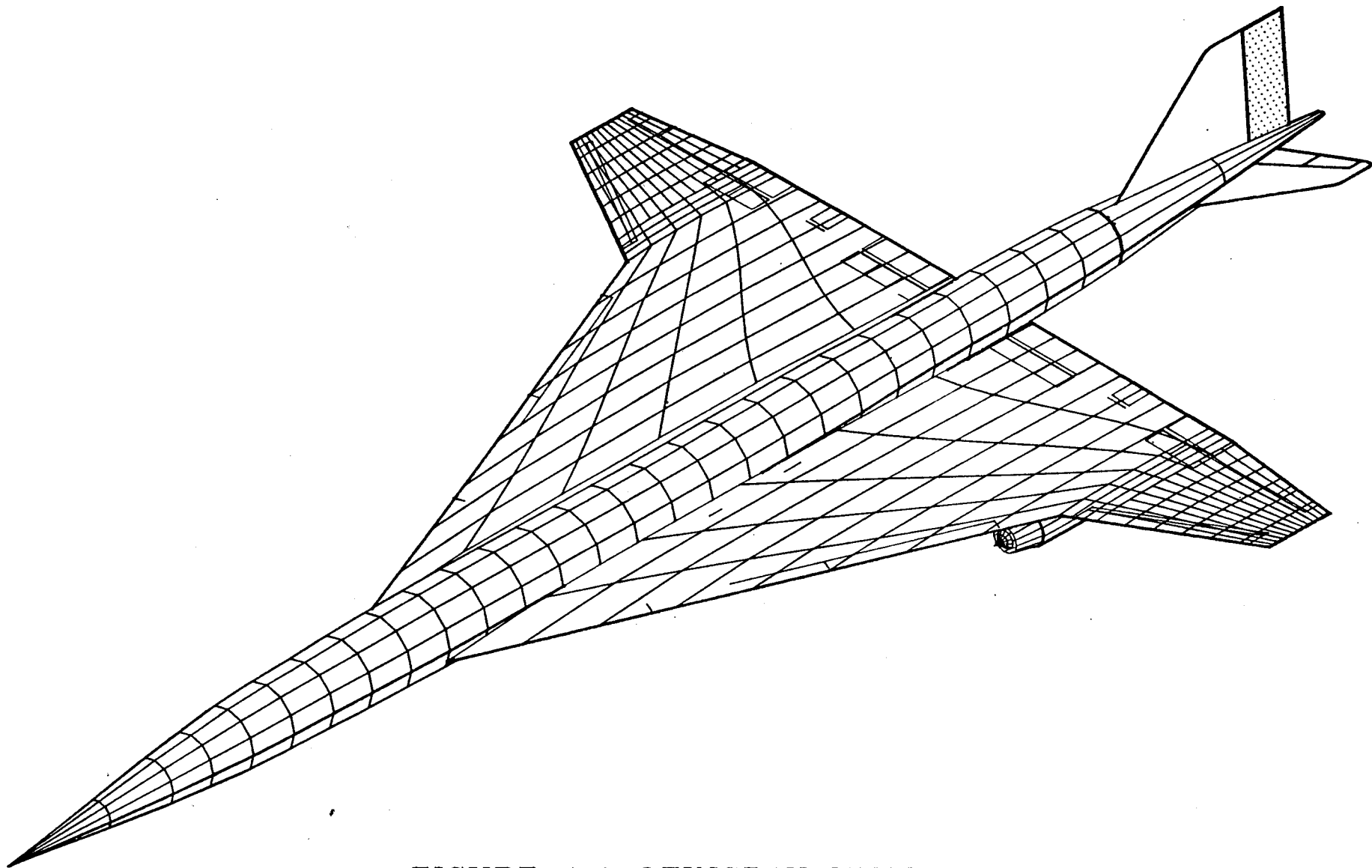
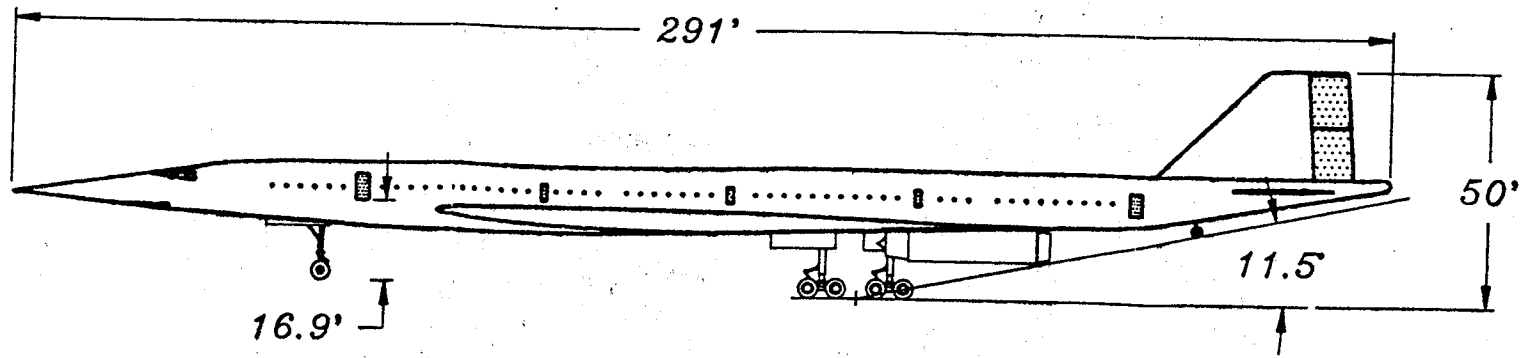
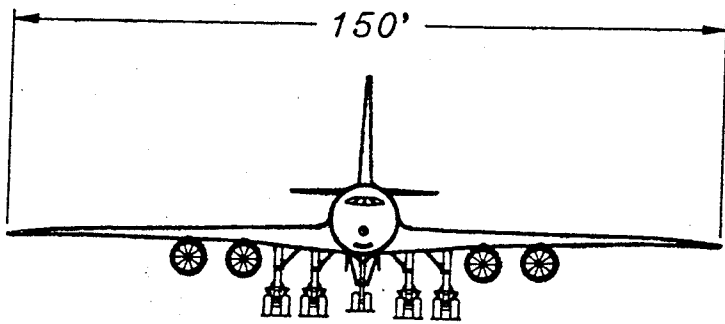
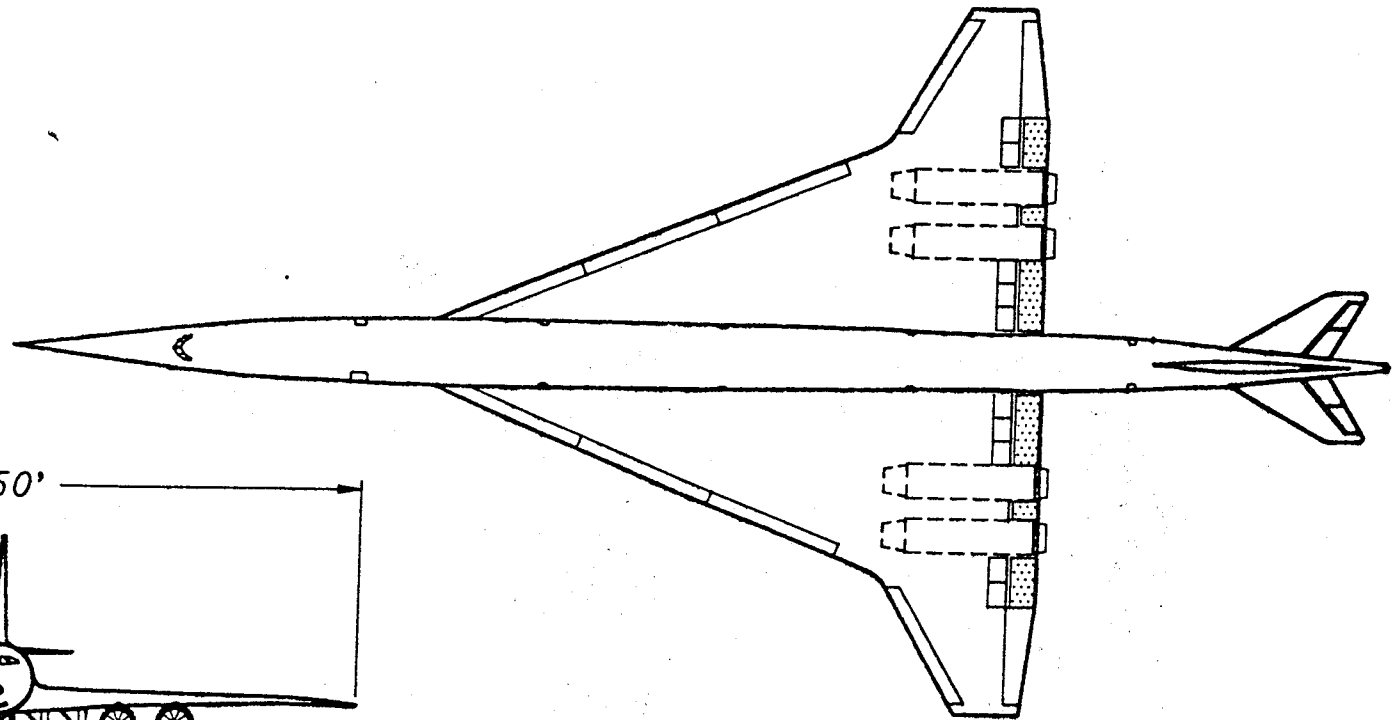


*FIGURE 1.1 STINGRAY ISOMETRIC*

# STINGRAY



## 2.0 MISSION PROFILE

The Stingray will perform missions similar to current commercial transports. The mission will consist of the following:

1. Engine startup, warmup, taxi, takeoff and climb out.
2. Climb at 250 knots IAS) to 10,000 ft as per FAA regulation.
3. Climb at best rate of climb to 30,000 ft.
4. Cruise at Mach 0.9 until aircraft is 100 nautical miles off coast and accelerate to Mach 1.2.
5. Climb to 60,000 ft. and accelerate to Mach 2.4.
6. Cruise at Mach 2.4.
7. Descend.
8. Cruise at Mach 0.9 to destination
9. Loiter
10. Descend.
11. Landing, taxi, shutdown.

The Stingray will carry international reserves, allowing to fly to alternates at a maximum distance of 300 nautical miles.

The primary difference between the Stingray and current subsonic transport is, of course, the cruise time. For example, the Boeing 747-400 flying the L.A.-Tokyo route would take 9.6 hours one-way. Comparatively, the Stingray would take only 3.2 hours one-way to fly the same distance. This corresponds to a time savings of 200%! Table 2.1 shows the time and distance breakdown between city pairs for the Stingray and the Boeing 747-400.



City Pair	Distance (nmi)	Cruise Time 747-400	Cruise Time Stingray
L.A.-Tokyo	4760	9.6	3.2
Tokyo-Singapore	2870	6.75	2.25
Singapore-Cairo	4469	9.45	3.15
Cairo-London	1875	4.05	1.35
London-New York	4067	8.85	2.95

**Table 2.1** Cruise Flight Time Comparison

This level of time savings is particularly important in routes such as Tokyo-Singapore, where time zone difference is only 3 hours. Therefore, the Stingray will be crucial not only in Trans-Pacific or Trans-Atlantic travel, but in Intra-Asia travel as well. It is also possible for the Stingray to complete the Great Circle in order to maximize the load factor of the aircraft all year round.

Table 2.2 provides weight, time and distances travelled throughout the mission. Figure 2.1 shows the mission profile of the Stingray.

Flight regime	Wt (lbf)	dW (lbf)	Wt %	dR (nm)	dt (min)	%time
Start Takeoff	725000					
Start First Segment Climb	713000	11721	3.25%	0	10	3.99%
Start Subsonic Cruise	695000	18753	5.20%	45	6.5	2.60%
Start Second Segment Climb	686000	8114.2	2.25%	75	4	1.60%
Start Supersonic Cruise	656000	30293	8.40%	200	15	5.99%
End Supersonic Cruise	402000	254065	71.78%	4405	191.94	76.64%
End Descent	394000	8114.2	2.25%	175	18	7.19%
Taxi	394000	360.63	0.10%	0	5	2.00%
Reserve	371000	22540	6.25%	300		
Block	354000		99.48%	5200	250.44	100.00%

4.174 hours

**Table 2.1** Stingray Mission Breakdown

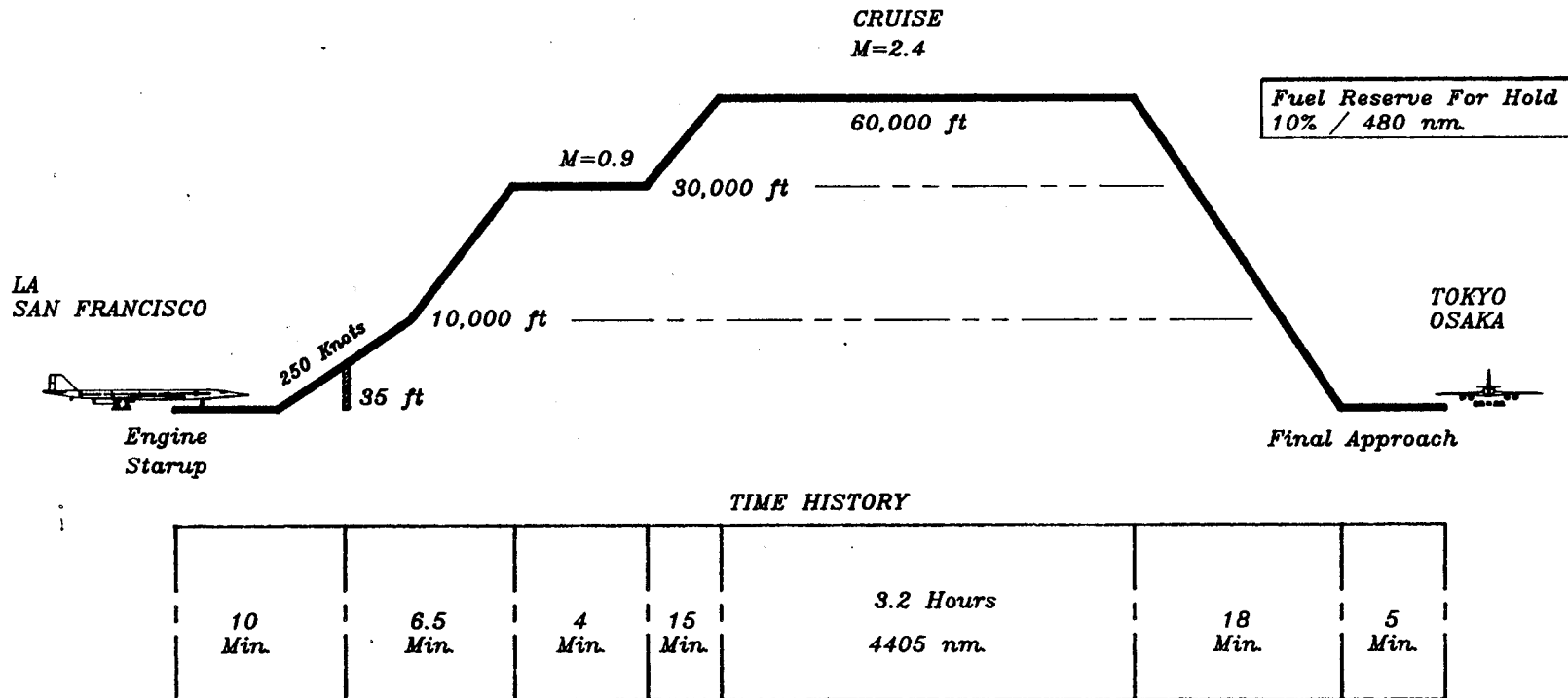


FIGURE 2.1 STINGRAY MISSION PROFILE

### 3.0 PRELIMINARY SIZING

#### 3.1 PRELIMINARY WEIGHT ESTIMATES

Preliminary sizing of the Stingray was accomplished using the weight fraction method described in (Ref. 1). The flight was broken down into nine regimes, each requiring a fixed fraction of the mission fuel. Empirical data is very scarce for supersonic commercial transports. Data from the British-French Concorde, NASA AST-100, Boeing 747-400, Boeing 2707, Rockwell XB70A Valkerie, and the Tupolev TU144 were used for analysis (Ref. 15). The mission fuel fraction was most sensitive to range, cruise specific fuel consumption (SFC), and the cruise lift to drag ratio(L/D), (Ref. 24). Initial estimates using a 250 passenger 5500 nautical mile range aircraft flying at Mach 2.7 resulted in gross takeoff weights between one and two million pounds. These aircraft were considered to be too heavy for current airport runways to handle so the decision was made to reduce the range and Mach number. The final weight fractions and weights given by the initial sizing are given in Table 3.1 below.

Number of Passengers	250
Cruise Mach Number	2.4
Cruise Altitude	60,000 ft
Range	5200 nmi
Cruise L/D	9.7
Cruise SFC	1.17
Mission Fuel Fraction	0.51
Operating Empty Weight	322,000 lbs.
Fuel Weight	358,000 lbf
Payload	53,800 lbf
Gross Takeoff Weight	729,000 lbf

**Table 3.1** Initial Sizing by Weight Fraction

### 3.2 SENSITIVITY STUDY

A sensitivity study was performed using the method in (Ref. 2) and the above weight estimate. The aircraft weight was found to be extremely sensitive to endurance, specific fuel consumption, and lift-to-drag ratio. The results are presented in Table 3.2. These indicate that the three most important factors to be considered during the design are decreasing the supersonic drag (aerodynamics), empty aircraft weight (structures and systems), and engine fuel performance (propulsion).

$\partial WT/O / \partial Range$	392	lbf/nm
$\partial WT/O / \partial Endurance$	538816	lbf/hr
$\partial WT/O / \partial Velocity$	-1826	lbf/knot
$\partial WT/O / \partial Lift / Drag$	-309272	lbf
$\partial WT/O / \partial SFC$	2511181	lbf/SFC

**Table 3.2** Sensitivity Factors

### 3.3 DESIGN POINT

Preliminary wing area and engine sizing were accomplished using the methods in (Ref. Roskam 2). The primary constraints for this aircraft were stall speed ( $C_{Lmax}$ ), FAR 25 takeoff and landing requirements, and thrust to weight (T/W) after an engine failure. Because of the low aspect ratio delta planform the  $C_{Lmax}$  limit was 1.03 for landing and 0.95 takeoff. The leftmost vertical line on Figure 3.1 represents the wing loading limit of around 95 psf. This constraint was set by the FAR 25 landing distance requirement. The horizontal line, the minimum necessary T/W was set by a landing configuration single engine failure. In this configuration the T/W is a direct function of lift to drag (L/D) ratio. The L/D = 6.2, which yields a T/W of 0.34. The sloped line represents a takeoff  $C_{Lmax}$  at takeoff of 1.0 and doesn't really set any design constraint. The design point was picked as low and far to the right as possible in an attempt to keep the

wing area and engine size as low as possible. The final wing loading and T/W of the aircraft are 93 psf and 0.34 respectively. The wing loading provides greater passenger comfort but increases the takeoff speed and distance.

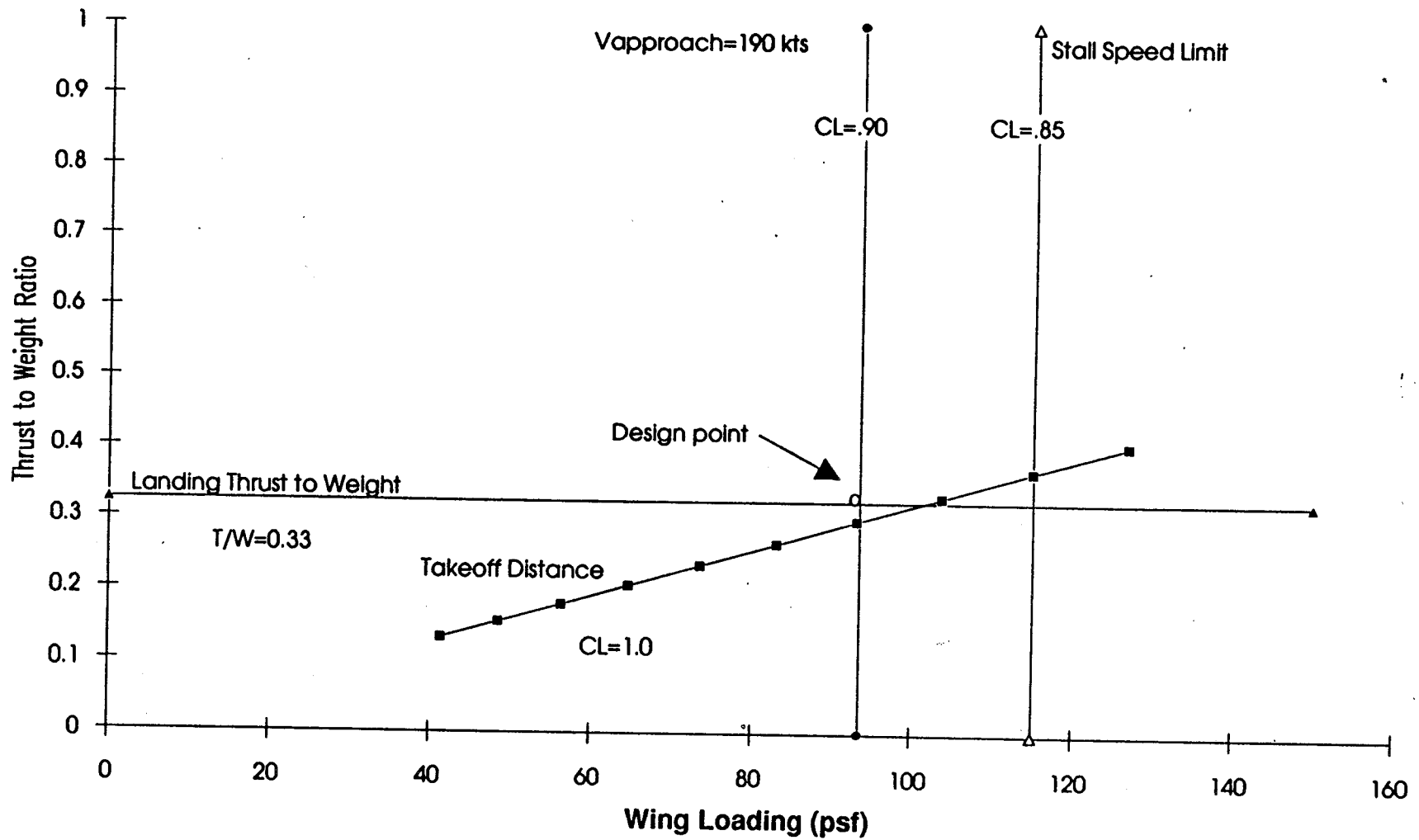


Figure 3.1 Stingray Design Point

## **4.0 AIRCRAFT CONFIGURATION**

### **4.1 CONFIGURATION SELECTION**

The configuration of the Stingray aircraft was selected after consideration of several designs. There were three primary design considerations in the configuration selection: low weight, aerodynamic efficiency and complexity. A low aircraft weight will reduce structural (especially landing gear) loads and engine thrust requirements. Aerodynamic efficiency (the lift-to-drag ratio) was another factor in the determination of the Stingray's range capability. Complexity became a concern since increasing complexity, for example, in a swing wing, also increases aircraft weight and cost, both in manufacturing and maintenance.

The double crank delta selected for the Stingray was chosen after a careful study of the following possibilities:

- Full swing wing
- Swinging wing tips
- Oblique wing
- Arrow wing
- Double crank delta

The swing wing was considered because it possesses good aerodynamic performance at all flight conditions. During takeoff, landing and subsonic cruise, the wing sweep could decrease to provide better subsonic handling. Supersonically, the wing could be swept back for good aerodynamic efficiency. The aerodynamic center shift for a swing wing is also minimized, allowing for better handling during transonic flight. However, the aerodynamic benefits were outweighed by the high weight penalty and complexity. The pivoting mechanism would not have easily fit into the thin wing section needed in a

supersonic aircraft. A thicker wing section could be used, but that would greatly increase wave drag since a larger cross-sectional area would be presented to the flow. In addition, the redundancy required for the pivot to counter a pivot failure would have further increased the wing weight and complexity.

The oblique wing was also considered due to its subsonic and supersonic aerodynamic flexibility. It was rejected because it has poor roll control and one engine out characteristics. Structurally, the pivot for the oblique wing would need a backup system in case of primary pivot failure, which would increase wing weight. Also, since the landing gear cannot be mounted on the wing, the tip-over angles would be very high. Research has indicated that people prefer to travel on a conventional aircraft as opposed to an unconventional aircraft.

Finally, the arrow wing, which is optimum at supersonic speeds above Mach 3.0 was rejected since the Stingray is only flying at Mach 2.4. In addition, flutter on the wing tips would cause severe structural problems.

The double crank delta wing was chosen since it has high fuel volume, even with thin wing sections. Also, the aerodynamic center shift is small (only 4% on the Stingray). Finally, the stall characteristics of a double crank delta are very good compared to other planform designs such as the arrow wing. The disadvantages are that delta wings yield low takeoff L/D values. This leads to increased engine required thrust and higher flap deflections (which will increase drag). In addition,  $C_{L\alpha}$  values are low, leading to higher angles of attack on takeoff and landing, and higher induced drag in cruise conditions.

A canard configuration was considered and weighed against a tailless or tailed aircraft. In order to maintain aerodynamic flexibility (high lift, low drag), a study of a retractable canard was considered, but was rejected since, like the swing wing, the weight penalty would be high.



The horizontal tailless concept (used in the Concorde) was rejected due to aerodynamic and stability and control considerations. In a tailless aircraft, there is less control power and less space for high lift devices available since the trailing edge of the wing must carry both control surfaces as well as high lift devices. The tailed design provided a longer moment arm to the center of gravity, reducing control surface sizing on the wing. In addition, the tailed design allowed for more high lift devices on the trailing edge of the wing, which was required for takeoff and landing. Finally, the horizontal tail can be used to counter pitching moments created by the deflection of high lift devices. Aerodynamically, however, a horizontal tail will increase skin friction drag since it will add more surface area to the aircraft. Also, a horizontal tail will increase the aircraft weight. After considering the advantages and disadvantages of each configuration, the Stingray incorporated a crank delta wing and a horizontal tail.

The fuselage characteristics were determined by considering passenger comfort, aerodynamic drag, and airport compatibility. The length of the fuselage could not exceed 320 ft. (which was the diagonal of the "box" created by the Boeing 747-400). Figure 4.1 compares the Boeing 747-400 box with the HSCT in the diagonal. A length exceeding 320 ft. would not fit into conventional airport terminals. The aircraft length also played an important role in drag considerations. A longer aircraft reduces wave drag and sonic boom, but will also increase parasite drag. The final length was 292 ft., which not only will carry the 250 passengers specified in Ref. 25, but also will reduce supersonic wave drag while not increasing parasitic drag substantially.

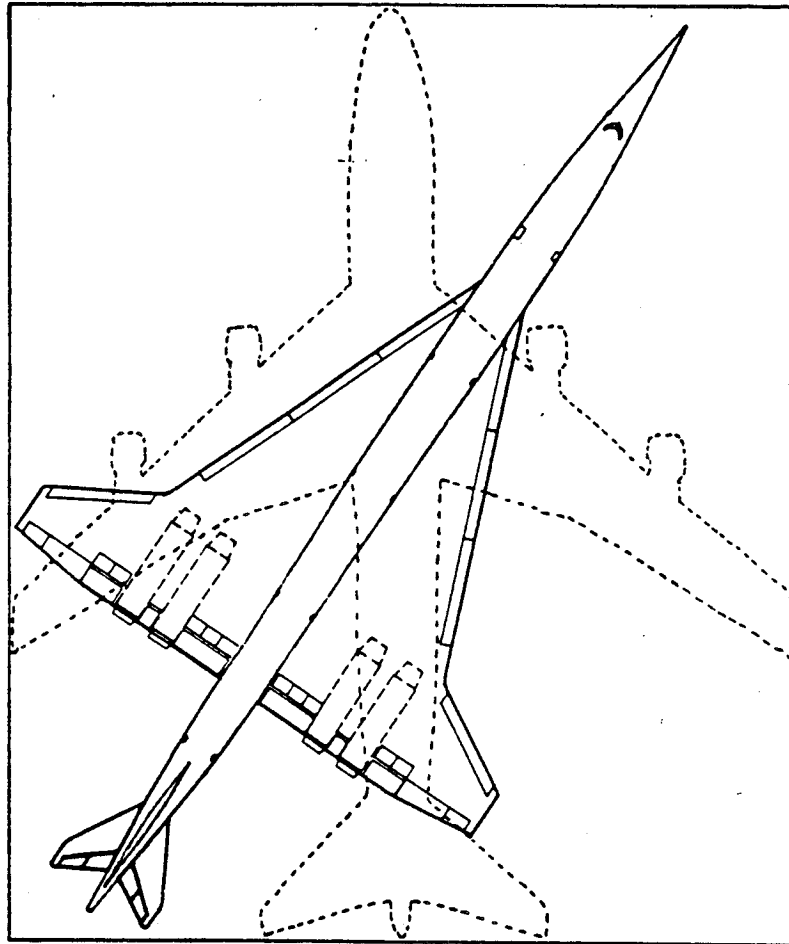


**Figure 4.1** Boeing 747-400 Box

The diameter of the fuselage was selected in order to minimize the cross-sectional area. A large diameter fuselage could hold more passengers, but would increase both surface area (hence increasing parasitic drag), and wave drag. Area ruling was performed to minimize cross-sectional area distribution, reducing wave drag. For this reason, the fuselage cross-sectional area was minimized while still emphasizing passenger comfort.

The landing gear comparison was made between two, three and four truck configurations for the main gear. The two and three truck configuration yielded load classification numbers (LCN) of greater than 100. Since the Stingray's LCN should be no more than that of the Boeing 747-400 (which has an LCN of 92), these configurations were not acceptable. The four truck

configuration provided an LCN of 82. In terms of weight, the four truck configuration would increase the weight but would enhance lateral stability on the ground, enhancing both passenger comfort and preventing engine strike on rotation. The two and three truck configurations would reduce weight, but have significant scrubbing problems. The four tire truck was selected in order to minimize scrubbing effects. For these reasons, the four truck, four tire configuration was selected.

## 4.2. WING DESIGN

### 4.2.1 WING CONFIGURATION

The primary needs driving the wing selection was high supersonic and subsonic efficiency, high fuel volume, stability and control considerations and low wing weight. The final configuration chosen for the Stingray was the double crank delta wing shown in Figure 4.2.

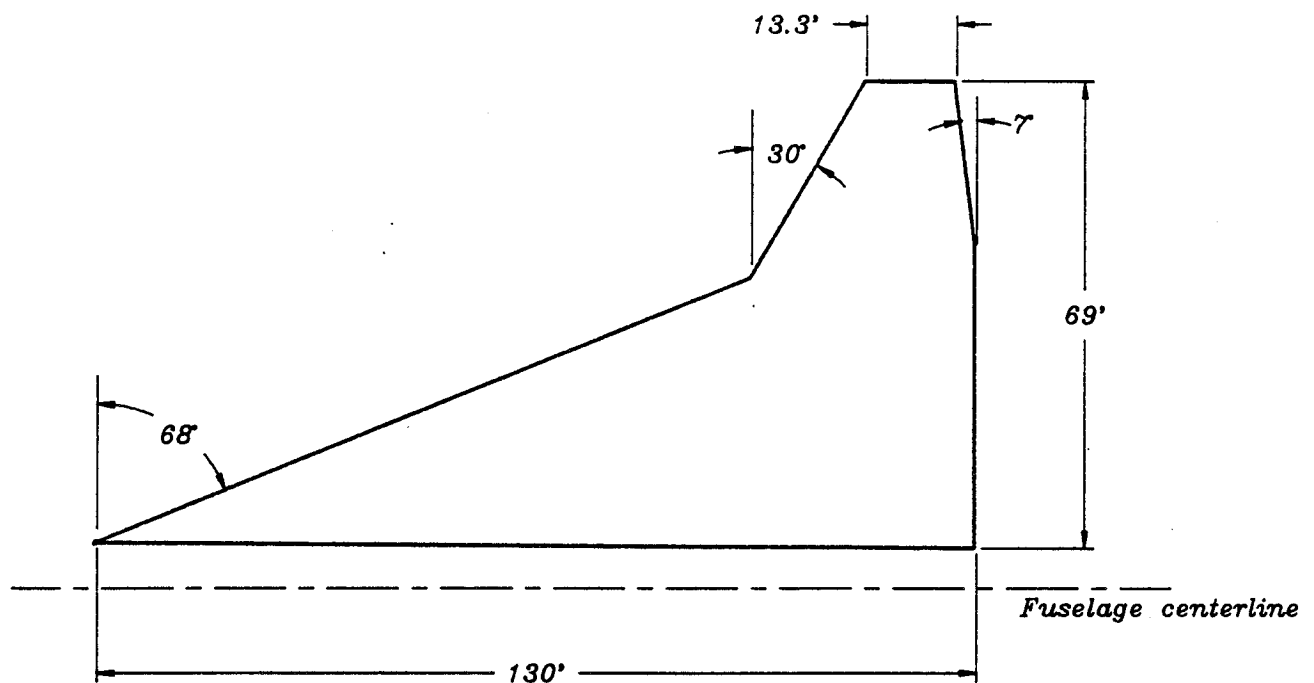


Figure 4.2 Stingray Wing Planform

### 4.2.2 WING PLANFORM

The aerodynamics of a supersonic transport poses some unique problems not typically found in conventional commercial transports, among them being aerodynamic center shift, wave drag, and supersonic handling

qualities. Since the Stingray spends most of its time in supersonic flight, a wing with an outboard supersonic section and inboard subsonic section was used. This will solve one of the primary aerodynamic problems since the inboard section will be subsonic during supersonic flight, leading to lower induced drag while the outboard section will be supersonic in order to provide supersonic roll control.

Table 4.1 lists the general wing planform characteristics of the Stingray.

Aspect ratio	2.87
t/c (root)	0.035
t/c (tip)	0.025
Taper ratio	0.106
Root chord	124.2.4 ft
Tip chord	13.3 ft
$\Lambda$ , delta1	68°
$\Lambda$ , delta2	30°
$\lambda$ , c/4	57°
Wing span	150 ft

**Table 4.1** Stingray Wing Planform Characteristics

Delta wings are typically used to reduce the movement of the aerodynamic center during transonic flight. The aerodynamic center of the Stingray shifts 4.4% of mean aerodynamic chord between subsonic and supersonic flight. A fuel management system will be implemented to control center of gravity travel. Since fuel will be stored in the wing, the fuel management system will be greatly simplified, minimizing the center of gravity travel.

The first sweep angle of  $68^\circ$  allows a subsonic leading edge during supersonic flight, producing less induced drag. The  $30^\circ$  outboard delta will remain supersonic during supersonic flight. The  $7^\circ$  forward sweep along the outboard trailing edge of the wing was required for area control; the wing area could be changed without significantly changing the aspect ratio. Also, the decrease in area increased the wing loading without decreasing the aspect ratio significantly.

The thickness ratios are small for a delta wing configuration due to the long chord line. The 3.5% thickness ratio at the root will provide more than adequate fuel volume. The taper down to 2.5% is beneficial in supersonic flight since it reduces the maximum cross-sectional area of the wing.

The taper ratio for the wing is 10.6%. Short wing tips were chosen for high speed roll control and, more importantly, for structural considerations: since more lift is generated at the tip of the wing, a longer tip would mean higher stresses and bending moments, hence, more structural weight. The average dihedral for the wing is zero. The wing twist angle is set at  $-1$  degree for good roll characteristics at high angle of attack. With this twist angle, the Stingray will be stable in all axes.

#### **4.2.3 AIRFOIL SELECTION**

After comparing several NACA wing sections, a thin wing section was selected. The advantage of a thin wing is that it provides less frontal area, hence leading to lower supersonic wave drag. The three disadvantages are that the fuel volume is reduced (compared to subsonic wing sections) and the landing gear must be specially tailored so as to minimize wing landing gear volume. In addition, the structural moments of inertia will decrease. Finally, thin wing sections are structurally heavier. Since aerodynamic drag was the main

concern in the supersonic wing design, the one advantage outweighed the three disadvantages.

The airfoil chosen for the Stingray was a modified NACA 65-206 (Figure 4.3). This thickness ratio of this airfoil was modified so as to meet the needs of the Stingray. The data for NACA 65-206 was used and assumed to be valid for preliminary design. The section was modified to 3.5% at the root chord to provide adequate fuel volume and to 2.5% at the tip in order to reduce the maximum cross-sectional area. With the 3.5% t/c, the maximum thickness of the wing was 4.55 ft.; if the 6% airfoil was used, the maximum thickness would have increased to 7.8 ft.

The leading edge radius of 0.240% will induce suction on the first crank delta in supersonic flight. Since this section is behind the Mach cone, the leading edge will be subsonic during supersonic cruise. The disadvantage of the sharp leading edge is that it is not efficient under high aerodynamic heating conditions when compared to a round leading edge.

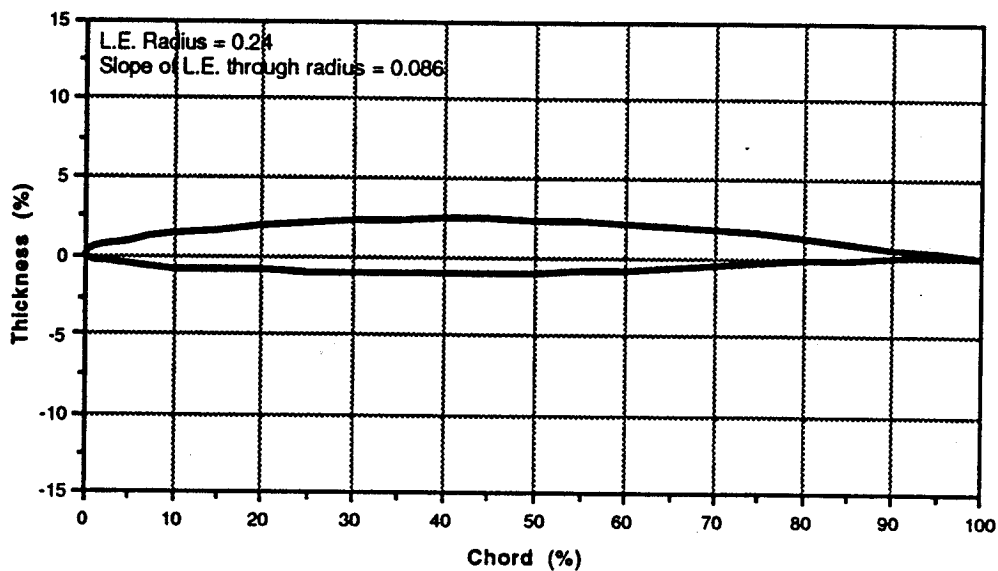


**Figure 4.3** Stingray Airfoil Section (Modified NACA 65-206, Ref. 26)

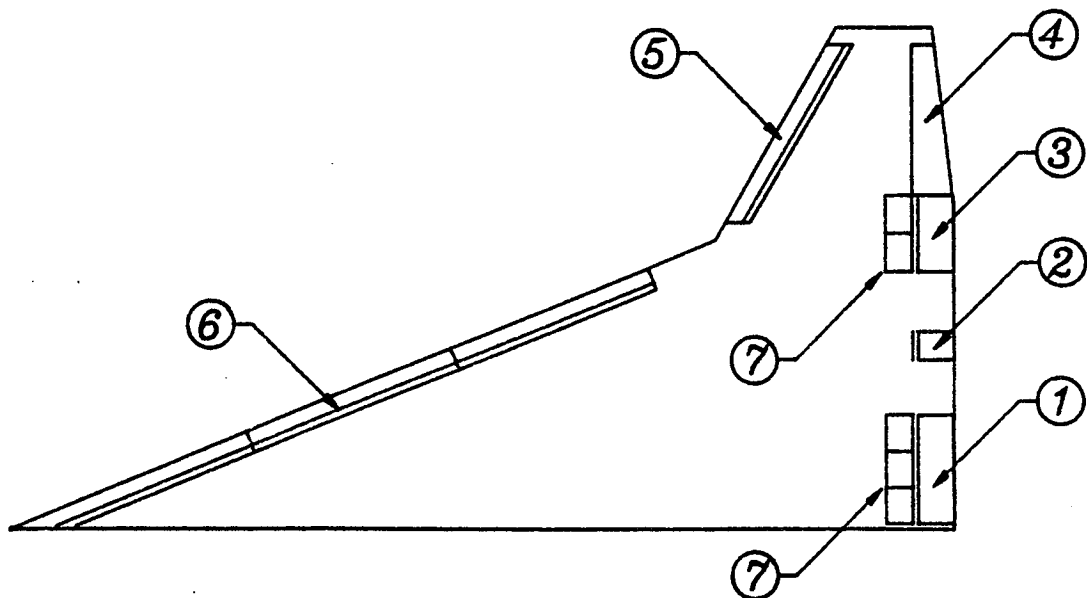
#### 4.2.4 HIGH LIFT DEVICES

The size, location, and flap type for the wing were estimated using (Ref. 2). A comparison was made between plain flaps, single-slotted and double-slotted Fowler flaps. It was determined that single slotted Fowler flaps located on the inboard section of the wing would enhance both takeoff and landing lift coefficients. Placement of these flaps would also leave sufficient space for placement of high speed ailerons. Plain flaps require a larger percent of the wing span to produce the same amount of lift. Double-slotted Fowler flaps were not needed since the single-slotted flaps provided sufficient lift. In addition, leading edge flaps were placed along the inboard delta wing to aid in low-speed lift.

Flap deflections of the Fowler flaps at takeoff is 25 degrees. This coincided with an increase in the lift coefficient of 0.43, providing a  $C_L$  of 0.9. A 45 degree flap deflection at landing provides a change in  $C_L$  of 0.46, with a  $C_L$  of 0.93

The flap area at takeoff and landing conditions was calculated using (Ref. 6). The critical case is takeoff, where the wing area/flap area ( $S/S_{wf}$ ) was 0.877. Landing required a flapped area of 0.599. The Stingray was easily able to make these requirements since Fowler flaps were placed along 53% of the trailing edge and leading edge flaps were placed along 90% of the wing. A flap and control surface layout is provided in Figure 4.4.





Item	Description	Area per Half
1	Fowler Flap	11000
2	Fowler Flap	1400
3	Fowler Flap	7600
4	Aileron	11600
5	Leading Edge Flap	10400
6	Leading Edge Flap	39000
7	Spoiler Panels	11300

**Figure 4.4** Stingray Control Surface Placement

#### 4.2.5 FUEL VOLUME

Delta wings generally have a great deal of volume available located in the wing. With the capability to carry over 96% of the mission fuel in wing tanks, the Stingray is no exception. When compared to the Concorde, which carries fuel in the fuselage due to its smaller wing, the Stingray will be able to carry almost 400,000 gallons of fuel in its wings. Figure 4.5 shows the fuel tank location on the Stingray

The fuel volume calculation was started by laying out the major wing structure, landing gear volume, control surfaces, and engines. The remaining volume of the wing was then broken up into 12 prismatic shapes for which conservative volumes (0.8-0.9 of actual) could be easily calculated. Each volume was multiplied by 50.4 pounds per cubic foot of volume to obtain the weight of fuel (JP-5) that that section of the wing can hold. The weight and volume capabilities of each fuel tank is shown in Table 4.2. The equations for transport aircraft, straight tapered subsonic wings, and for delta winged military aircraft, larger structural volume, both greatly underestimated the available fuel volume. A fuselage tank was added because an additional 5% more fuel was necessary to complete the mission. The fuel located in the fuselage was initially located in the tail but was moved into the wing box to keep the center of gravity forward. The aircraft can carry 8 percent more fuel than it needs for the mission, including reserves. This additional fuel volume can be used as surge tanks or to control the center of gravity location.

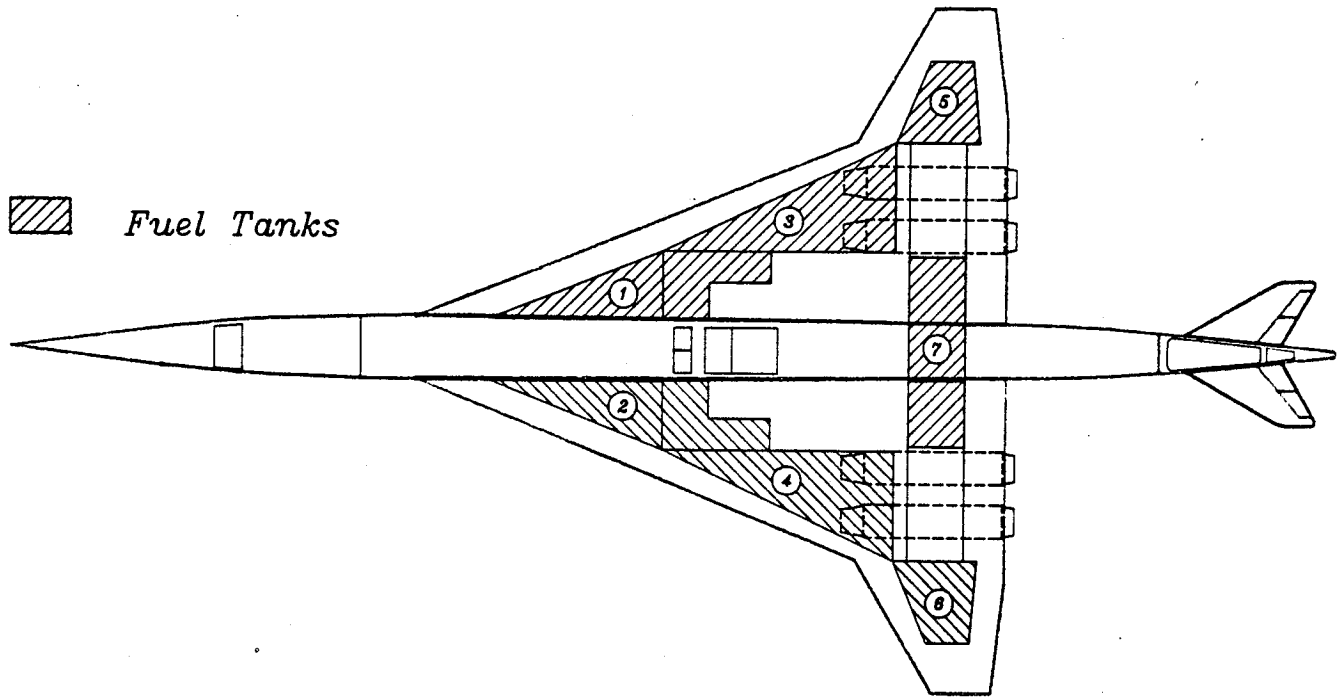


Figure 4.5 Stingray Fuel Tank Location

Tank	% Weight	Volume (ft <sup>3</sup> )	Weight (gal)
1	12.40%	940	48000
2	12.40%	940	48000
3	26.60%	2020	100000
4	26.60%	2020	100000
5	2.80%	210	11000
6	2.80%	210	11000
7	16.20%	1240	63000
Total	100%	7580	381000

Table 4.2 Fuel Tanks

## 4.3 FUSELAGE DESIGN

### 4.3.1 INTERIOR LAYOUT

The interior arrangement of Stingray provides accommodations for three classes and 250 passengers. A breakdown of the cabin layout is presented In Figure 4.7.

The spacious 2-2 seating in first class (Figure 4.6) comprises 10% of the total seating. The aisle width in this class is typically 28" between arm rests. The first class seats have a seat pitch of 42" and typical aisle height of 84". Some of the luxuries of first class seating includes individual pop-up LCD movie monitors and earphones for music entertainment for the duration of the four hour flight.

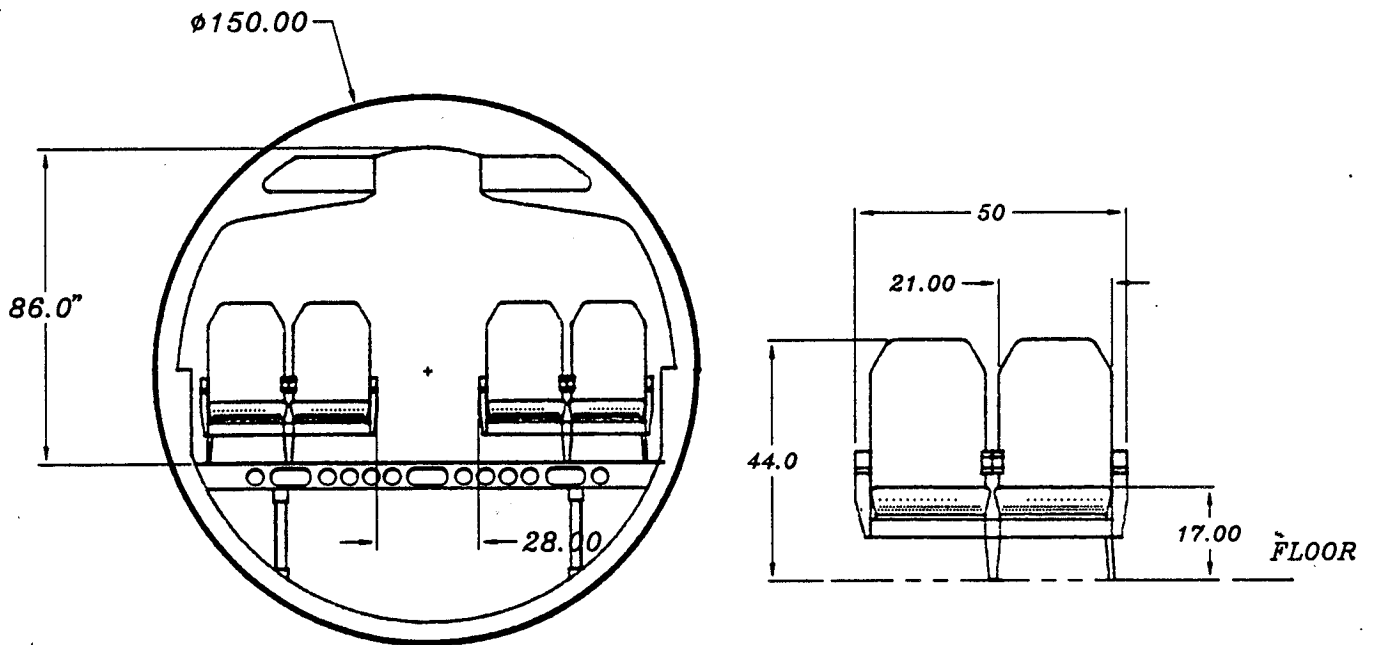
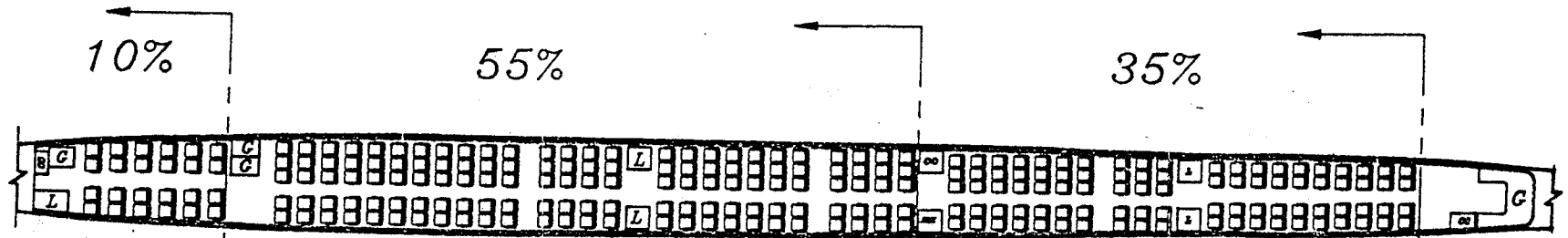


**Figure 4.6** Stingray First Class Cross-Sectional Layout

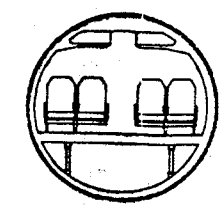
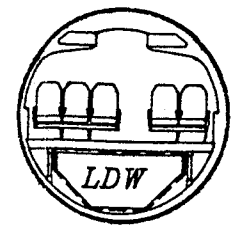
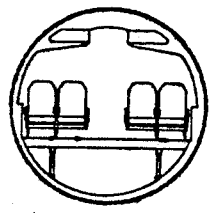
# STINGRAY



FIRST

BUSINESS

ECONOMY



AISLE HEIGHT  
 AISLE WIDTH  
 SEAT PITCH

86 IN.  
 28 IN.  
 42 IN.

84 IN.  
 22 IN.  
 38 IN.

80 IN.  
 22 IN.  
 34 IN.

FIGURE 4.7 STINGRAY CABIN LAYOUT

The 3-2 seating arrangements in both business and economy were carefully selected based on passenger comfort, accessibility of emergency egress, aerodynamic drag penalties, and airport compatibility when compared to a typical 2-2 seating or 2-1-2 seating. A 2-2 seating would eliminate the "middle man squeeze" associated with a triple seating, however, this configuration would make the aircraft nearly 320 feet long, posing airport compatibility problems. The 2-1-2 seating arrangement would have increased the cross-sectional diameter to a minimum of 184", which is too large for wave drag considerations.

The business seating (Figure 4.8) comprises 55% of the total seating arrangement. To compensate for the potential discomfort of triple seating, 20" wide seats are incorporated. The spaciousness of the seats and additional arm rests between the seats would diminish the "middle man squeeze" problem. The typical aisle width of the business class is 22". The typical aisle height ranges from 86" in the first class to 80" in economy class. As a compliment to the business class, telefax and telephone machines will be placed at the center of the business class section.

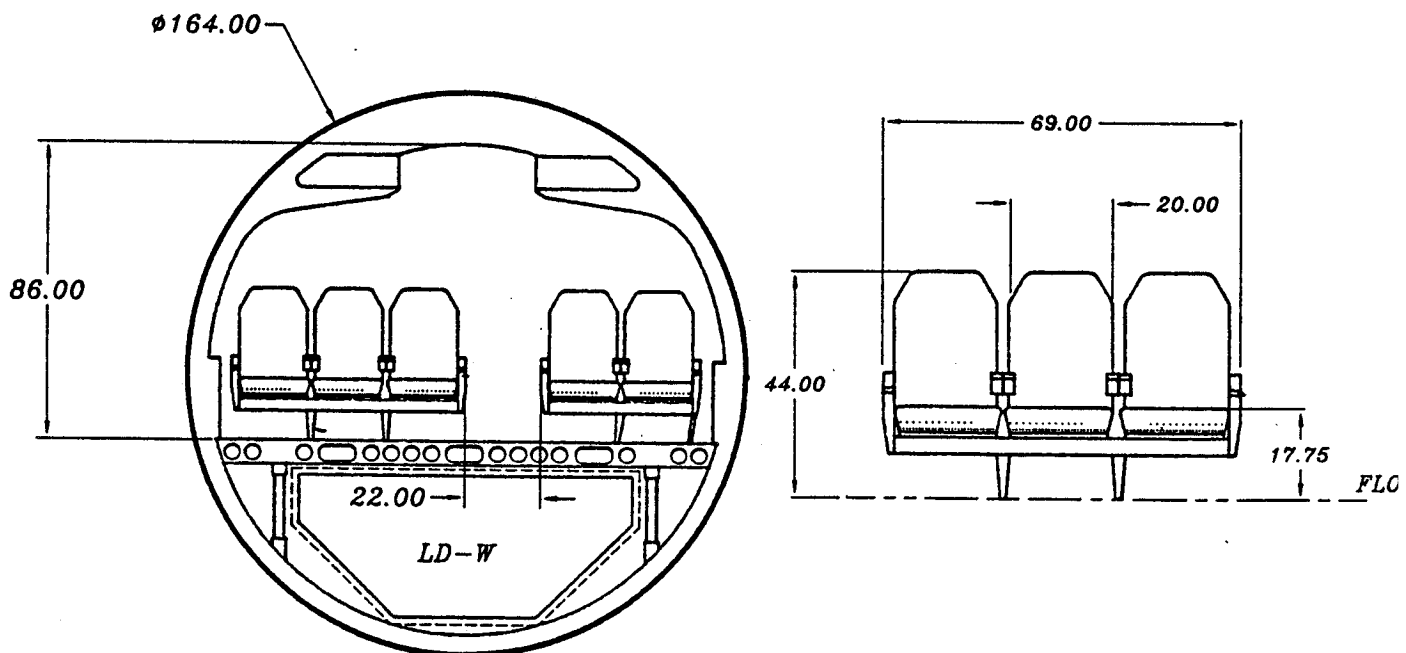


**Figure 4.8** Stingray Business Class Cross-Sectional Layout

The economy class (Figure 4.9) is comprised of 35% of the total seating arrangement. The seating arrangement shifts from a 3-2 seating to a 2-2 seating as the aircraft tapers down. The seat width of the economy class is 19". Also the aisle width is 20"-2" more than the minimum FAR requirement of 18". The aisle height is 80".

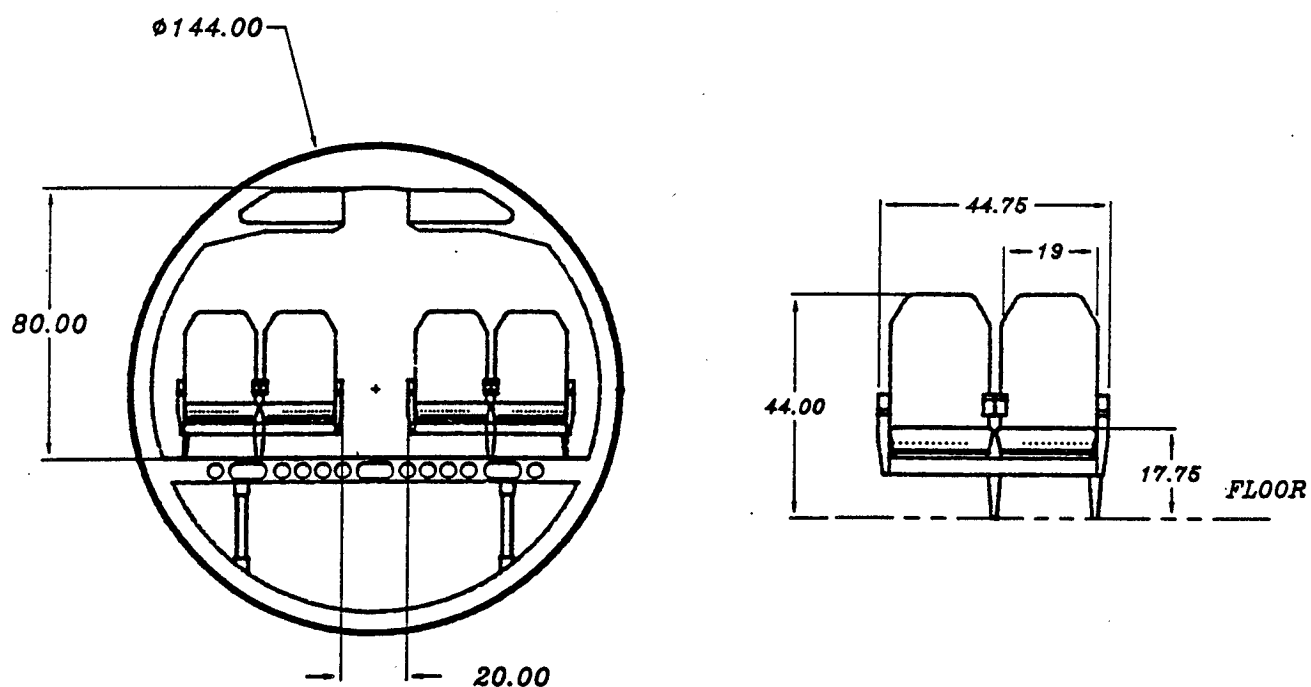


**Figure 4.9** Economy Class Cross-Sectional Layout

The Stingray was designed to provide maximum interior flexibility. This was achieved by efficient modification to the interior layout to accommodate seasonal travelling. This is achieved by changing the seat pitch or adding additional seats in the tail cone. The primary changes occur in the transition between business and economy class.

Galleys, lavatories and closets have been placed throughout each class. Due to the slenderness of the fuselage, the galleys and lavatories incorporated into the cabin are those standard on the Boeing 737 or McDonnell Douglas DC-10. While these are standard items, each galley and lavatory service a smaller number

number of passengers when compared to the 737 and DC-10, making them much more comfortable for both passengers and flight attendants. Because of the additional space, jump seats for the flight attendants can be provided. The closets provided for all classes on the Stingray are larger than those currently in conventional aircraft, such as the Boeing 747-400. Standard comfort items on the Stingray include telephone jacks and power outlets (for laptop computers).

All passengers will board through a main door 72"X42" located in front of the business class seating on the left hand side of the aircraft. The size of the boarding door offers generous boarding or exiting with carry-on luggage. Three service doors are located adjacent to the galleys on the right hand side of the aircraft. The service doors are Type B, 34"X72" (Ref. 2).

#### **4.3.2 CROSS-SECTIONAL DESIGN**

A seat track system provides maximum flexibility for 4 and 5-across seating. Due to careful placement of the seat track, seasonal changes in seating arrangement is possible. The utility systems, including lights, audio, and emergency oxygen are positioned for easy accessibility from each seat.

The general illumination is provided through glare free indirect lighting and is complemented with individual reading lights for each passenger. Besides underseat storage, spacious overhead sidewall modules of 1.86 ft<sup>3</sup> per passenger provides safe storage for personal belongings, blankets and pillows.

Windows will be placed at each seat location throughout all three classes. The windows will be circular and 8 inches in diameter and will be made of current standard materials. Circular windows were chosen over rectangular windows to order to minimize stress in the fuselage skin.

The cargo compartment of the Stingray was designed to accommodate LDW containers currently in use in narrow-bodied jet transports. The use of



containers will ensure quicker turn around time. A total of eighteen containers were needed to accommodate for a pre-load baggage volume of 40 lb. per passenger. Due to structural penalties created by doors, only one loading door will be incorporated. These containers will be on systematic tracks which speeds up the loading and unloading of cargo.

### 4.3.3 COCKPIT LAYOUT

The flight deck crew consists of a pilot and copilot. The flight engineer position has been eliminated through the use of advanced avionics and an integrated flight management system. However, a flight engineer station may be outfitted if the airline desires more manual control of flight management systems and less dependence on automated control. In addition to these three seat positions, a jump seat is incorporated into the flight deck for an observer.

It is worth noting that the inclusion of a copilot is purely for redundant purposes and, perhaps, to keep the pilot company. It would be completely within the capacity of the airline to have the Stingray flown with a single pilot. This would be very attractive from an operating cost standpoint.

Figure 4.10 illustrates the layout of the flight deck. Advanced avionics technology and flat screen displays will minimize the workload on the pilot by displaying information efficiently and in the form of graphic images where possible so as to avoid a "numbers overkill", or the display of so many numbers that the pilot loses track of the function of the numbers.

Flight control surfaces will be actuated through the use of a sidestick controller, located on the outboard side of each pilot, and conventional rudder pedals. The rudder pedals will also provide braking to the main gear wheels while on the ground.

The engine throttles will be located on the center panel, within reach of both pilot and copilot.

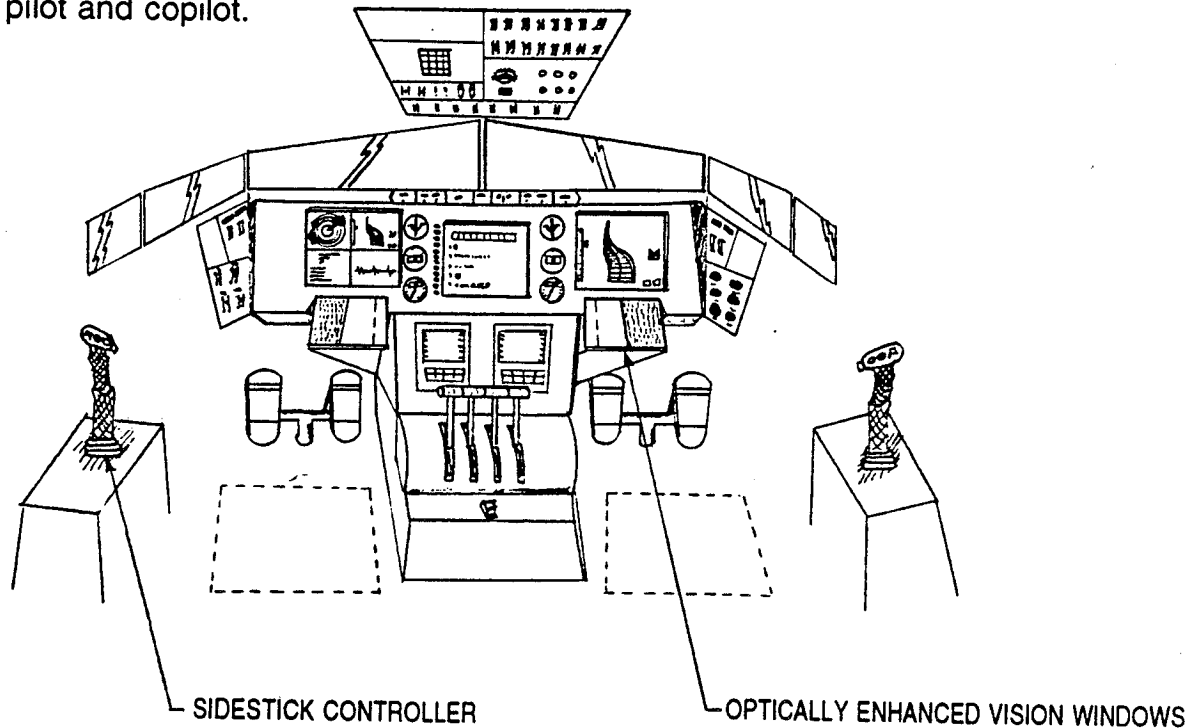


**Figure 4.10** Stingray Flight Deck Layout

Due to the shallow curvature of the aircraft nose, two possibilities were considered for pilot visibility. The first was a droop nose, the second, an optical system. The droop nose, which is used in the Concorde, was rejected since it would add considerable weight and complexity, thus increasing maintenance and cost. In terms of optical systems, a "see-by-wire" system was studied as well as a fiber-optic "periscope" system. Neither system would replace the windshield, but would provide forward visibility at high angles of attack. The "see-by-wire" system would involve computer imaging of the runway and terrain on a video screen. While this system has the ability to provide additional information to the pilot and will work in all types of weather, pilot acceptance of this system has not been favorable.

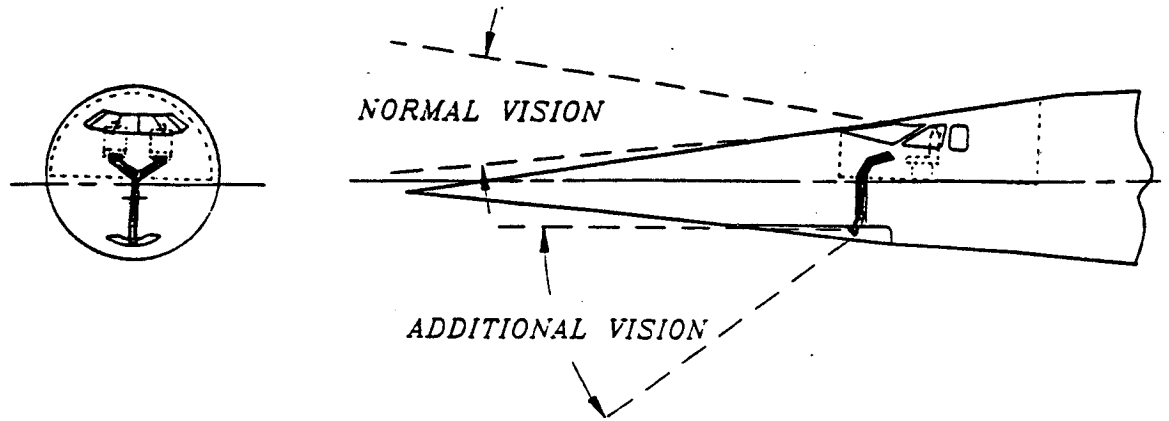


Figure 4.11 Stingray Visual System

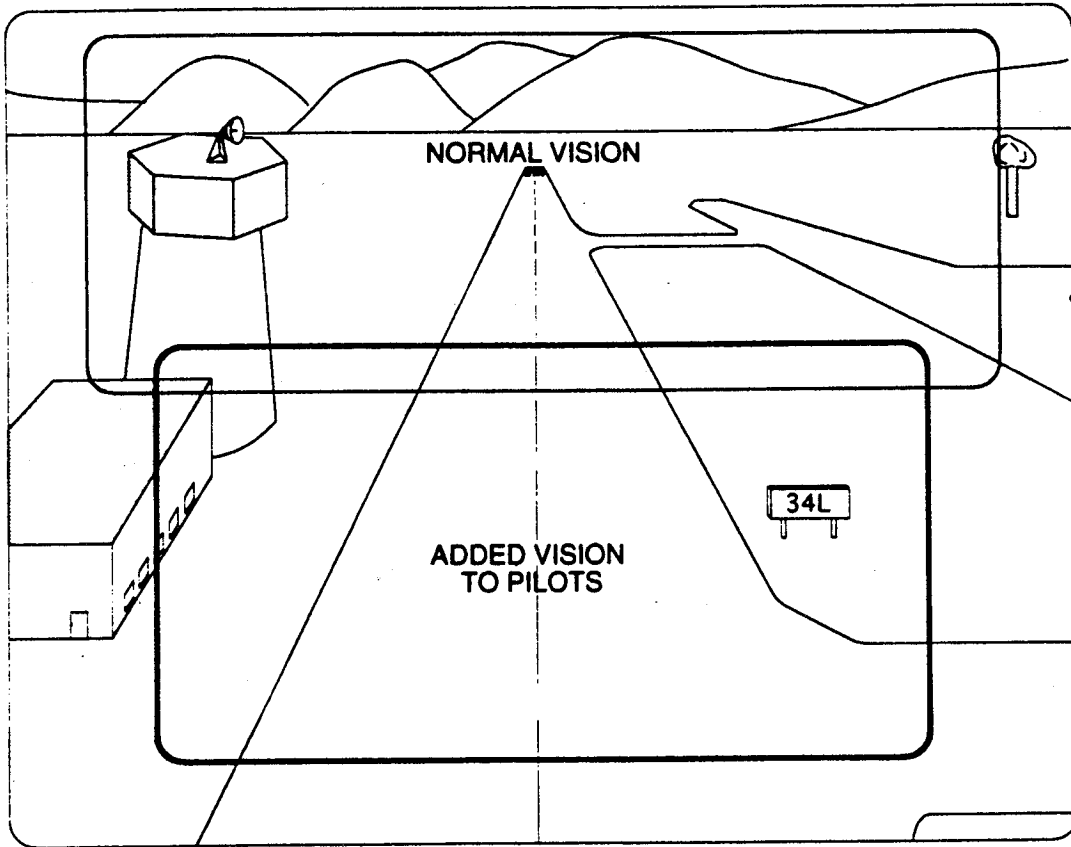


Figure 4.12 Pilot's Expanded View Using Stingray Visual System

## **4.4 EMPENNAGE DESIGN**

### **4.4.1 HORIZONTAL STABILIZER**

The initial sizing of the horizontal tail volume was achieved by looking at the values for existing supersonic cruise aircraft. Balancing horizontal control power, flight trim conditions based on static margin, and parasitic drag on the horizontal tail, the tail volume was set to 0.065. This is at the low end of the range but compares favorably with other conventional delta wing supersonic cruise aircraft.

Horizontal control power is provided by two split segment elevators, each of the four segments having its own electrohydrostatic actuator for redundancy. The tail was designed to provide enough control volume to provide adequate control power in the case of individual surface failure. The layout of the horizontal empennage is shown in Figure 4.13. The whole horizontal stabilizer has a trim capability of plus or minus 20 degrees and the elevators have a capability of plus or minus 15 degrees. The horizontal stabilizer is intended mainly as a trim surface but has a small enough inertia and an actuator sized to act as a control surface (stabilator) if necessary. As shown in Figure 4.13, the tail is swept to minimize drag at cruise Mach numbers, but has a higher aspect ratio than the wing to improve its lift curve slope during takeoff and landing. The 3.5% thick symmetric airfoil provides adequate aerodynamic performance as well as adequate structure volume.

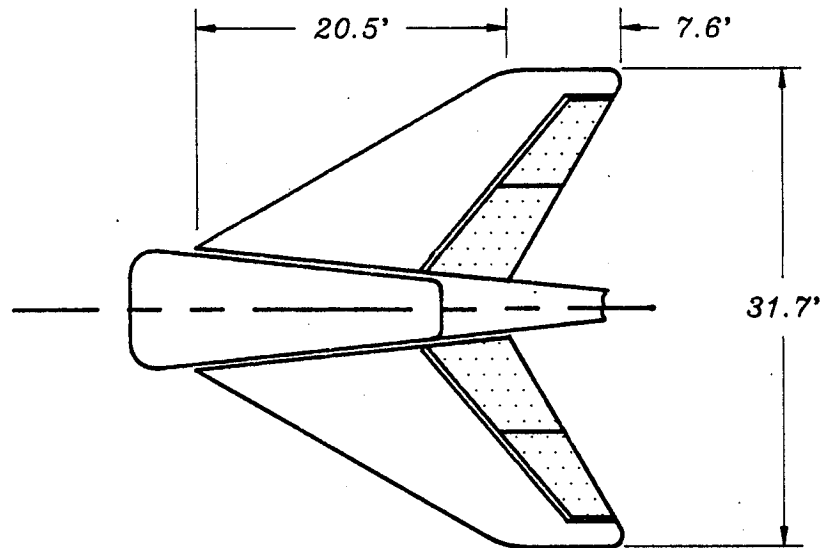


**Figure 4.12** Horizontal empennage

#### 4.4.2 VERTICAL STABILIZER

The preliminary vertical stabilizer volume coefficient was chosen by looking at existing supersonic cruise aircraft. The initial value chosen was 0.066, comparable to the NASA AST-100, and slightly smaller than the Concorde or the TU-144. Several of the directional derivatives degenerate at high Mach numbers but the condition that sized the tail was the single (outboard) engine out condition in the landing configuration. Delta wing aircraft generally require a very large vertical tail for acceptable directional stability at high angles of attack. The rudder is split into two sections, each controlled by a separate actuator for redundancy. Both sections are deflected during low speed maneuvering, while the lower section provides all control power at high Mach numbers to minimize the bending moment on the tail. The rudder provides 10 degrees of movement in both directions to provide directional control. The major factors driving the design of the vertical empennage were, takeoff one engine out FAR required control power, roll to roll performance, and degraded lateral directional handling qualities at high Mach numbers (dutch

roll). The basic parameters associated with the vertical empennage are shown in Figure 4.13.

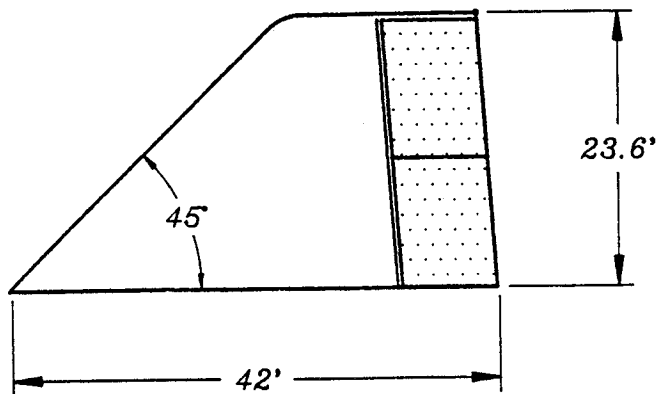


**Figure 4.13** Vertical empennage

The structure and low speed control requirements of the vertical stabilizer set its 45 degree leading edge and 4 percent thick symmetrical airfoil. The low speed control requirements outweighed the high speed drag penalty of having a supersonic leading edge on the vertical stabilizer.

## 5.0 PROPULSION SYSTEMS

### 5.1 ENGINE SELECTION

The engine selected for the Stingray was a mixed flow, low bypass ratio turbofan whose data was provided by NASA-Lewis Research Center. Sufficient data was available to accurately determine whether or not this engine met the needs of the Stingray. The thrust-specific fuel consumption (with units of lbs-f/lbs-T/hr) for this engine is 0.78 in takeoff, 0.89 in subsonic cruise, and 1.17 in supersonic flight at 60,000 ft. at Mach 2.4. A technology improvement of 5% was taken for all SFC values since this engine will not be certified for another 20 years (Ref. 11). Further improvements in SFC would reduce aircraft weight and increase range. Figure 5.1 shows a picture of the NASA-Lewis engine used in the Stingray and Table 5.1 provides engine parameters at different flight conditions.

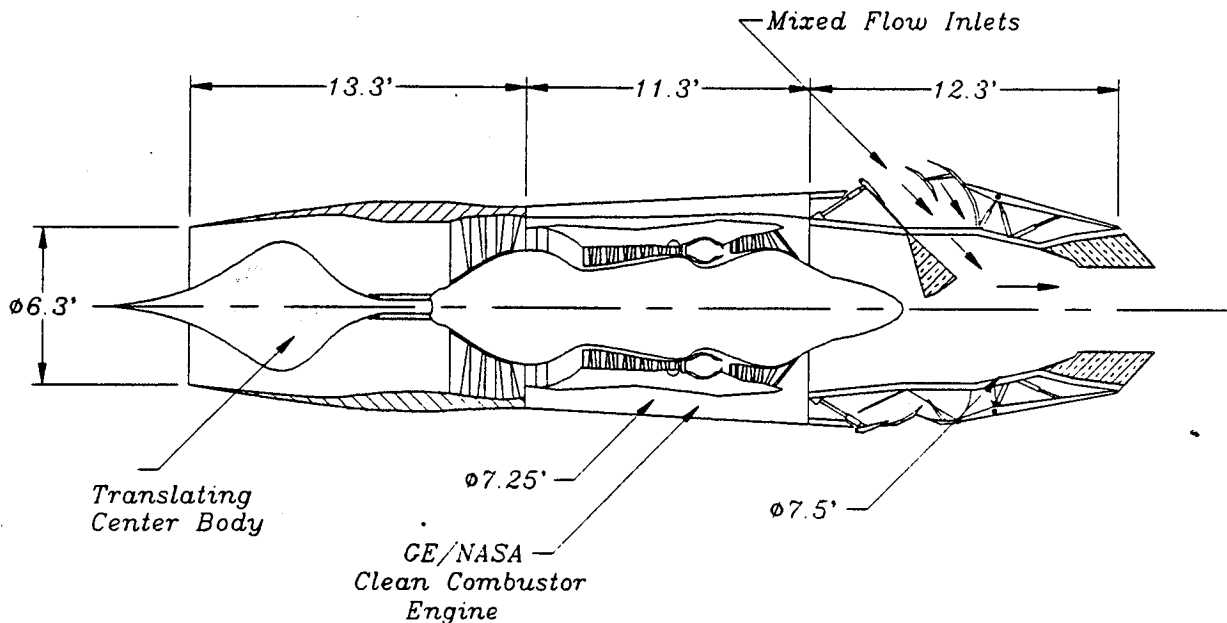


Figure 5.1 NASA Lewis Engine Cutaway (Ref. 24)

Available Thrust (in lbs.)		Excess Thrust (in lbs.)	
Takeoff	242280	Takeoff	120345
Landing	242280	Landing	163035
Subsonic	96896	Subsonic	47929
Supersonic	79607	Supersonic	7821
Required Thrust (in lbs.)		SFC (in lbs-f/lbs-T/hr)	
Takeoff	121935	Takeoff	0.78
Landing	79245	Landing	0.78
Subsonic	48976	Subsonic	0.89
Supersonic	71786	Supersonic	1.17

**Table 5.1** Engine Parameters with All Engines Operational (Ref. 24)

## 5.2 ENGINE SIZING AND LOCATION

The NASA-Lewis engine was not sufficient by itself to meet the Stingray's needs. An afterburner was considered for the critical condition of one engine out on takeoff, producing a scaling factor of 1.07. This meant that the engine needed to be sized for supersonic cruise. However, this allowed for no excess thrust in cruise, decreasing the maneuverability of the Stingray. A scaling factor of 1.19 was needed in order to meet the FAR 25 one engine out requirement with no afterburners. This correlated to only an 800 lbs. savings in engine weight and no decrease in engine length. For this reason, it was decided to scale the engine by 1.19 and keep the engine dry at all conditions, allowing sufficient excess thrust at all flight conditions.

The thrust-to-weight ratio for that condition was 0.34, or a takeoff thrust of 242,000 lbs was required. This scaling factor enabled the Stingray to meet the FAR requirements without adding the weight of an afterburner. For all other



flight conditions, the engine was more than capable of meeting required thrust levels. Table 5.2 shows the critical case which sized the Stingray engine.

T/W	0.34
Thrust	242280
Scaling Factor	1.19

**Table 5.2** Stingray Critical Engine Requirements

The four engines were placed under the wing near the trailing edge. Location was driven by the landing gear placement; engines need to be placed such that Foreign Object Damage (FOD) was minimal. Advantages in under-wing mounts is that accessibility of the engines for maintenance will be easier. Also, the exhaust plume will not interfere with flow over the wing.

The separation of the engine was governed by the one engine out conditions, catastrophic failure and landing gear placement. Outboard engine placement was limited by rudder control power necessary to counter the yawing moment induced by outboard engine failure. Additionally, should a catastrophic failure in one of the engines occur, the distance between engines will ensure that the other engine will not be damaged. The inboard engine was set by the placement of the landing gear. Because the engine inlet extends past the landing gear, the inboard engine must be outboard of the landing gear.

The final size of the engine, after consideration of placement, scaling factor for the critical condition, and thrust requirements led to the dimensions found in Table 5.3.

Component	Length (ft)	Diameter (ft)	Weight (lbs)
Engine	11.35	7.25	8500
Inlet	13.38	6.33	4200
Nozzle	12.31	6.23	4800
Engine Accessories	0	0	800
Nacelle	27	7.08	1500
Total Pod	37.05	8	19800

**Table 5.3 Engine Dimensions**

### 5.3 INLET DESIGN

Since this engine is designed for supersonic flight, a built-in shock system will be necessary to compress and slow the air flowing into the engine core. The Stingray engine uses an axisymmetric internal 3-shock system with a translating center body. The translating "spike" will enhance pressure recovery in all stages of flight regime. The pressure recovery with the movable spike was 96% at takeoff and subsonic cruise, and 93% at supersonic cruise.

The inlet is designed to be 12.84 ft. long. This dimension was provided by NASA-Lewis (Ref. 27) and is sized by diffusion of the flow necessary before compression. The airflow into the engine using this inlet was slowed from Mach 2.4 down to Mach 0.69, a typical number for supersonic engines. Due to boundary layer theory, a predicted boundary layer of 6 inches must be manipulated such that it does not enter the engine. For this reason, an 8 inch long pylon was used to place the engines below the boundary layer. A small drag penalty is paid due to interference between the wing and the engine.

## 5.4 ENVIRONMENTAL CONCERNS

There are two main areas under which the Stingray engine must be environmentally conscious. First, it must meet at least FAR 36 Stage III noise requirements and second, the nitrous oxide (NOx) emissions must cause minimal (if any) damage to the earth's fragile ozone layer.

The Stingray engine will meet FAR 36 Stage III by using a mixed ejector system as a noise suppressor. Typically, exit jet velocities above 1400 ft/sec will require some type of noise suppression (Ref. 17). With the Stingray's exit velocity of 3200 ft/sec, the ejector will be needed. The ejector will take bypassed flow as well as outside flow and eject the flow into the nozzle, enhancing flow mixture. According to NASA-Lewis, the ejector will provide 19 EPNdB of noise suppression, enough to meet FAR 36 Stage III. The disadvantage with the ejector is that it causes a loss of 4 to 5% of thrust. This, however, has been accounted for in the engine scaling. The mixed ejector is shown in Figure 5.2.

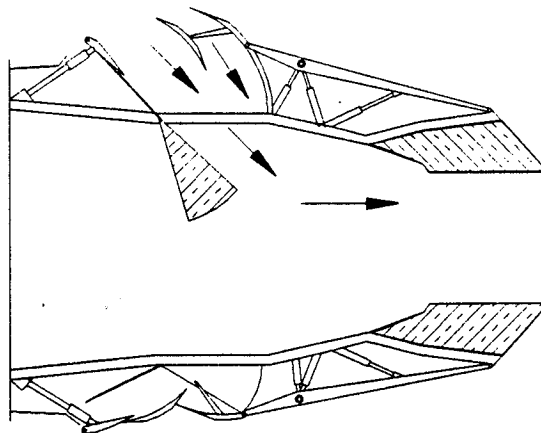


**Figure 5.2** Stingray Noise Suppressor-Mixed Flow Ejector

The nitrous oxide emissions are not a problem for the Stingray engine. NASA-Lewis has incorporated the use of the NASA/General Electric clean combustor which will reduce the NOx to less than 8 grams NOx per 1 kilogram fuel burn, minimizing ozone damage. This will have no effect on thrust output on the engine due to the fact that the data available from NASA-Lewis was based on the incorporation of the clean combustor.

## 6.0 LANDING GEAR

### 6.1 LANDING GEAR OVERVIEW

The landing gear for the Stingray was designed with the following limitations in mind. First, the landing gear needed to absorb all landing and taxiing shocks, minimizing stresses and vibrations on the airframe. Since the Stingray is a heavy aircraft, the landing gear must be able to distribute the load on the runway such as not to damage the pavement. Finally, the landing gear must optimize the utilization of existing technology to cut down production and development costs.

The final configuration of the landing gear system for the Stingray are presented in Figure 6.1. The nose gear layout resembles the traditional McDonnell-Douglas nose gear design. The main gear configuration resembles the landing gear system for the Boeing 747-400.

Both nose and main gear, however, required critical modifications before aircraft integration due to the slenderness of the Stingray. This layout yielded a load classification number (LCN) of 82, less than that of the Boeing 747-400, which has a LCN of 92. As seen from Figure 6.1, a tail wheel was incorporated to prevent the engines from striking the ground during rotation for takeoff. This wheel will be retracted forward into the fuselage after takeoff. Table 6.1 shows the load distribution of the landing gear at takeoff and operating empty weight.

	TOGW	OEW+PAX
Nose Gear	6.5%	10.0%
Main Gear	94.5%	90.0%

**Table 6.1** Landing Gear Load Distribution

# STINGRAY

LCN COMPARISON	
BOEING 747-400	92
STINGRAY	82

TURN-OVER	44°
TIP-OVER	41°

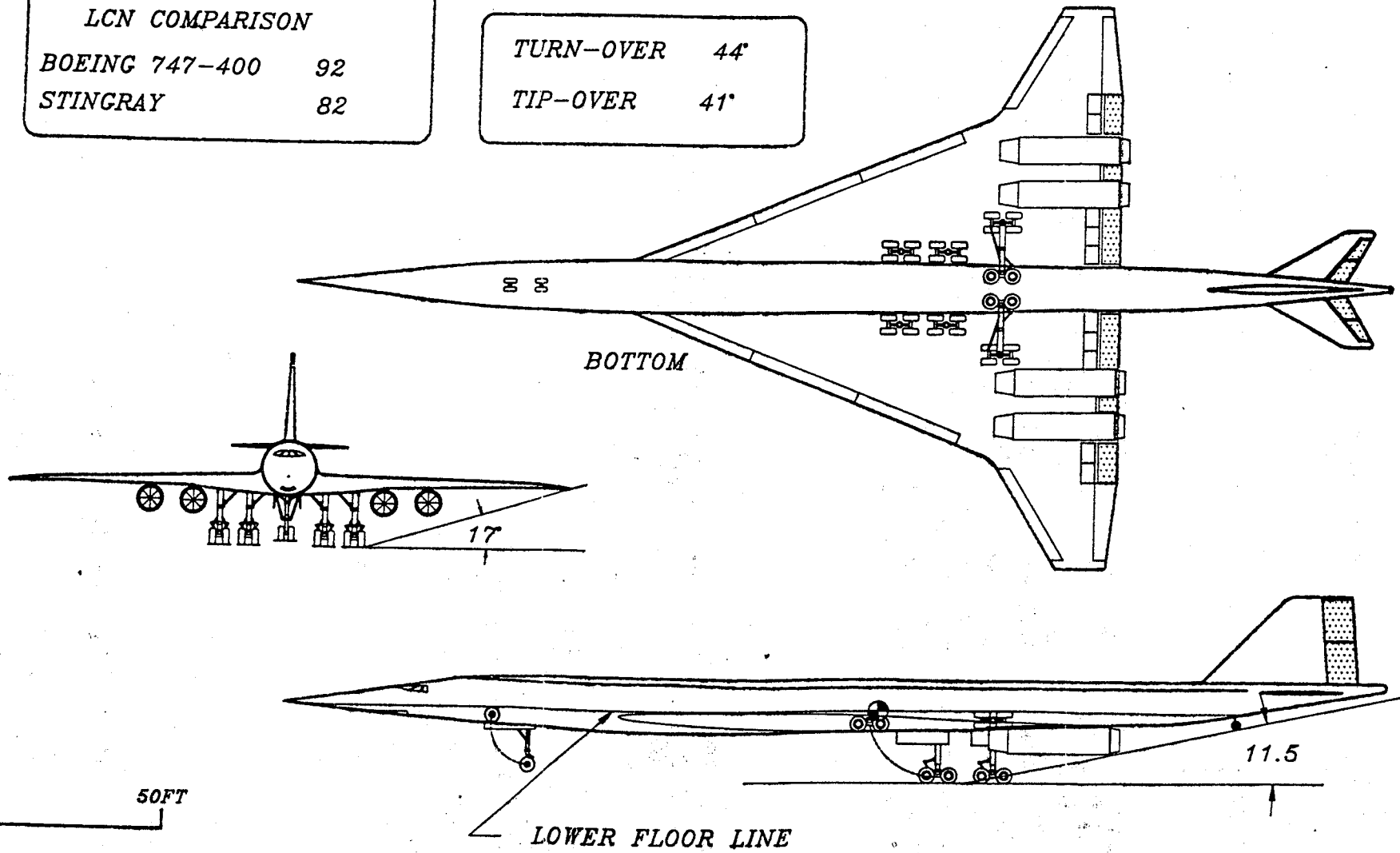


FIGURE 6.1 STINGRAY LANDING GEAR LAYOUT

The landing gear design involved an iterative process in sizing the tires, struts, and shock absorbers to handle the aircraft weight, impact loading, and c.g. excursions. It also involved a detailed study of the retraction systems before modifications could be made. Upon completion of the sizing and modifications, the landing gear was integrated into the aircraft for fit & function, tolerance, and interaction with other systems such as propulsion, structures and fuel tanks. The final sizing, corresponding sample calculation, and load distribution analysis are presented in the Ref. 24.

The load distribution and the rotation for takeoff led to the use of Oleo pneumatic strut on all gears. To prevent the entire load of the aircraft from being distributed on the back main gear upon takeoff rotation, an Oleo pneumatic strut system with interconnected cylinders were incorporated onto the main gears. This technology is currently incorporated into the Boeing 747-400 landing gear system (Ref. 4). In terms of energy absorption and dissipation, Oleo pneumatic struts are about 90% efficient.

The tire pressures for both nose gear and main gear are presented in Table 6.2.

	Tire Size	Tire Pressure
Nose	48 X 18	175 psi
Main	50 X 20	175 psi

**Table 6.2** Tire Parameters

## 6.2 NOSE GEAR

The dual tire configuration of the retractable nose gear is presented in Figure 6.2.

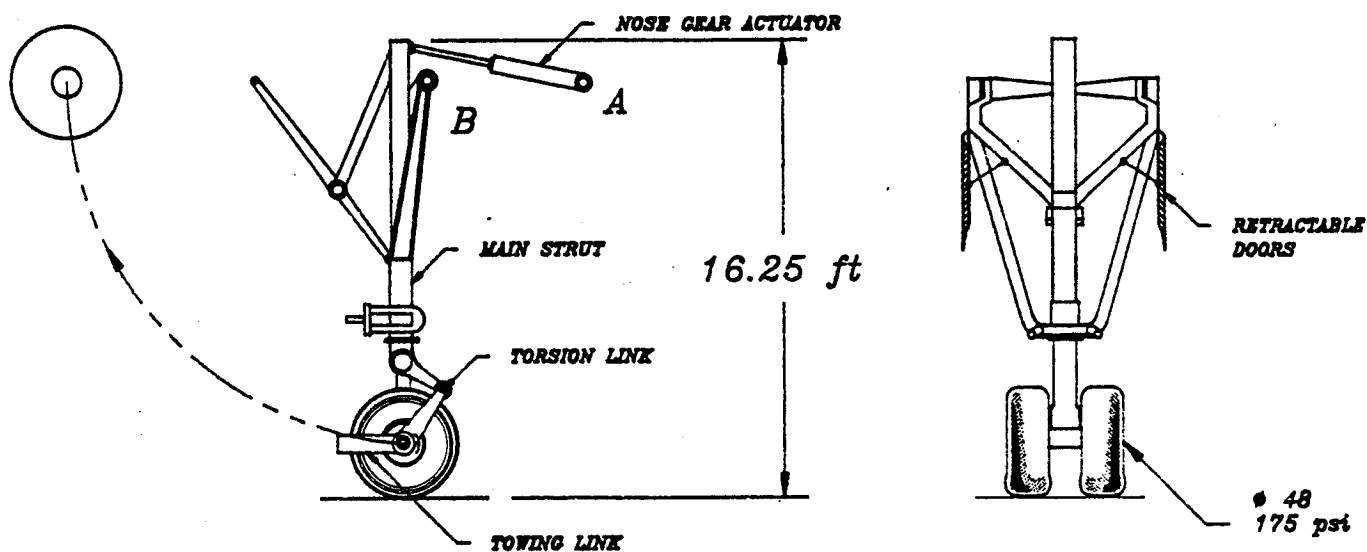


**Figure 6.2** Stingray Nose Gear Configuration

The nose gear has freefall capabilities, as specified by the FAR 25. This nose gear was designed to handle both the static and dynamic impact loading from the gross takeoff weight upon emergency landing. A load distribution of 6.5% on the nose gear at gross takeoff weight allows for controlled steering while taxiing and taking off. A load distribution of 6.5% on the nose gear at Operating Empty Weight ensures taxiing capability under this load condition.

To ensure static stability, a positive rake is incorporated. This feature is stable because a positive rake tends to lift the aircraft if the nose gear begins to swivel. To ensure dynamic stability a slight positive trail was incorporated. This feature allows the runway-to-tire friction to rotate the tire back to its originally intended position. The positive trail also helps to reduce an oscillatory dynamic instability called shimmy. Due to gear stiffness, strut size, and load on nose gear a shimmy damper is not needed. A drag strut is incorporated to prevent



accidental damage to Oleo pneumatic cylinder caused by the tremendous drag force during taxi and landing. Other features of the nose gear system include a nose gear actuator, steering cylinder, towing link, torsion link and retractable doors. The nose gear does not have braking capability; the braking of the aircraft will be adequately handled by the main gears.

### 6.3 MAIN GEAR

The retractable front and back main landing gear of this aircraft has a twin tandem configuration as shown on Figure 6.3a and 6.3b respectively. The main gear layout resembles that of the 747-400. The utilization of existing landing gear technology was intended to minimize the research, development and pre-production cost of a new design.

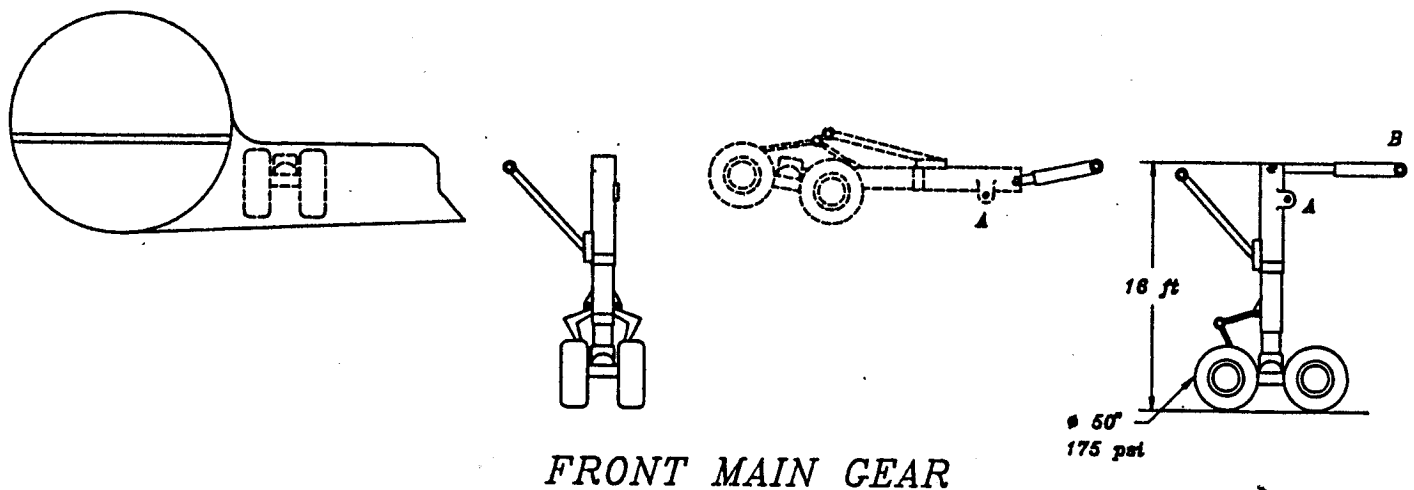
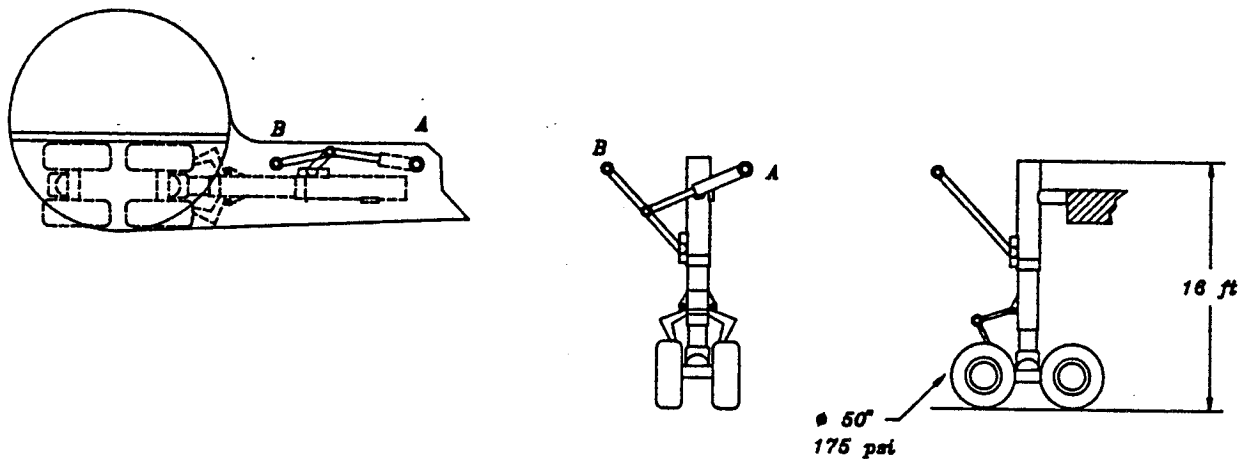


**Figure 6.3a** Stingray Main Gear Configurations



### BACK MAIN GEAR

**Figure 6.3b** Stingray Main Gear Configurations

Furthermore, this four truck configuration was one of the few design options that yielded a reasonable LCN, structural loading on the thin wing sections, and retraction mechanism. In addition to these advantages, this twin tandem configuration does not have as bad of a scrubbing problem when compared to conventional six or eight wheel trucks.

Due to the fact that all four struts on the main gear are interconnected with hydraulic lines, the constant loading on front and back main gears can be regulated by differentiating the strut extension and compression during rotation for takeoff. This feature also improves the lateral stability of the aircraft when taxiing along the runway as shown on Figure 6.4.

The penalty for this configuration was the additional weight due needed for the two additional struts when compared to a two strut configuration. The design results, however, yielded identical strut sizes for the main landing gear

to make use of compatibility of spare parts. In addition, the tradeoff for the ability to land on any existing international airports in the world without causing damage to the runway, lowered concentrated loading on the wing structure, and performance made this choice reasonable.

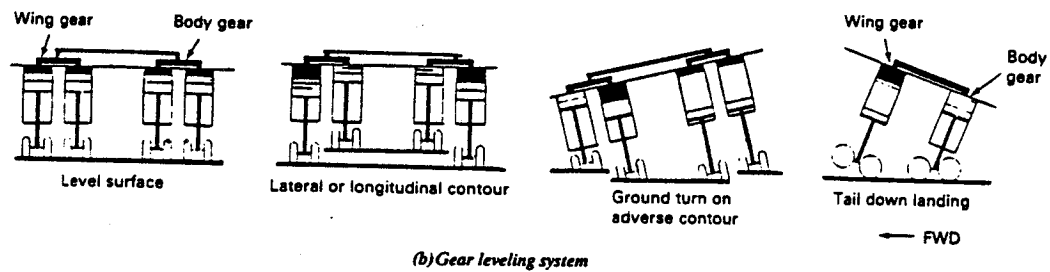


**Figure 6.4** Stingray Landing Gear Leveling System (Ref. 18)

Another feature of the main gear is differential braking, which enhances the steering capability of this aircraft. The four truck configuration resulted in smaller brakes. This will both increase the brake area and dissipate heat faster when compared to larger, but fewer brakes.

The brakes on the gears are composed of disc brakes made of anti-skid carbon. This type of brake is 40% lighter than conventional steel brakes but costs nearly twice as much. Given time, the cost should come down with increased utilization of these brakes by other aircraft. This braking system is capable of holding the aircraft while running the engines at full throttle. Heat sinks are incorporated to prevent over heating from the inside. Carbon brakes dissipate heat quicker than steel, which is desirable for decreasing turn around time.

## 7.0 STRUCTURES

### 7.1 MATERIALS

Material selection for the HSCT poses a unique challenge uncommon in conventional subsonic aircraft design. Due to thermal heating experienced as a consequence of supersonic flight, the materials utilized will have to provide high strength to weight characteristics at elevated temperatures. A cruise velocity of Mach 2.4 induces unadjusted skin temperatures averaging 340 degrees Fahrenheit. Since this exceeds the practical operating limit of aluminum alloys (Figure 7.1), more exotic materials will have to be used over much of the airframe.

Four main design criteria determined the final material selection. The first and most important was the material thermal characteristics. The strength to weight ratio is also especially critical for this type of aircraft because of the high weight associated with supersonic flight. The large fuel volume required to fulfill the mission requirements drove the gross take-off weight to a high number which reinforced the necessity for minimizing the structural weight of the aircraft. Material consistency was also a major concern because of the stresses induced at the interface of dissimilar materials with incompatible thermal expansion coefficients. Economic factors were also of primary concern in the determination of the final material layout illustrated in Figure 7.1. Titanium was selected as the primary structural material contributing to approximately 60 percent of the airframe. Aluminum alloys are the second largest contributor, composing 35 percent of the airframe. Special composites will be utilized to a minor degree on some control surfaces for reasons addressed later.

Due to material selection, the airframe cost inflates beyond conventional subsonic aircraft such as the Boeing 747. To offset this initial increased

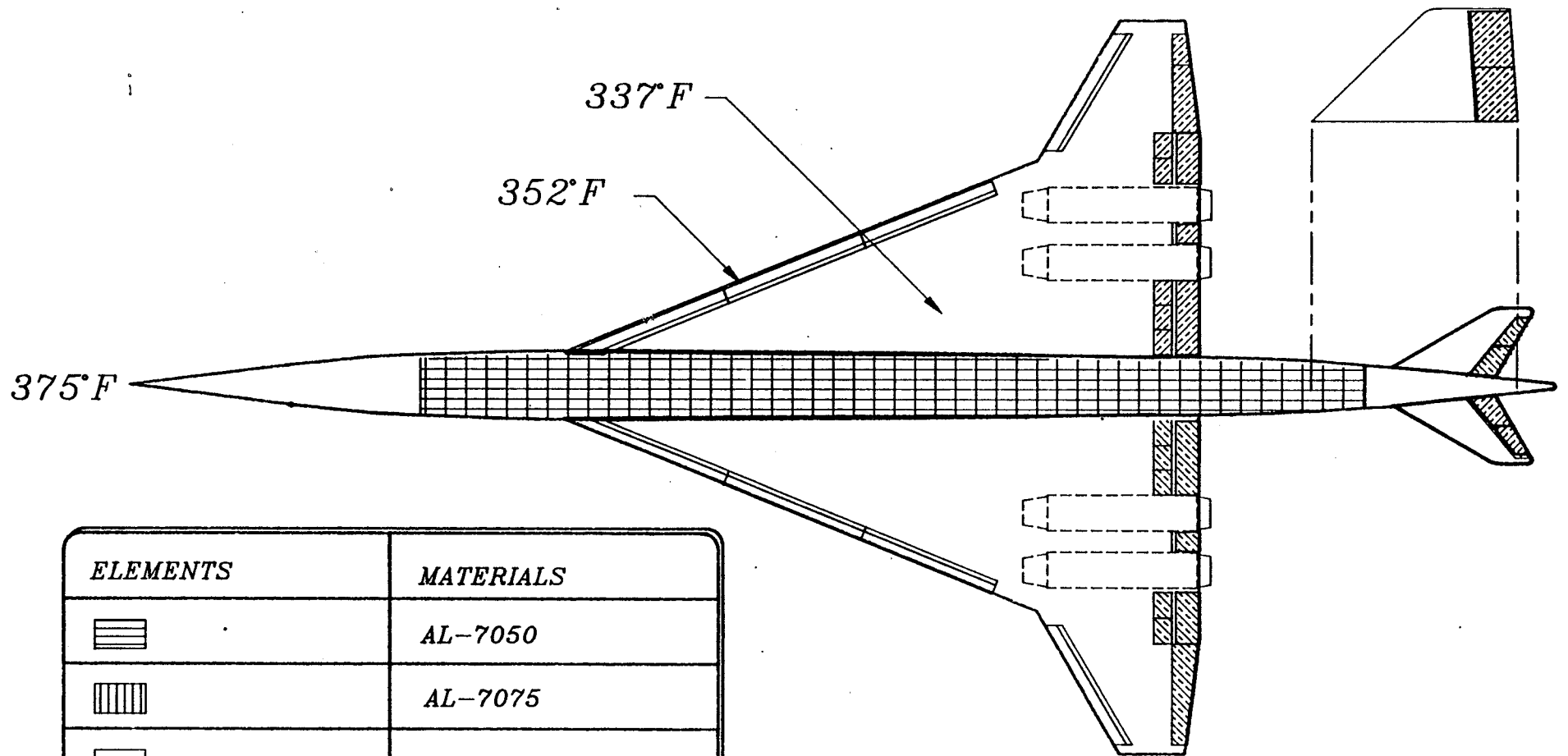
investment, the structural design is intended to reduce long term maintenance costs. This will be achieved through the use of unusually large single forgings bonded together by adhesives over much of the airframe. Bonding component interfaces with adhesives and minimizing the number of rivets required will increase the life expectancy of the airframe and consequently reduce long term maintenance costs. A reduction in manufacturing cost is also accomplished by the elimination of thousands of holes that would have to be precisely drilled into very hard titanium surfaces to accommodate rivets.

Titanium was selected over other potential materials such as advanced metal matrix composites due to lower investment cost. Composite structures of this type could not be implemented due to the extreme initial capital investment. The lack of empirical knowledge about the performance of load carrying composite aircraft structures reinforced this decision. FAA certification and airline acceptance of structural composite materials is not yet widespread enough to justify their use. Manufacturing costs for the large titanium structural components would be reasonable because they require conventional methods, which when optimized, can be adequately efficient. The lack of property variations at projected operating temperatures made titanium a suitable material. The strength to weight ratio of titanium remains virtually constant in the temperature range of concern.

Aluminum, maintaining production costs nearly half that of titanium, is utilized in areas in which it satisfied operating requirements. This occurs on the upper fuselage where relatively low skin temperatures exist.

Composites will be utilized on all control surfaces except the leading edge flaps. The reason for this is the necessity to use the next generation metal matrix composite materials in limited simple forms to prepare for a transition of construction tactics in the future. Control surfaces, being independent

detachable structures subject to periodic replacement and repair, are simple enough to justify composite construction costs. A weight savings has also been confirmed by the use of composite structures in these areas. This provides a test bed for the development and use of these materials to greater extent by the airframer in the future. If it is determined that advanced composites are inappropriate for this type of application, the control surfaces can be easily replaced with metallic substitutes.



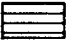


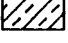
<i>ELEMENTS</i>	<i>MATERIALS</i>
	AL-7050
	AL-7075
	TI-6AL
	POLYMERIC COMPOSITES
CENTRAL FUSELAGE SKIN	AL-2024
LANDING GEAR	300M

Figure 7.1. (a)

## 7.2 V-n DIAGRAM

The V-n diagram in Figure 7.2 was constructed by the method shown in (Ref. 5). The criteria for FAR 25 certified aircraft were followed, including maximum maneuvering load factors of positive 2.5 gees and negative 1 gees. A cruise Mach number of 2.4 at 60,000 feet set the equivalent airspeed (KEAS) to 423 knots. The maneuver point was established by using the maximum cruise configuration (flaps and gear up) lift coefficient of 0.55. The dive point and maximum structural velocity line was established using the value recommended in (Ref. 5) of 1.25 times the cruise velocity. This may be slightly higher than necessary for this class of aircraft in supersonic cruise, but at lower altitudes this velocity will be critical. The maximum structural velocity ( $V_{\text{dive}}$ ) sets a dynamic pressure limit ( $Q_{\text{bar}}$ ) of 850 psf. The gust load criterion for FAR 25 aircraft resulted in the sloped dotted lines shown in Figure 7.2. These lines all fall within the previously defined maneuver envelope indicating that gust criterion have no additional impact on structural design. This makes sense because gust sensitivity is a function of the lift curve slope and wing loading. A highly loaded delta wing is not very sensitive to gust loading.



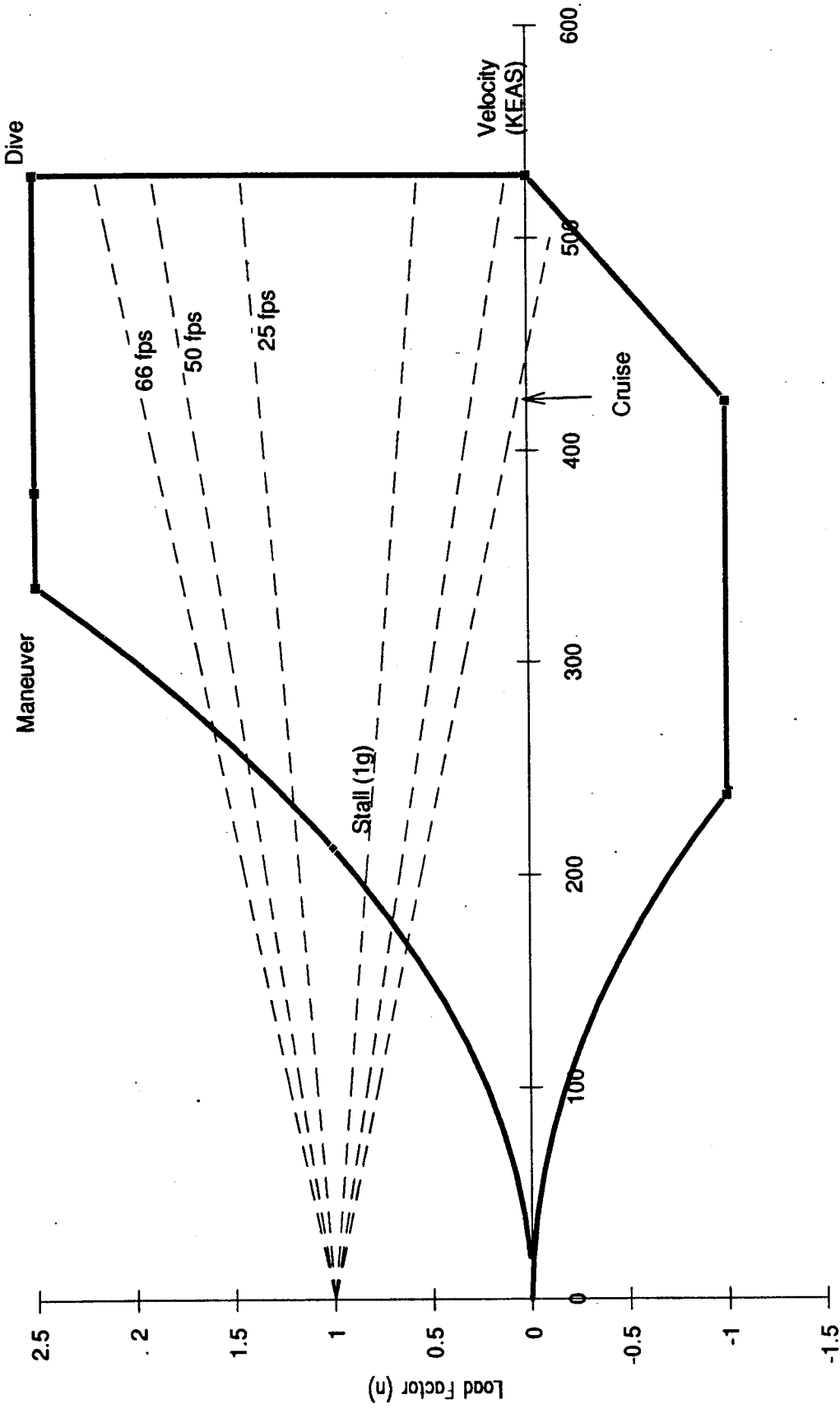


Figure 7.2 V-n Diagram

### 7.3 STRUCTURAL LAYOUT

Conventional methods similar to those used on existing aircraft were used to determine the structural layout of the Stingray (Ref. 3, 18). The wing was to be the only exception as detailed later. Aerodynamic loads were determined using the critical case of a 2.5 g maneuver as dictated by the V-n diagram (Figure 7.2).

A minimum skin thickness of 0.07 inches was required on the fuselage to maintain cabin pressurization in the aluminum section. This thickness was continued throughout the titanium section of the fuselage to accommodate rivets. Fuselage frames were spaced at a standard distance of 18 inches which allowed plenty of room for the inclusion of windows (Ref. 18). The minimum frame depth for the aluminum fuselage section was calculated to be 5.5 inches (Ref. 3). Cabin and fuselage dimensions allowed a frame depth of 6 inches to accommodate the extra fuselage torsion due to the unusually long length. Fuselage longeron spacing was maintained at a conventional 10 inches which also helped to accommodate the selected window diameter of eight inches (Ref. 18).

Most of the nose cone, due to extreme temperatures, is composed of titanium. A small portion of the tip is composed of kevlar to allow for the use of radar equipment. A high temperature silicon sealant will be used at the titanium/aluminum interface to help absorb the stresses induced by incompatible expansion ratios. The empennage section is constructed similar to the nose cone with similar treatment of the interface between it and the aluminum fuselage section.

The horizontal stabilizer and rudder followed conventional design characteristics utilizing main spars, stringers, and ribs.

The main wing will be constructed of titanium skin and substructure with composite rear control surfaces. The unique feature of the wing is the intended use of adhesives as the primary bonding agent instead of rivets. This should allow the wing to have more flexibility and a more consistent load distribution, reducing the number of stress risers. Rivets will be used sparingly as a means of protection against adhesive failure. The reduction of stress risers will increase the fatigue life of the wing considerably, which is especially critical in the type of operating environment expected (Ref. 28). High temperatures will cause the wing to expand (6 inches in overall length) and flex against the applied loads. If the design does not in some way compensate for this expansion, the consequences could be disastrous and costly. It is critical that the adhesive chosen has favorable strength characteristics at elevated temperatures. It will also have to exhibit limited flexibility characteristics. A weight savings (maximum 15%) should also coincide with the extended use of adhesives, but since the extent of the savings is yet undetermined, it has been omitted from the weight analysis (Ref. 28). Another advantage to the use of adhesives is the utilization of the large interface between structural components without drilling holes and destroying the integrity of the structures.

Wing spars were located to pick up component loads, lifting forces, and to act as fuel tank barriers. A wing carry through box is included at the rear portion of the wing to help provide a smooth load redistribution into the reinforced fuselage frames. The number of ribs will be limited due to the utilization of fuel storage bladders in the wing. This results in unusually thick ribs to compensate for wing twist. The use of internal fuel bladders may prove critical due to the expansive characteristics of the wing. If the structures acted as fuel barriers also, leaks would undoubtedly become an issue. The wing skin has not been designed to be a load carrying member at this point of the design

stage. As a consequence, the skin thickness is dictated by the minimum required for riveting, which is 0.06 inches for most structures. A skin thickness of 0.07 inches is used on the Stingray wing. Stringers have not been incorporated into the design at this time, but will be utilized and placed once a more accurate analysis has been completed.

Wing spars are sized to resist bending and shear loads experienced at the critical design condition of a 2.5 g maneuver as determined by the V-N diagram. A typical section is composed of two caps, a web, and stiffeners and is sized to the maximum proportions above. A typical wing spar profile, rib profile and structural layout are included in Figure 7.3. The shear and moment diagrams for this particular spar are included in Figure 7.4 and Figure 7.5 on the following page.

# STINGRAY

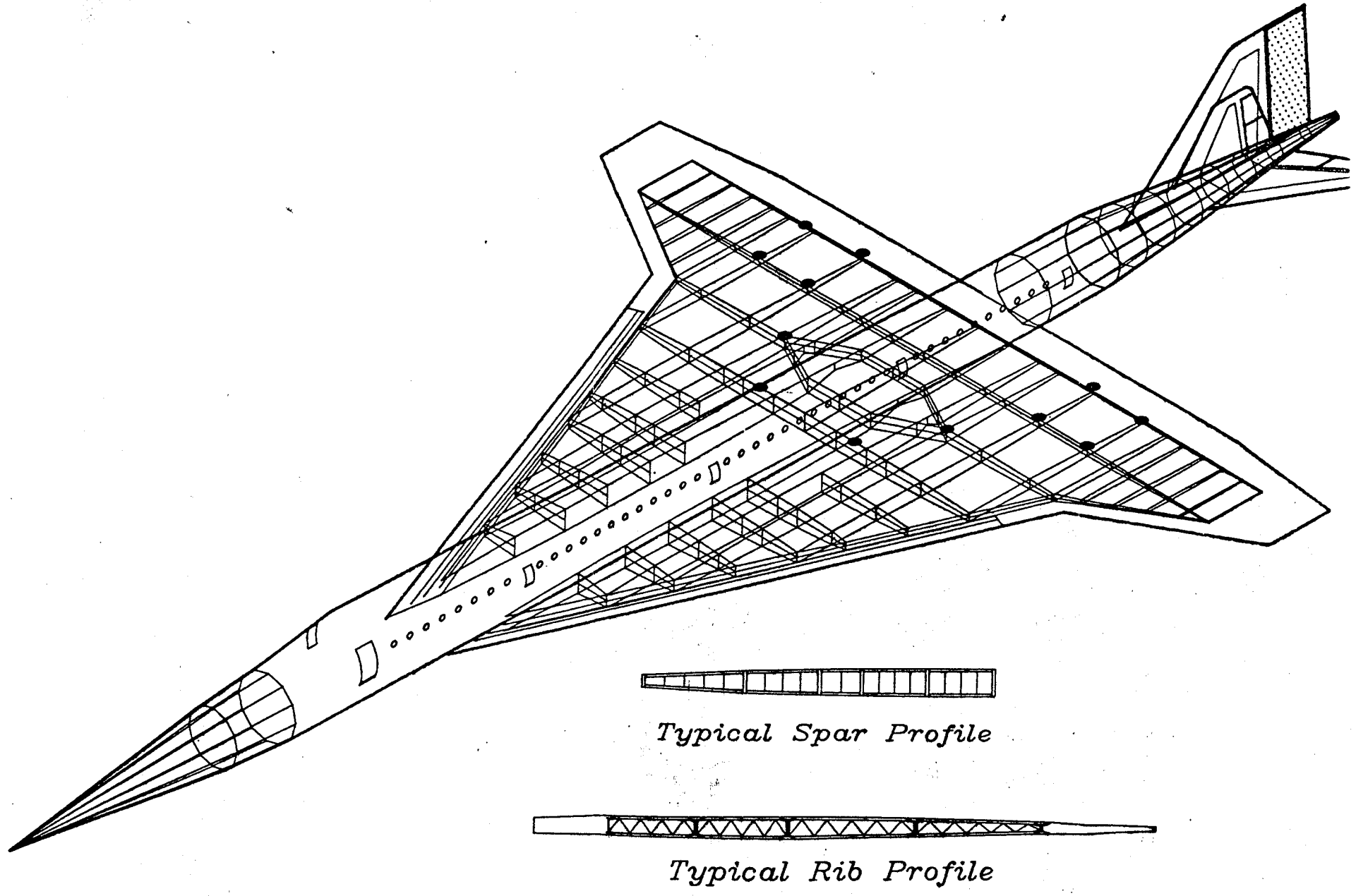


FIGURE 7.3 STINGRAY STRUCTURAL LAYOUT

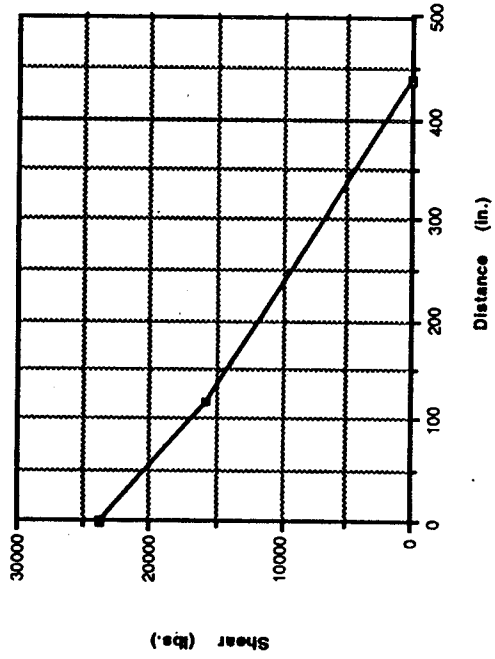


Figure 7.4 Shear Diagram

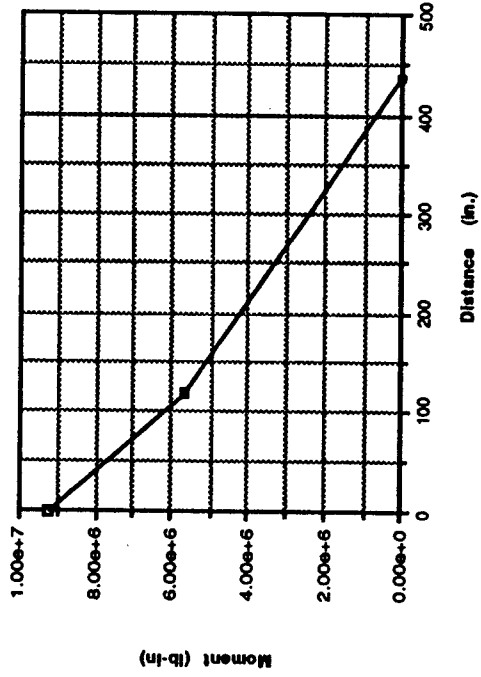


Figure 7.5 Moment Diagram

## 8.0 AERODYNAMICS

### 8.1 LIFT PREDICTION

The lift distribution for the Stingray was calculated using the NACA 65-206 airfoil data. The Stingray wing is designed to ensure a good aerodynamic performance for both subsonic and supersonic flights. The lift prediction for different flight conditions is shown in Table 8.1.

	$C_L$	$C_{L\alpha}$ (1/deg)
Subsonic Cruise	0.328	0.043
Supersonic Cruise	0.153	0.035
Take-Off	0.90	0.09
Landing	0.93	0.09

**Table 8.1** Stingray Lift Prediction for Different Flight Conditions

The maximum clean lift coefficient for the Stingray was calculated to be 0.47 at an angle of attack of 10.0 degrees. With a flap deflection of 25 degrees at takeoff,  $C_L$  increased to 0.90 with an angle of attack of 10.0 degrees. The reason for choosing an airfoil with camber is to provide the aircraft with extra lift. The result has proved it to be correct. Without the camber, the  $C_L$  at the same angle of attack would decreased by approximately 0.11. Although camber increases induced drag, this penalty is small compared to the lift benefits. The use of leading and trailing edge flaps also provides the aircraft with the necessary lift. Figure 8.1 shows the variation of aircraft  $C_L$  with flaps up and flaps down.

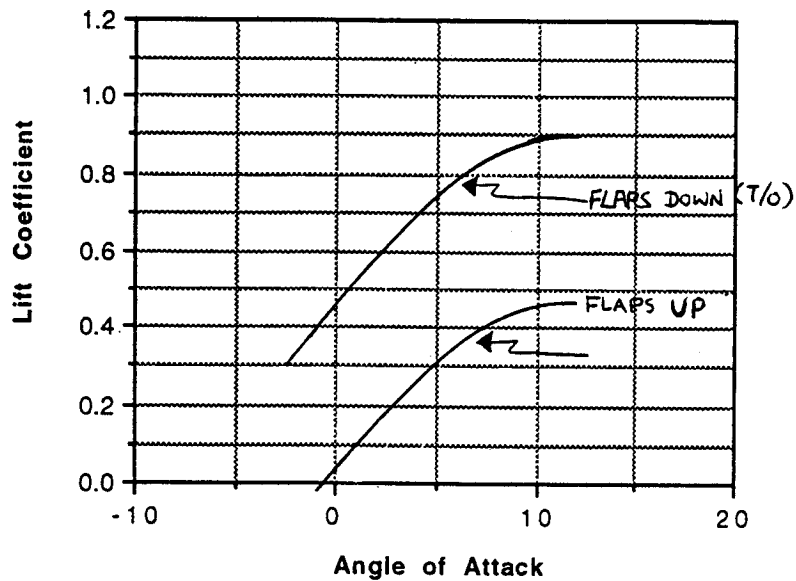


**Figure 8.1** Variation of Aircraft Lift Coefficient vs. Angle of Attack with Flaps Up and Flaps Down

## 8.2 DRAG PREDICTION

Drag polars were calculated for takeoff, landing, subsonic and supersonic cruise conditions. Zero lift drag was calculated using skin friction coefficients on each exposed surface of the aircraft, including flaps and landing gear. Because the Stingray spends most of its mission in supersonic flight, wave drag contributions were calculated using area ruling methods and the Sears-Haack area ruling distribution (Ref. 11).

In order to calculate the zero-lift drag (for all flight conditions), the aircraft was divided into components to be analyzed separately. Interference and form factors were calculated for each component as well. Base drag from the engine was neglected due to the jet exhaust plume. Since the aerodynamics of the Stingray are optimized for supersonic flight, a fineness ratio of 21.58 was used, minimizing the bluntness of the body.



Induced drag (or drag due to lift) was calculated in subsonic flight by using (Ref. 11). The Oswald span efficiency factor was calculated as a function of the aspect ratio and the sweep angle. Induced drag for supersonic flight was calculated by (Ref. 9) assuming a subsonic leading edge. This equation is a function of the inverse of the lift curve slope.

Wave drag in supersonic flight was analyzed by comparing the Stingray's area distribution to that of the Sears-Haack body. Ref. 11 provided a method to calculate the wave drag as a function of maximum cross-sectional area, the length and the Mach number. An area distribution plot was made over the length of the aircraft and a maximum cross-sectional area of 279 ft<sup>2</sup> was used in the wave drag calculation. The wave drag contribution to total drag in supersonic flight, therefore, is minimal.

Figure 8.2 shows the drag contributions in both supersonic and subsonic cruise. Figures 8.3 and 8.4 show the drag polar curves for takeoff, landing, subsonic cruise and supersonic cruise. The lift-to-drag ratio (L/D) for supersonic cruise was calculated at an average weight of 582,000 lbs and was found to be 9.77. The subsonic cruise L/D was found at an average weight of 700,000 lbs and was calculated as 15.1. These are average values calculated at average weights for each flight condition. Although no improvements were assumed in these calculations, L/D values will improve as wing optimization factors are accounted for. Since L/D values play a crucial role in range, weight, and fuel consumption, improvement in this area will increase mission range, decrease aircraft weight, and lessen the amount of fuel necessary per mission.

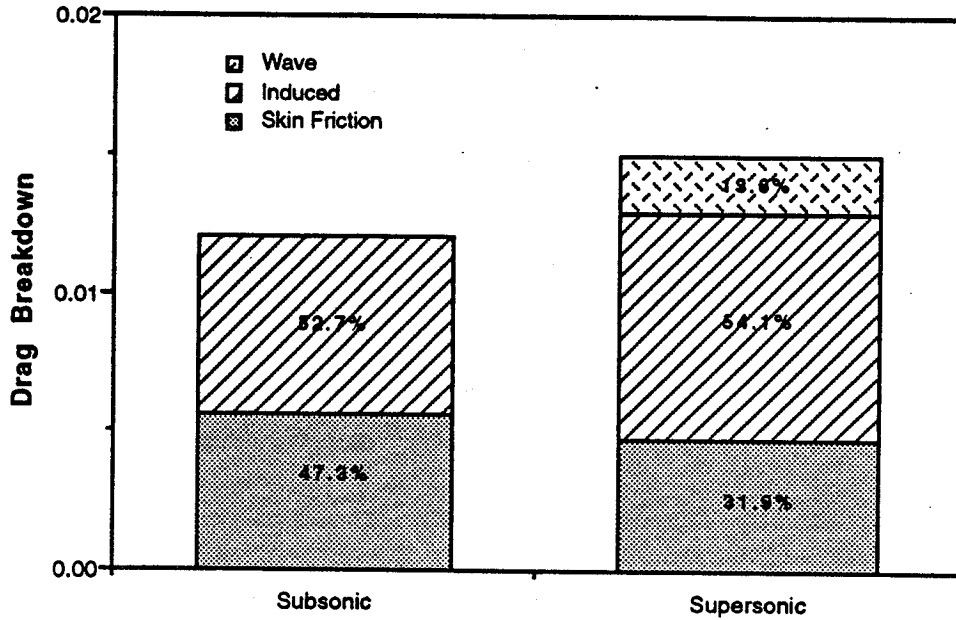


Figure 8.2 Stingray Drag Breakdown

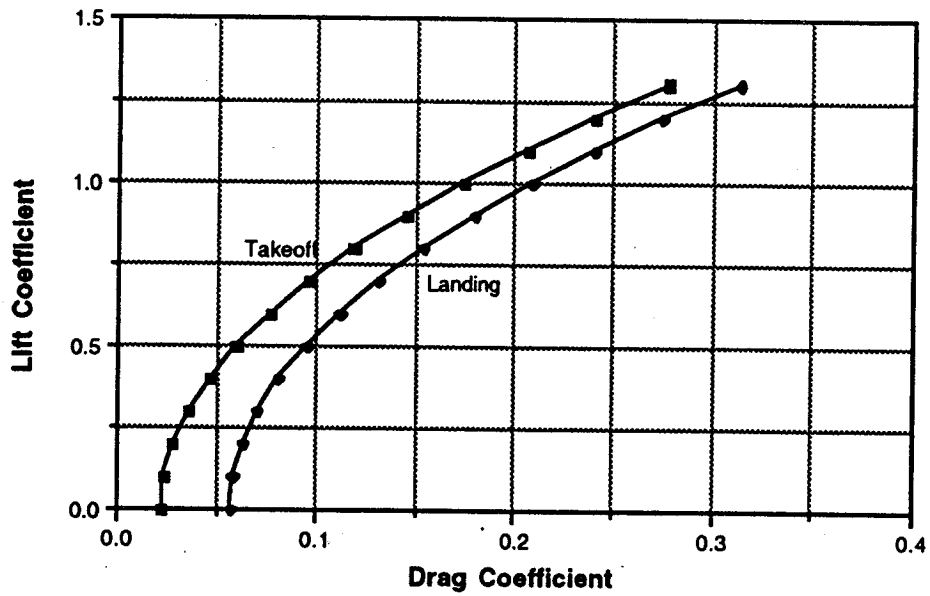


Figure 8.3 Stingray Takeoff and Landing Drag Polars

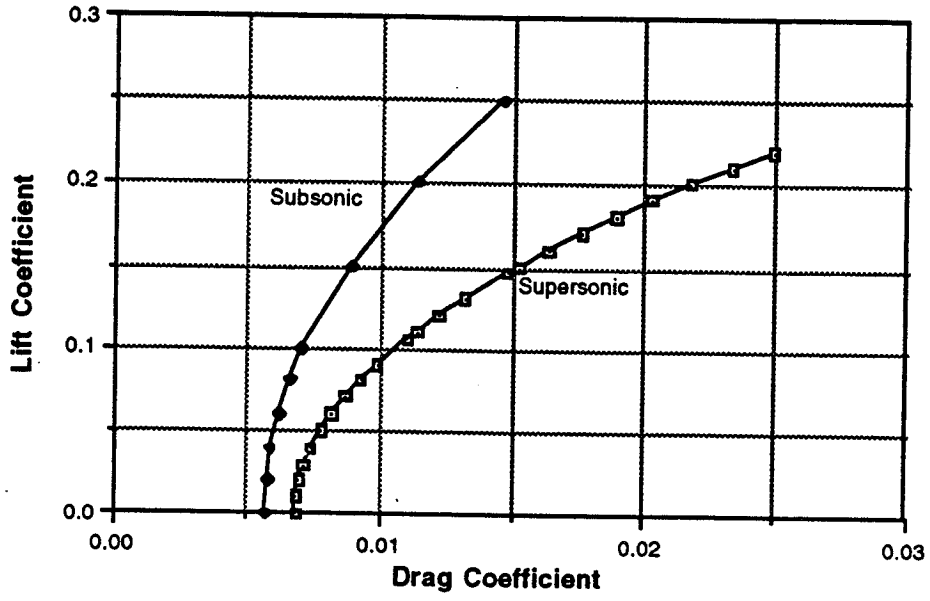


Figure 8.4 Stingray Cruise Drag Polars

## **9.0 PERFORMANCE**

### **9.1 TAKEOFF AND LANDING PERFORMANCE**

The Stingray is designed to takeoff and land in conventional airports, allowing considerable compatibility with current international facilities. The mission specifications require that the Stingray be able to takeoff and land on a 12,000 foot runway. The takeoff and landing distances were calculated using the method of (Ref. 11). The total takeoff distance was calculated to be 9800 ft. The decision point length was calculated using (Ref. 7), with a distance of 6600 ft. resulting.

The landing distance was calculated using a similar method to takeoff. The landing distance was calculated component-wise by analyzing the approach, flare, free roll, braking with thrust reversers and braking with no thrust reversers. The total landing distance was found to be 7800 ft. on dry asphalt.

### **9.2 CLIMB PERFORMANCE**

Climb performance is specified by the FAR 25 regulations. As dictated by FAR requirements for one engine out, the climb gradient for liftoff must be 0.005 radians per second with a second segment climb gradient of 0.03. The Stingray meets these requirements easily. The height achieved by the Stingray at the end of the runway is 184 ft, easily clearing the 35 ft obstacle. The takeoff and second segment climb gradients are 0.16, a full 13% above the FAR requirements. The rate of climb with one engine out is 2900 feet per minute, more than adequate performance in an emergency.

The flight ceiling was specified by the FAR 25 requirements. For subsonic flight, the rate of climb must be 300 fpm. This corresponds to a flight service ceiling of 45,000 ft. The rate of climb at 30,000 ft., where the Stingray

will climb to, is 1154 fpm, well within the FAR requirements. The supersonic flight ceiling corresponds to a rate of climb of 1000 fpm. Since the Stingray is accelerating at constant Mach number (not velocity), the Stingray's rate of climb will be well within FAR requirements for any potential climb condition. Figure 9.2 plots the subsonic rate of climb and flight ceiling (supersonic rate of climb is not displayed since it is of no concern).

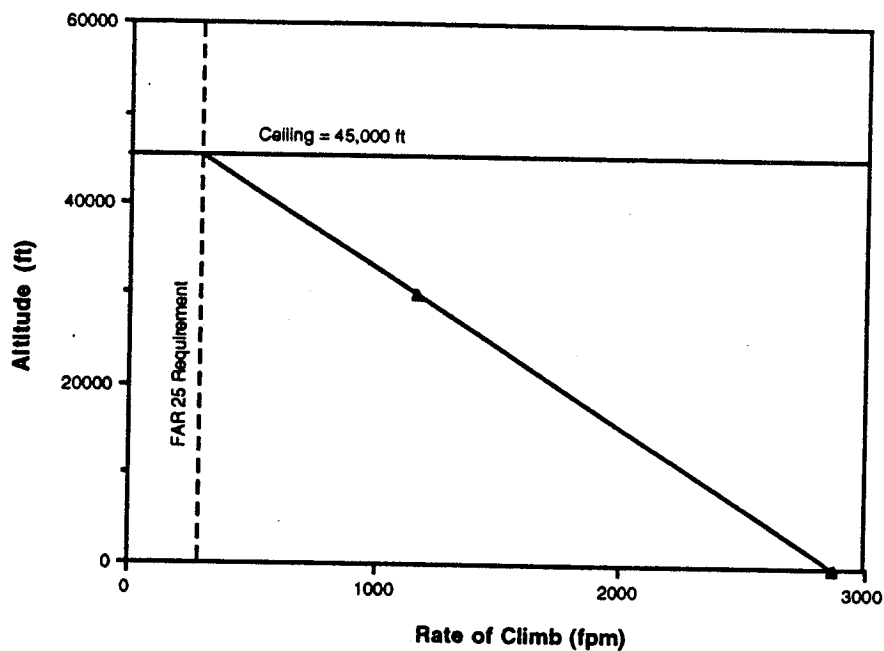


**Figure 9.2** Stingray Flight Ceiling

### 9.3 RANGE-PAYLOAD

The range for the Stingray was set by the mission specifications to be 5200 nautical miles. By using the Breguet range equation found in (Ref. 7), the range of the Stingray was found to be 5400 nautical miles. Figure 9.3 presents the range payload diagram.

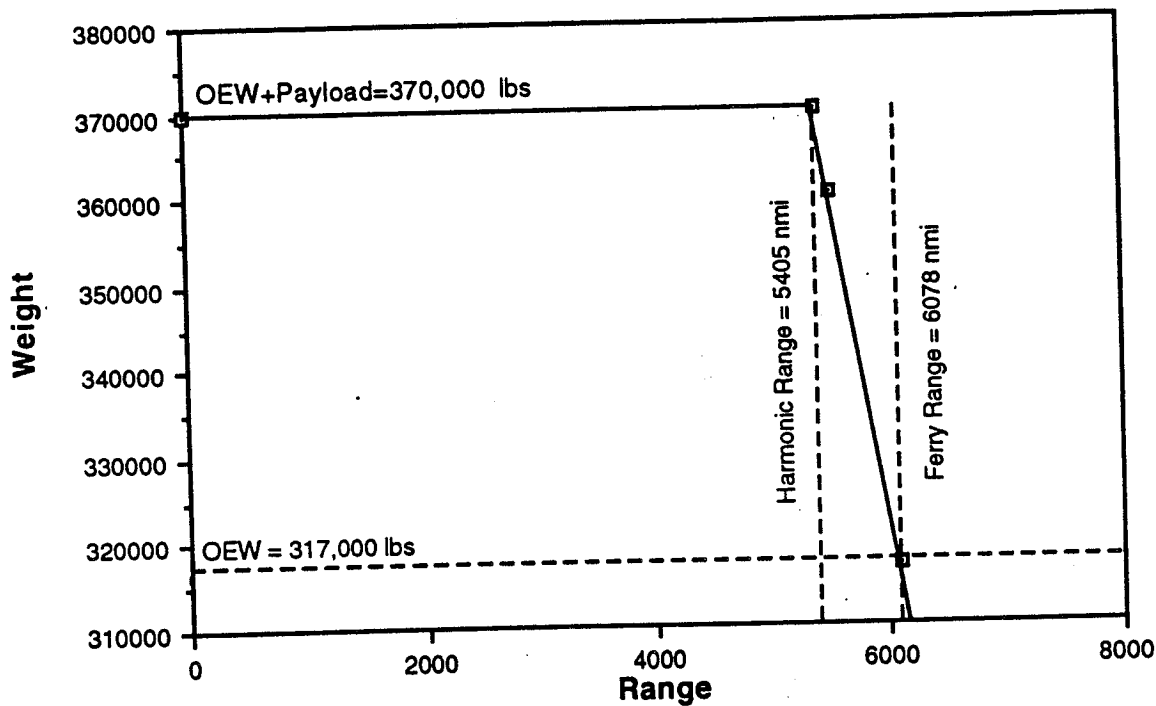


**Figure 9.3** Stingray Range-Payload Diagram

The harmonic range (or maximum payload) of the Stingray was found to be a maximum of 5404 nautical miles (point B). This is the range computed with no tradeoff between fuel and payload. The range using the maximum fuel capacity (point C) was 5511 nmi. This requires a loss of 48 passengers; a tradeoff not economically feasible. The ferry range (point D), with no passengers and maximum fuel, was 6078 nmi. Therefore, the Stingray will easily make its required range without sacrificing any passenger payload.

## 10 STABILITY AND CONTROL

### 10.1 WEIGHT AND BALANCE

The weight and balance was accomplished by methods described in Ref. 5 and Ref. 9. The aircraft was divided into several groups, each shown in Figure 10.1, containing specific components of the aircraft.

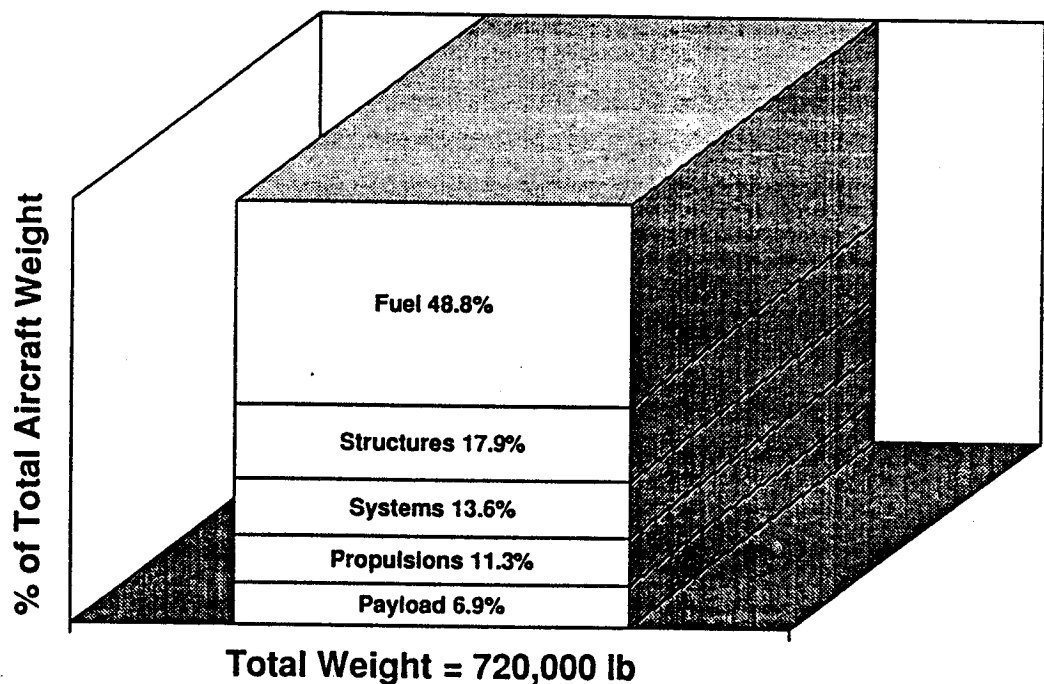


**Figure 10.1 Weight Breakdown**

Each component was placed on the aircraft and assigned a weight and a set of coordinates relative to an absolute zero. The weights assigned to each component were either calculated using the equations in (Ref. 7, 9) or assigned based on empirical data. The weight of each component and the moments created by it were then summed to give the weight and balance characteristics of the aircraft. The final aircraft configuration weights are given in Table 10.1.

Empty Weight (EW)	310,000 lbf	43%
Operating Empty Weight (OEW)	320,000 lbf	44%
Zero Fuel Weight	370,000 lbf	51%
Gross Takeoff Weight (GWTO)	720,000 lbf	100%

**Table 10.1 Aircraft Weights**

## 10.2 CG EXCURSION

The center of gravity (CG) for the aircraft were calculated by taking the sum of the moments created by each aircraft component about a reference point. These total moment were then divided by the aircraft gross takeoff weight to yield the aircraft center of gravity. The center of gravity for each axis was calculated. Because the aircraft is symmetric and has a conventional layout the center of gravity of the Y axis (roll) is right down the centerline of the aircraft. The center of gravity of the Z axis (yaw) fell very close to the wing center in that axis. The most important center of gravity is that of the longitudinal axis. Some of the constraints that restrict the center of gravity are stability and control, and landing gear position. FAR 25 longitudinal tipover criterion restricted the aft most position of the center of gravity to a 40 degree angle relative to the main landing gear. The four truck longitudinally spread landing gear helps to relax that requirement by moving the critical point aft. The nose gear location also limits the CG envelope of the aircraft on the ground. The CG cannot be too far forward or the static and dynamic loads on the nose wheel require a heavier gear and additional weight in the structure of the fuselage. The CG cannot be shifted back too far or the nose wheel may lose steering authority during taxi, takeoff, or landing. Care must be taken to ensure that the aircraft can be moved around while it is empty and that the aircraft can be loaded in the proper order without tipping over or overloading any of the struts.



This aircraft, with its long slender fuselage and highly swept delta wing provided a great deal of flexibility in loading to provide an optimum CG envelope. Because there are several wing fuel tanks located in various areas of the wing, fuel can be pumped from one tank to the others to control the center of gravity.

The CG excursion diagram, Figure 10.2, shows the center of gravity envelope for the Stingray. The outer solid lines show the maximum CG shifts for the aircraft full of passengers. The forward CG path, shown in figure 10.3, was calculated by subtracting fuel from tank 1 and 2 first, while the aft CG path was calculated by subtracting the fuel from tank 7 first. The vertical dotted lines represent the subsonic neutral point (35%) and the supersonic neutral point (39%). The CG envelope brackets these points nicely, indicating that the fuel management systems can control the C.G. such that the trim drag can be minimized during cruise flight.

The best CG travel history during flight falls inside the envelope defined in figure 10.3. The aircraft begins at the OEW and travels along the straight line to the OEW+Fuel point as the aircraft is fueled. The addition of passengers moves the CG forward to GWTO. During the ground handling the aircraft CG is close to the front main gear but doesn't get close to the rotation point halfway between the main gear locations. If the fuel management system should fail while the aircraft is being fueled the aircraft may get very close to the aft tipover point. The aircraft takes off with the CG at point (3) and the neutral point at the 35% line. The fuel is initially burned from tanks 1 and 2 during the climb, moving the CG forward. At point (5) the aircraft begins to accelerate from Mach .8 to Mach 2.4, causing a aft shift of the neutral point and requiring a aft movement of fuel to move the CG close to the 39% line. As the aircraft passes

point (7) the CG moves forward as it follows the aft CG path, burning fuel from tank 7. If no loiter or divert is required the aircraft lands at point (9).

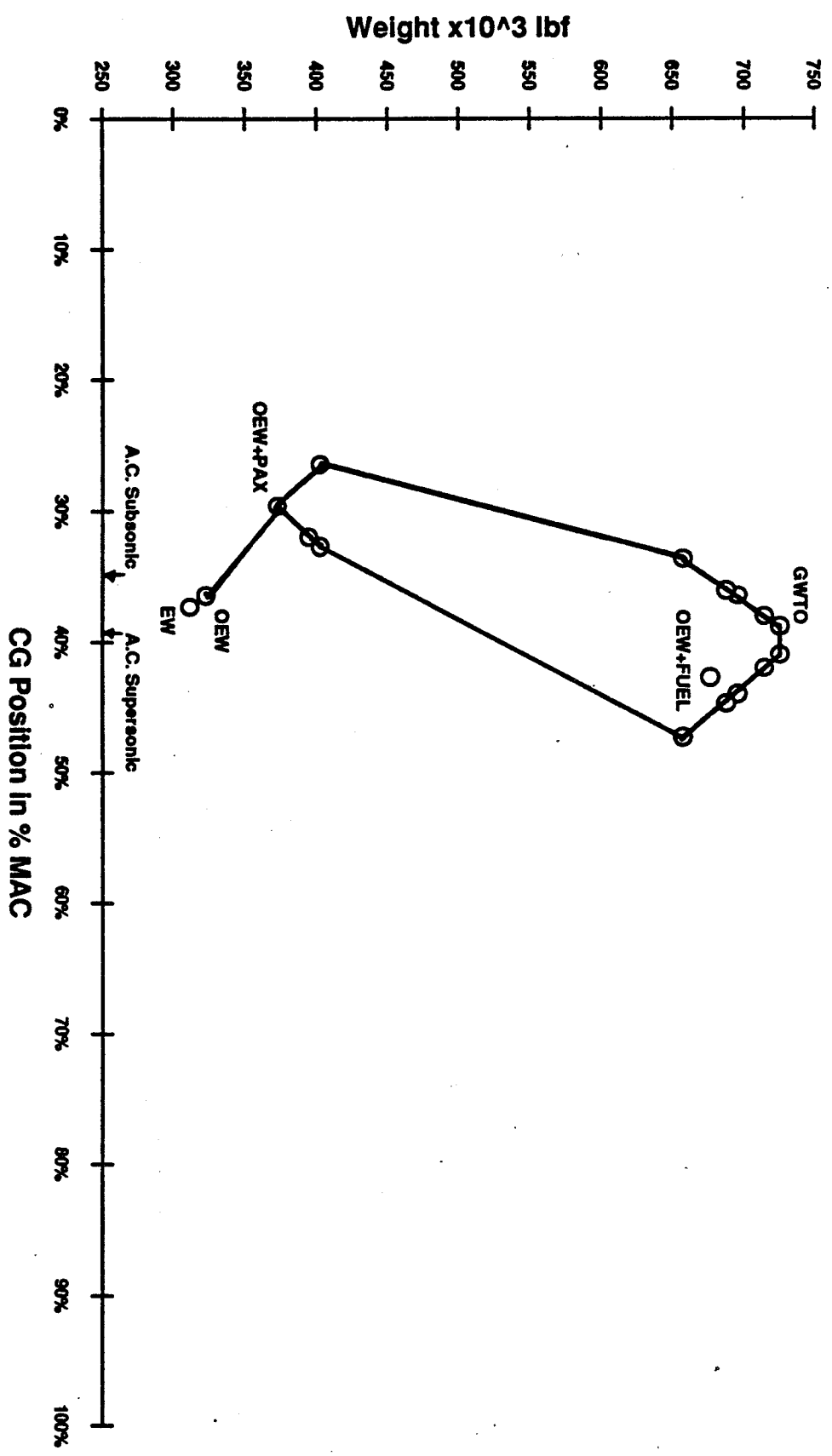


Figure 10.2 Stingray CG Excursion

### 10.3 MASS MOMENTS OF INERTIA

The moments of inertia of the aircraft were calculated using the mass properties of the components. These mass moments of inertia were calculated using formulas given in (Ref. 19). The components of the aircraft contributed a local moment of inertia due to their mass distribution and a moment of inertia due to their distance from the center of gravity of the aircraft. The contribution of each portion of the aircraft was calculated using equations from (Ref. 5) and summed to give the moments of inertia of the whole aircraft for several conditions. Because this is an extremely large aircraft, especially in the longitudinal axis, the moments of inertia are very large. The resulting numbers were slightly low when compared to the inertia's of existing aircraft. This deviation was most likely the result of the method of computation. The inclusion of additional local moments of inertia and more detailed weight analysis will improve the accuracy of the moments of inertia. The large magnitudes of the moments of inertia of this class of aircraft indicate a very low sensitivity to gusts, and slow response (frequency) to control inputs. This is typical of large transport aircraft.

## **10.4 LONGITUDINAL STABILITY AND CONTROL**

The longitudinal center of gravity plays a major roll in the longitudinal stability and control of the aircraft. great positive benefits in stability, control, and performance can be achieved with proper control of the CG. The aircraft begins its flight with a static margin of -3.5%. The horizontal tail is sized to provide adequate control power for takeoff rotation, and to provide positive lift and control during the subsonic climb portion of the flight. The negative static margin requires the lifting tail, which helps the climb performance of the aircraft. The aircraft will be restricted to taking off with the CG forward of the 39% line. The aircraft will be controllable at a static margin behind the 39% line but depending on the conditions the tail might become saturated with its lifting requirement and lose its ability to provide longitudinal control.

The aircraft will be placarded to restrict flight with the C.G. in the aft-most configurations. When the aircraft is supersonic the horizontal tail provides adequate control power for any possible CG position. The best CG position for supersonic cruise would be somewhere very close to the supersonic neutral point. This would result in neutral stability and allow the tail to be unloaded, improving cruise L/D. Studies have shown that commercial transports can gain a 3-4 percent fuel savings (Ref. 20) by using a relaxed stability airframe with a stability augmentation system. As the aircraft finishes its flight it becomes more positively stable.

### **10.4.1 LATERAL STABILITY AND CONTROL**

Lateral stability and control derivatives (Table 10.2) were calculated using Ref. 7. The numbers for the stability derivatives falls within reasonable range for those of comparable aircraft.

	M=0.3	M=0.8	M=2.4
Altitude	0	35000	60000
<b>Lateral</b>			
$C_{Lav}$	1.473	1.48	1.425
$C_{y\beta}$	-0.216	-0.216	-0.212
$C_{Lw}$	0.55	0.307	0.1356
$C_{n\beta}$	0.103	0.097	N/A
$C_{l\beta}$	N/A	N/A	N/A
$C_{nT\beta}$	N/A	N/A	N/A
$C_{y\beta}$	0.0113	0.0113	N/A
$C_{l\beta}$	2.29	2.29	N/A
$C_{n\beta}$	0.007	0.007	N/A
$C_{yp}$	-0.0167	-0.0167	N/A
$C_{np}$	0.155	0.0328	N/A
$C_{nq}$	0	0	N/A
$C_{yr}$	0.251	0.251	0.247
<b>Control</b>			
$C_{Dh}$	0	0	0
$C_{Lh}$	0.115	0.115	0.115
$C_{mh}$	-0.149	-0.155	-0.149
			-0.16
$C_{D\delta t}$	0	0	0
$C_{L\delta t}$	0.057	0.057	0.057
$C_{m\delta e}$	-0.074	-0.08	-0.074
			-0.08
$C_{y\delta a}$	0	0	0
$C_{l\delta a}$	0.078	0.078	0.078
$C_{n\delta a}$	-0.0013	-0.0013	-0.007
$C_{y\delta s}$	0	0	0
$C_{l\delta s}$	0.0029	0.0029	0.0029
$C_{n\delta s}$	0.0286	0.0286	0.0286
$C_{y\delta r}$	0.106	0.106	0.107
$C_{l\delta r}$	-0.0053	-0.0053	0.0036
$C_{n\delta r}$	0.0726	0.0726	0.0734

Table 10.2 Stingray Lateral Stability and Control Derivatives

#### 10.4.2 HANDLING QUALITIES AND AUGMENTATION

The negative static margin during the early portions of the flight and the degradation of the lateral directional handling qualities at high Mach numbers require stability augmentation system. Initial handling quality parameters (frequency, and damping ratios) showed that an unaugmented aircraft is controllable but requires excessive pilot workload (Class 3). The aircraft control surfaces along with the flight control system provide enough redundancy even with multiple actuator/surface failure.

The aircraft will takeoff with unstable, burn fuel in the climb, then cruise with the Center of Gravity as close to the aerodynamic center. Cruising with a static margin of zero causes  $C_{m\alpha}$  to approach zero, decreasing the longitudinal short period, decreasing the handling qualities. The horizontal surface is sized to provide adequate control authority to handle the instability and the neutrality during the supersonic cruise. A rough gain calculation taking into account the maximum negative static margin and the horizontal control power showed longitudinal stability augmentation to be possible ( $K_a=1.8 < 5$  deg/deg).

## 11.0 SYSTEMS LAYOUT

### 11.1 AVIONICS

All conduit running through the fuselage will utilize a "4-point" distribution, as illustrated in Figure 11.1. The purpose behind this is to avoid a complete catastrophic failure in the event a portion of the aircraft becomes inoperable.

A set of two independent, identical, advanced avionics computers, capable of being powered by any of the electrical power sources for maximum redundancy, will automatically control fuel management, stability augmentation, and pre-programmed flight path management (navigation). Each will utilize Integrated Flight and Propulsion Control (IFPC) for maximum fuel efficiency and be capable of Category IV, all weather landing. Each computer will be capable of handling all functions should the other fail.

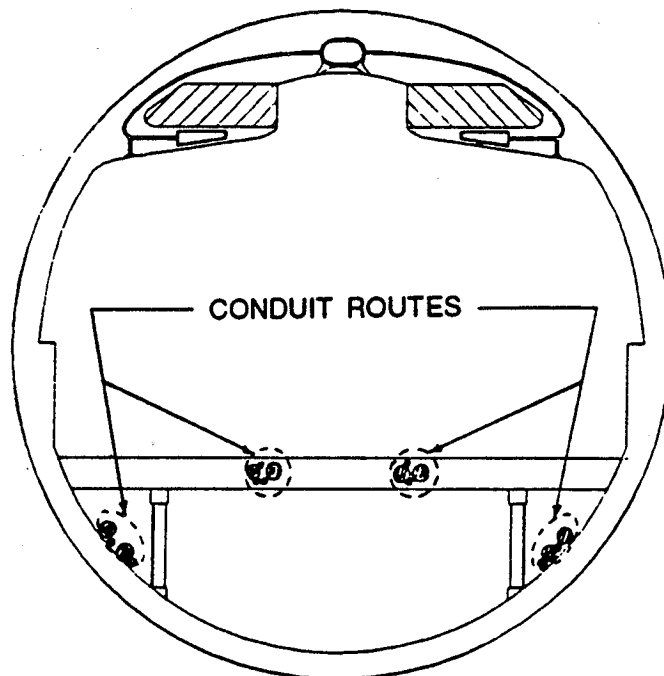


**Figure 11.1** Stingray Conduit Layout through a Fuselage Cross Section.



## 11.2 ELECTRICAL SYSTEM

A schematic of the electrical system is shown in Figure 11.2. The primary power generating system will be an AC generator at each engine. Secondary power from the auxiliary power unit (APU) and stored battery unit will act as standby power. Each engine source will power a separate electrical generator bus, allowing for four independent electrical sub-systems. The APU and battery unit will connect to each of the buses for maximum redundancy and the battery unit will be used to supply power to the APU starter. The generator buses will provide power for heavy loads. Branching from each generator bus is an AC bus, for light AC loads, and a DC bus, fed through a transformer/rectifier unit, for DC loads. Electrical power will be used to power exterior and interior lighting, flight control actuators, fuel pumps, avionics racks and heating elements for water and galleys.

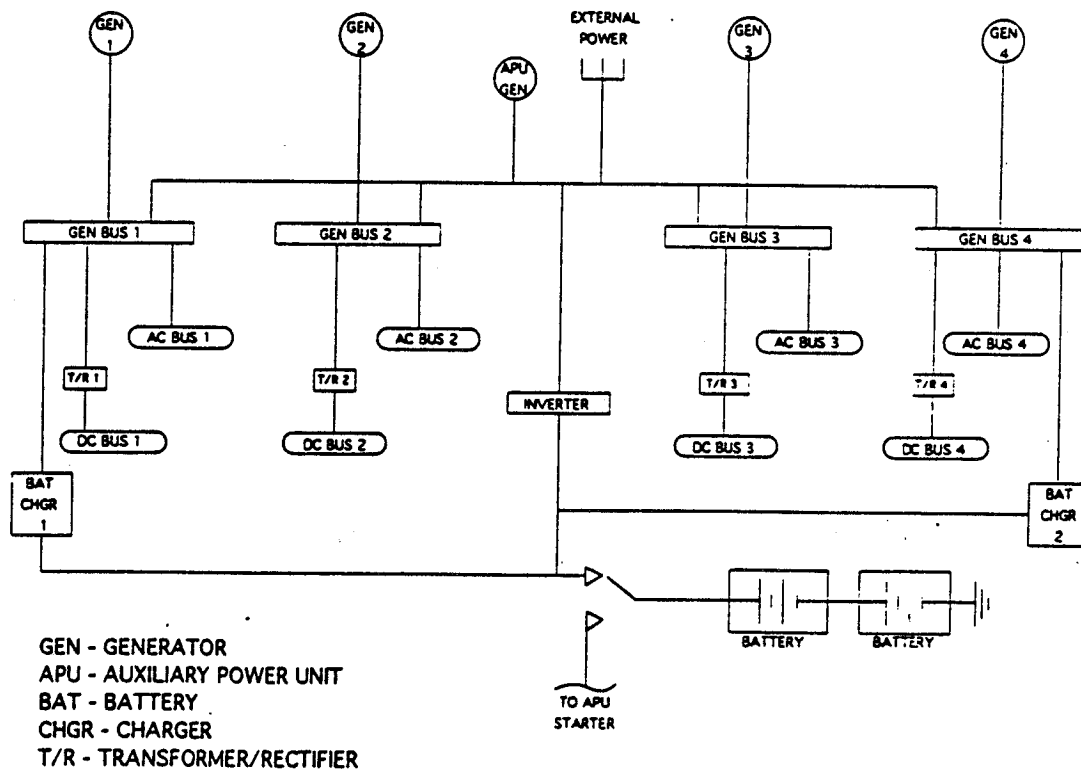


Figure 11.2 Stingray Electrical Schematic

## **11.3 PNEUMATIC SYSTEMS**

### **11.3.1 HIGH PRESSURE SYSTEM**

Figure 11.3 shows the layout of the high pressure air system. There is one independent air source from the APU in addition to an independent source from each engine, which allows for sufficient redundancy. These sources of high pressure air provide for the following:

- Ice protection - An anti-ice system is located on each engine cowl inlet, horizontal stabilizer leading edge, and wing leading edge slats. These systems would only be activated under subsonic icing conditions. Skin temperatures will prevent ice formation during supersonic flight.
- Air conditioning.
- Cabin pressurization - The cabin will be controlled automatically for an internal pressure equal to that at 7,500 ft. MSL, as required by FAR regulations. This system will contain sufficient fail-safe mechanisms to prevent adverse pressure conditions.
- Cargo heating.
- Fuel tank pressurization - Bleed air will provide pressurization to fuel tanks during flight at high altitudes.
- Potable water system pressurization.
- Cross engine starting - The engines are started using high pressure air. This gives the aircraft the capability to start any engine with another running engine and provides redundancy to the normal APU pneumatic source.

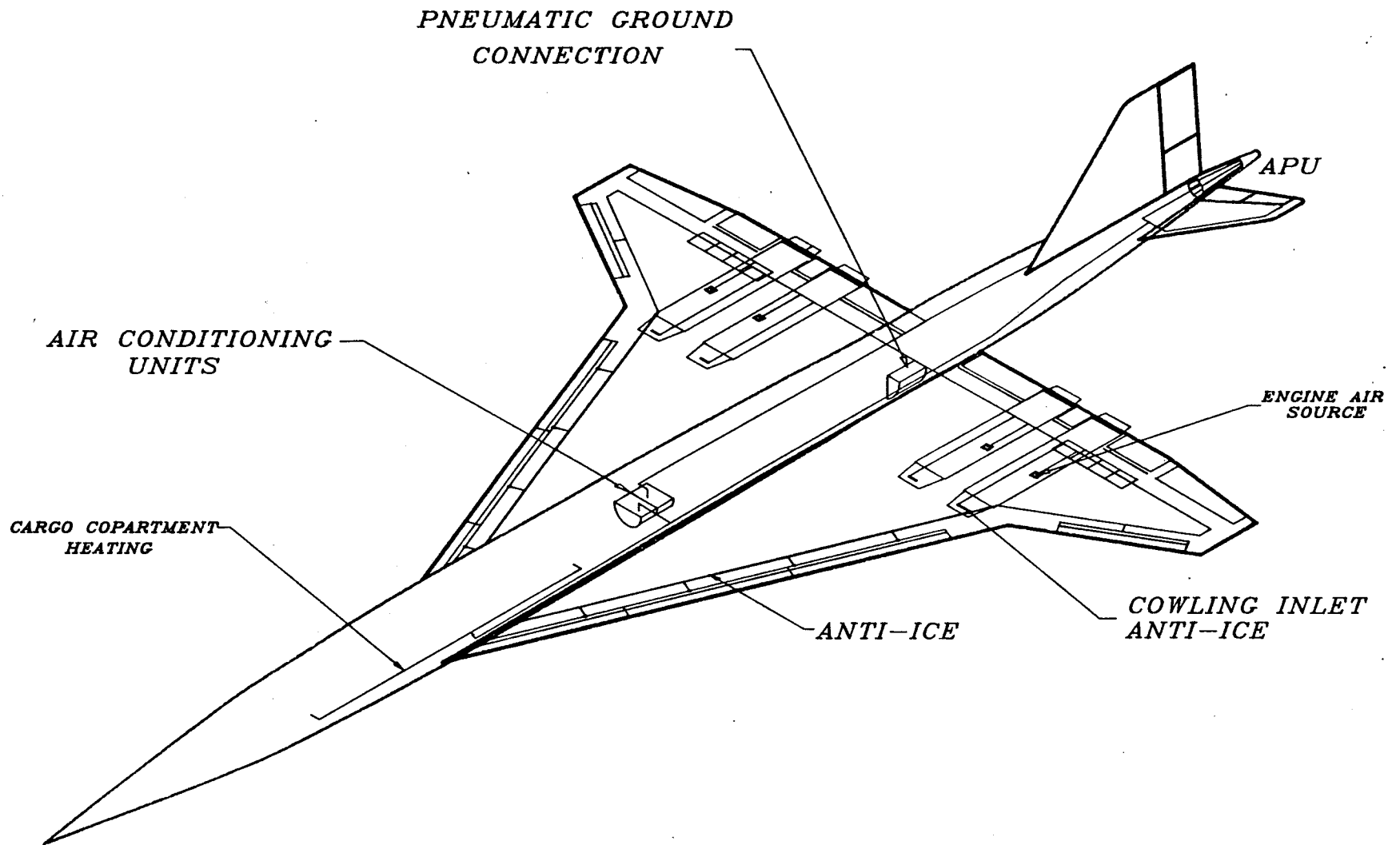


FIGURE 11.3 STINGRAY HIGH PRESSURE SYSTEM

### 11.3.2 AIR CONDITIONING SYSTEM

Figure 11.4 shows the layout of the major components of the air conditioning system. The general flow of air starts in the passenger cabin, moving laterally and into the lower fuselage, moving to the rear of the fuselage and exiting. Figure 11.5 illustrates a typical flow pattern in the fuselage cross-section. If there is a significant variance in temperature along the length of the passenger cabin due to aerodynamic heating, the cabin may be broken into separate temperature control zones. This ensures an even temperature distribution for passenger comfort. The lateral-flow nature of the cabin air circulation may localize the temperature variations but has the benefit of minimizing travel of odors and other air particulates.

The ratio of recirculated air to fresh air in the passenger cabin will be maintained at around 2 to 1. This is a reasonable ratio given the absence of smoking sections, which reduces the necessity for fresh air. A comfortable level of 20 cu. ft. per minute per crew member will be supplied to the flight deck, while the rest of the passenger cabin will be at a level of 15 cu. ft. per minute per passenger. Though passengers could be comfortable with as low as about 8 cu. ft. per minute, it is believed the former value is necessary to provide adequate cooling of the air due to the supersonic fuselage skin temperatures.

In addition to being fed cabin air from above, the cargo compartment will receive its own cool-air supply due to excessive aircraft skin temperatures in supersonic flight.

Separate, redundant cooling is supplied to the electrical/electronic equipment racks and avionics due to the criticality of keeping them at reasonable temperatures.

The galleys and lavatories will each be ventilated and the air immediately exhausted from the aircraft along with the cargo compartment, electrical equipment, and avionics air.

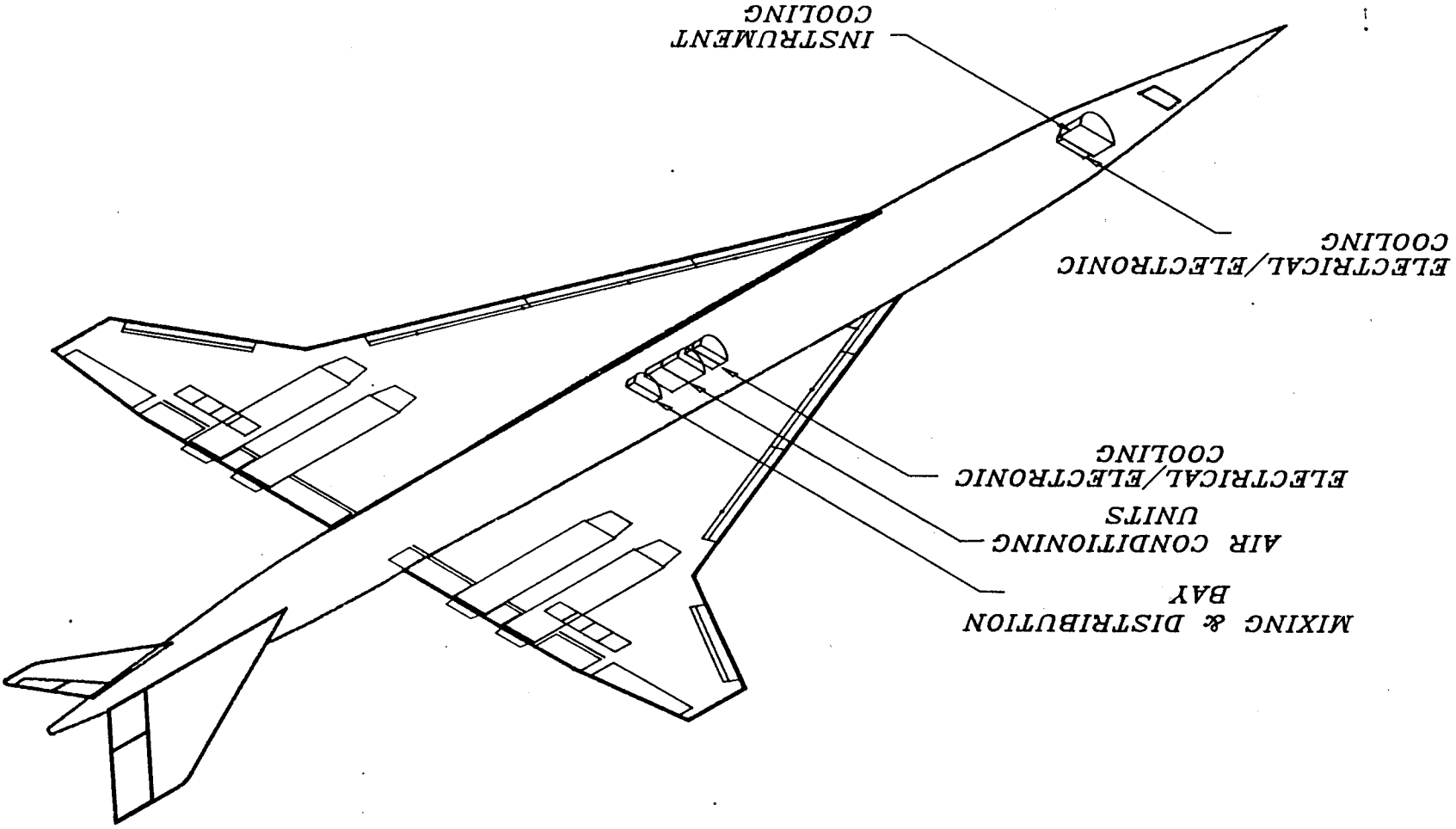
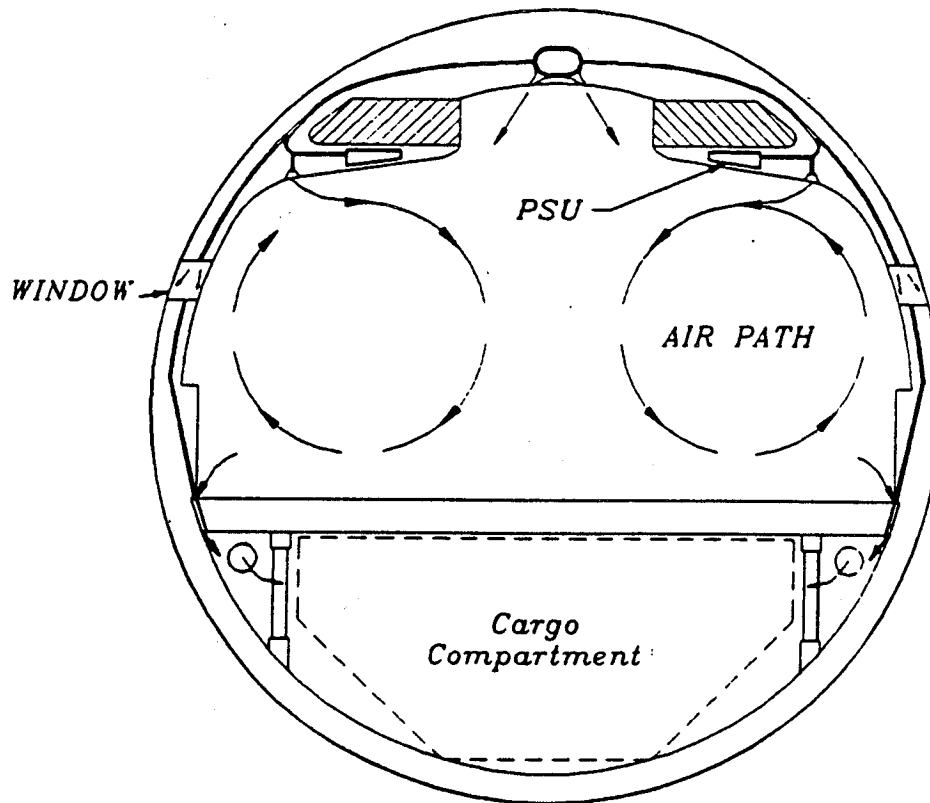


FIGURE 11.4 MAJOR COMPONENTS OF STINGRAY AIR CONDITIONING SYSTEM

Because of the use of the wing box in the fuselage as a center fuel tank, it is necessary by FAR Requirements to maintain a fume-proof enclosure around this tank at all times. Due to the natural pressure gradient between the passenger cabin and the lower half of the fuselage, and the fuselage's rearward airflow during pressurization, this requirement will be satisfied. If there is a loss of cabin pressure or when the aircraft is loading or unloading passengers and/or cargo at a terminal, the necessary rearward airflow will be provided by suction fans at the air system exhaust port.

Due to the amount of cooling expected to be needed from the air conditioning packs, this exhaust air will be utilized by the heat exchangers to carry the heat generated from cooling the air out of the aircraft.



**Figure 11.5** Stingray Cabin Air Circulation

## 11.4 FUEL SYSTEM

The fuel system layout is shown in Figure 11.6. Using the smallest number of fuel tanks minimized weight and cost, yet redundancy and safety are still maintained for an effective fuel management system. For example, dry bays are located near any critical areas such as landing gear wells and engine struts.

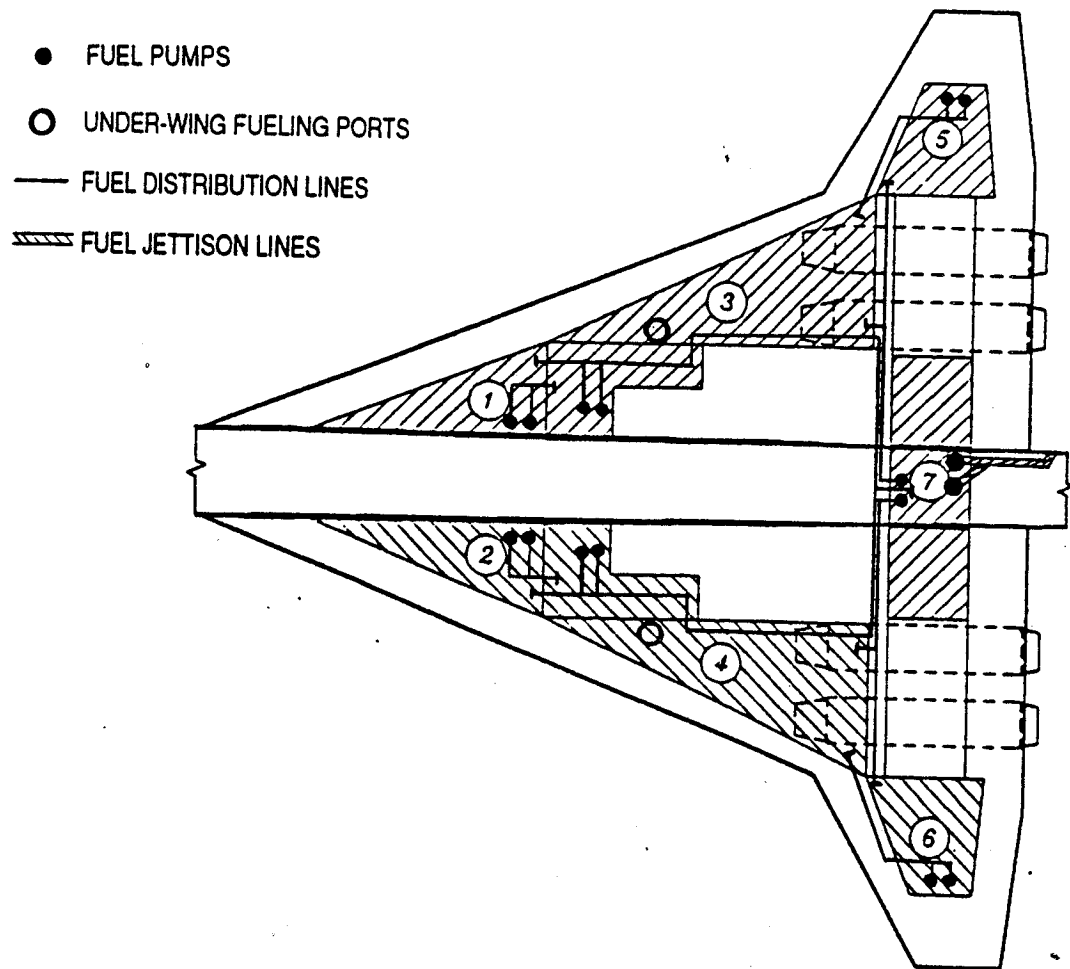


**Figure 11.6** Stingray Fuel System Layout

The Stingray will use conventional Jet-A fuel. The supersonic cruise flight temperatures encountered are well below those that might pose a hazard



to this type of fuel. Thus, the use of exotic fuels is avoided, increasing the Stingray's compatibility into today's market.

A sumping system will provide drainage and automatically remove condensed water from the tanks.

A venting system will prevent overpressurization in the tanks, utilizing surge tanks to collect and condense overflow fuel vapor. A source to each tank from the high pressure air system will provide pressurization during high altitude flight. For redundancy, there will be two fuel pumps in each tank, with no two from the same tank being run by the same electrical source.

Distribution lines will be run to each tank to enable fueling/defueling to be performed from fueling ports on the underside of the wing. It is assumed fuel will be fed from an underground source, eliminating interference with service vehicles. However, access to the ports by fuel vehicles is still possible. The fueling system will be pressurized, increasing fueling efficiency.

A fuel jettison system is integrated into the fuel management system if the need to land arises when the aircraft weighs more than the allowable landing or ramp weight.

## **11.5 ESCAPE SYSTEM**

In addition to the boarding and service exits, emergency doors will be located as indicated in Figure 11.7 to provide passenger egress in emergency situations.

Raft slides will be incorporated into the exits not over the wing. Figure 11.8 illustrates a similar type of raft slide used on the Boeing 767. Additional auxiliary life rafts will be stored in the cabin. For overwing exits, a slide will be stored on each side of the fuselage near the trailing edge of the wing. It will

automatically deploy if any emergency exit on the same side of the fuselage is opened.

A life jacket will be located under each passenger and attendant seat, as well as with each flight deck seat.

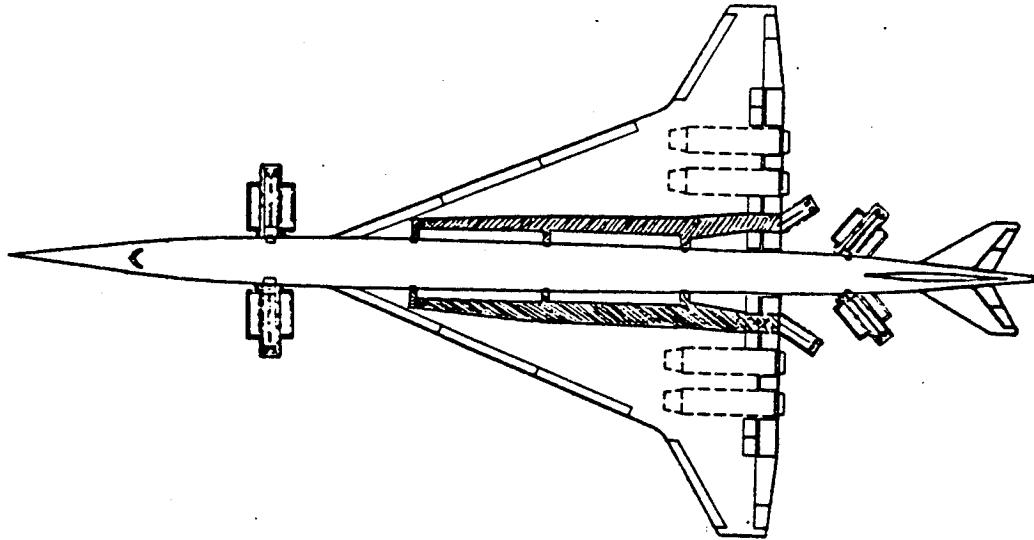


**Figure 11.7** Stingray Emergency Escape System

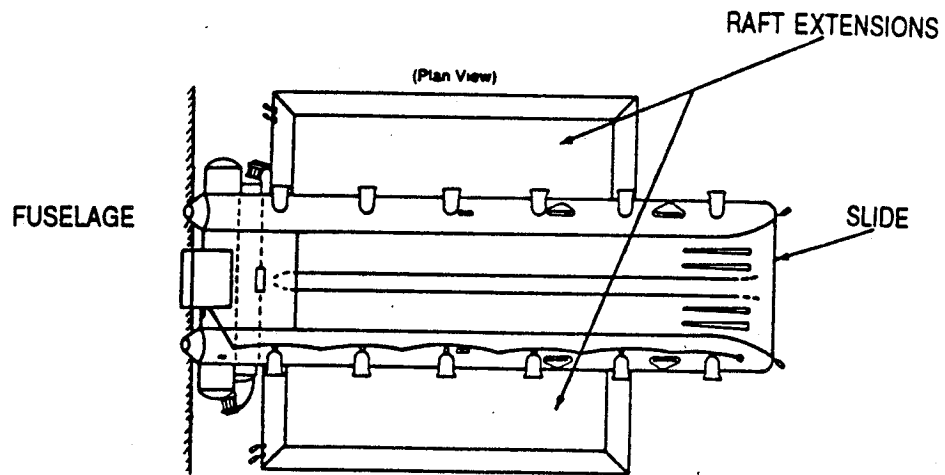


**Figure 11.8** Raft/Slide System. (Ref. 4)

## 11.6 OPTICAL SIGNALING SYSTEM

Signalling between the flight controls and the flight control actuators will be enacted using a "fly-by-light" system, or fiber-optic cables. Using an optical "fly-by-light" system over an electrical "fly-by-wire" system has several benefits. Glass fiber-optic cable provides a weight savings over metallic electrical wiring. Optical cable is also not susceptible to the electromagnetic effects of lightning strike or other electrical wiring. This is a very significant contribution by the "fly-by-light" system due to the sensitive tolerance of a flight control signalling system.

## 11.7 OXYGEN SYSTEM

In the event of failure of the cabin pressurization system, emergency oxygen is available (Figure 11.9), either activated automatically by the sudden pressure loss or manually by a crew member in the flight deck. Gaseous oxygen is supplied via oronasal masks to each crew member in the flight deck. Each passenger and flight attendant seat is supplied with oxygen, via an oronasal mask from the overhead passenger service unit (PSU), from a chemical oxygen generator (Figure 11.10). An additional mask is available at each row in case of another mask's (or even a generator's) failure. This is standard on present commercial transports such as the Boeing 737 and 767. Two oxygen masks are also provided in each lavatory. Portable oxygen cylinders will be available at various locations for purposes requiring first aid or oxygen mobility.

Although a chemical oxygen generator system weighs more than a gaseous oxygen system, the generator system provides a larger number of benefits. Only those generators whose masks are needed are used, the servicing of high pressure passenger oxygen bottles is eliminated, and

maintenance of the passenger system is reduced because of easy access, no bottle regulators or valves to leak, and the generators' 12-year shelf life. Therefore, this system should require less cost overall.

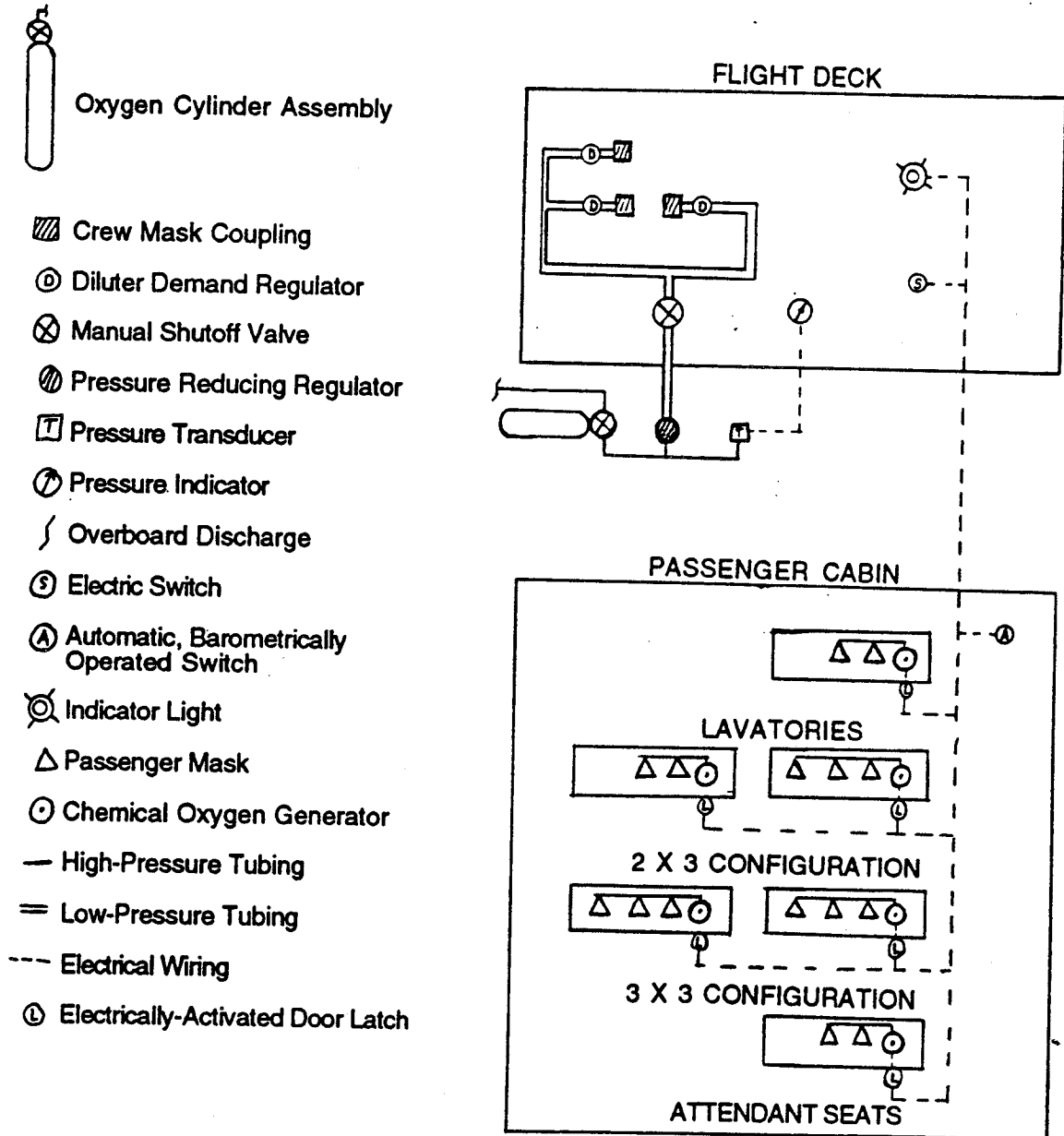
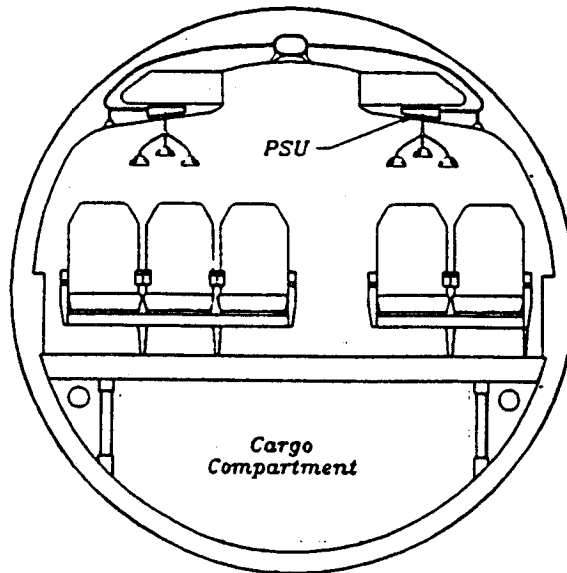


Figure 11.9 Schematic of Stingray Oxygen System



**Figure 11.10** Stingray Passenger Cabin Oxygen System

### **11.8 POTABLE WATER SYSTEM**

The pressurized water system is powered by bleed air from the high pressure air system. Water will be provided to each galley and lavatory. Warm water will be available by using electrically heated heat exchangers near each warm water faucet. Drain water from faucets will exit the aircraft through drain masts:

### **11.9 WASTE SYSTEM**

The self-contained waste system will be powered by vacuum flushing, using the in-flight pressure differential. This eliminates the need for gravity plumbing and assists in ventilation and odor control in the lavatories. Vacuum waste is stored in waste tanks located in the lower fuselage, outside of the passenger cabin, to prevent odor problems. Ventilation is provided to the waste tanks using the same pressure differential. Solid waste is prevented from entering the vent tubes by a water separator. When no significant pressure differential exists, blowers will be activated to prevent any "backdrafts".

## 12.0 AIRPORT OPERATION AND MAINTENANCE

The Stingray is designed to be compatible with existing ground handling equipment with minimum modification. Figure 12.1 shows how airport vehicles can service the aircraft concurrently. This will provide a one-hour turnaround time.

Galley access doors are located such that the wing will not interfere with servicing. Two galley trucks will service the first class and business class galleys. Another service truck will load the rear galley (in economy class) using a rear galley servicing door. Current galley trucks will be compatible with the Stingray.

A secondary boarding door at the rear of the aircraft will also double as a cleaning service door. This door will be used as a boarding door in airports where terminals are not available and passengers will board from the tarmac. In airports with terminals, this door will serve as an access door for cleaning services.

The main boarding door is located forward of the wing and is less than 17.6 feet above the tarmac. This will enable the Stingray to be compatible with all current terminals serving the Boeing 747-400. First class will board the airplane first, followed by business and economy classes.

Cargo trucks and conveyer belt will be used for loading the cargo bay. The cargo bay will handle 18 LDW containers, with 9 containers being loaded forward and 9 containers loaded aft of the loading door. There is only one cargo loading door since additional ones would cause structural problems due to the "breaks" in the fuselage.

Lavatory service will be performed by one truck located under the fuselage. Since the fuselage belly is 14 feet off the ground, a service truck will be able to fit under the fuselage without interfering with other service trucks.

Fuel loading receptacles are located on the underside of the wing. Due to the high fuel volume of the Stingray, two fuel trucks will load fuel into the aircraft simultaneously. This will cut turnaround time in half.

Potable water tank location under the wing will not interfere with other vehicles.

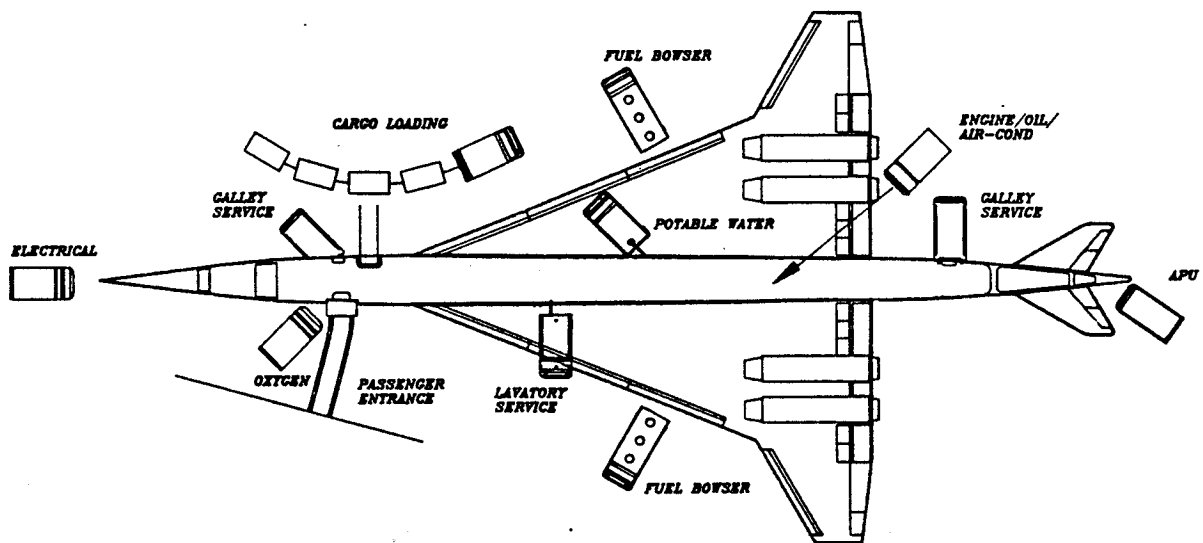


**Figure 12.1** Airport Ground Handling

### 13. MANUFACTURING

The final assembly will occur as outlined in Figure (13.1). The wing will be an independent structure and include a carry through wing box at the rear. Internal fuel bladders will be installed into the wing during the wing construction process. Since wing ribs will continue through the fuel cells, the fuel bladders will have to be composed of a material that can be applied in a liquid or gel form that will cure to the desired properties (similar to silicon gasket sealant or generic roofing tar). It will have to be applied near the end of the wing construction process. Since the wing is the largest independent component, the rest of the assembly process will have to be conducted around the wing.

The fuselage center sections will be mated to the wing structure. Fairing will then be added to provide a smooth aerodynamic interface. The fuselage fore and aft of the wing will be composed of two smaller sections each. Systems will be added during the construction process. The forward portion of the nose assembly will include the cockpit and certain avionics systems. The rudder and horizontal stabilizer will be mounted onto the most aft section after it has been attached to the rest of the fuselage assembly. Control surfaces, engines, and landing gear will then be attached to the wing body to complete the aircraft assembly. The interface between aluminum and titanium sections will have to be specially treated to reduce heat transfer and excessive stress buildup. Once again, silicon sealant is a potential candidate material to satisfy these needs.

Components will be designed to allow for construction in different areas or factories and final assembly to be completed wherever economic concerns dictate.



# STINGRAY

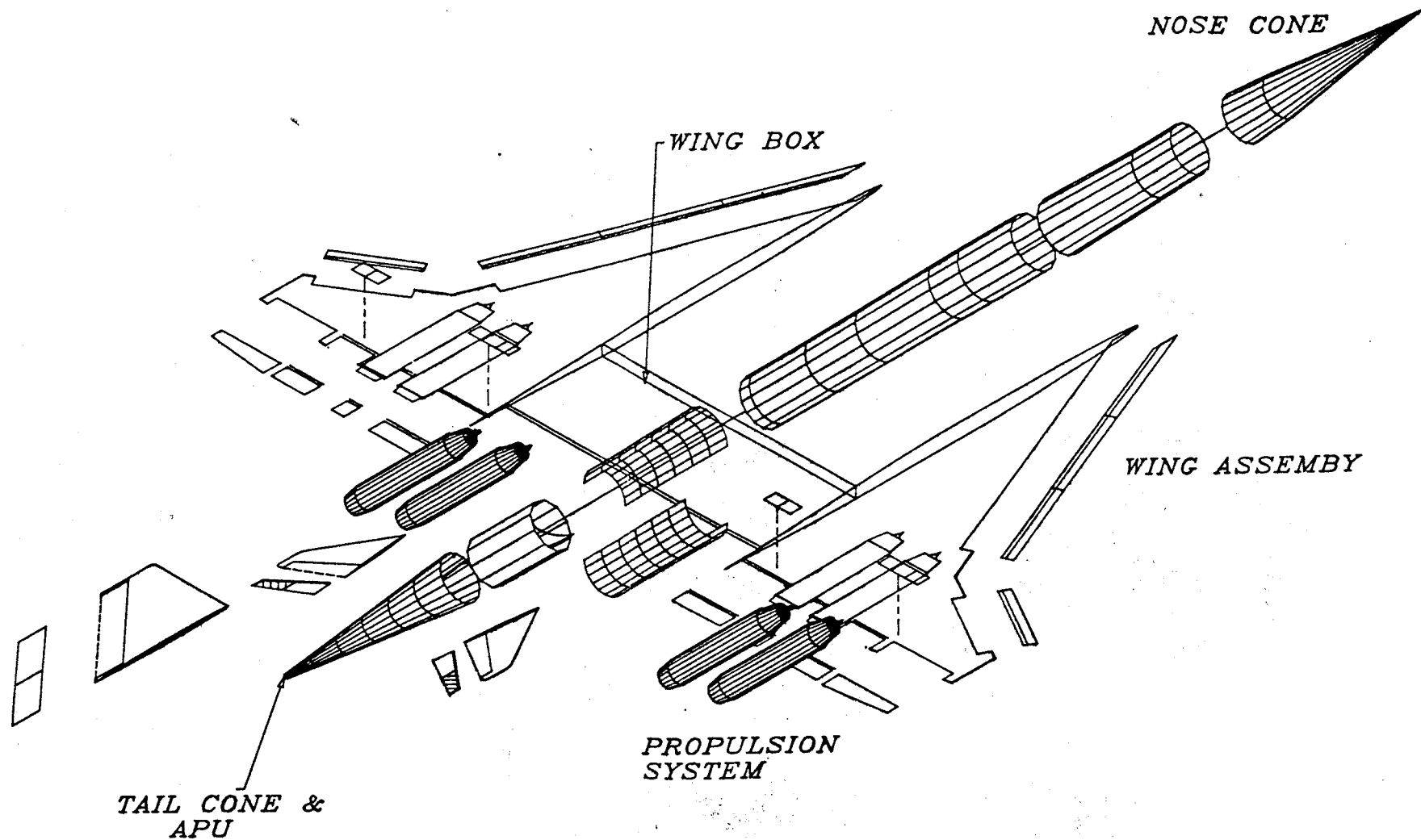


**FIGURE 13.1 STINGRAY ASSEMBLY**

## 14.0 COST ANALYSIS

The estimated cost of the Stingray was calculated using the method from Ref. 8. The projected life cycle cost (LCC) was estimated in U.S. dollars projected into the year 2005. The LCC includes the following:

- Research, Development, Test, and Evaluation Cost ( $C_{RDTE}$ )
- Manufacturing and Acquisition cost ( $C_{ACQ}$ )
- Operating Cost ( $C_{OPS}$ )
- Disposal Cost ( $C_{DISP}$ )

The breakdown of the above costs is shown in Figure 14.1.

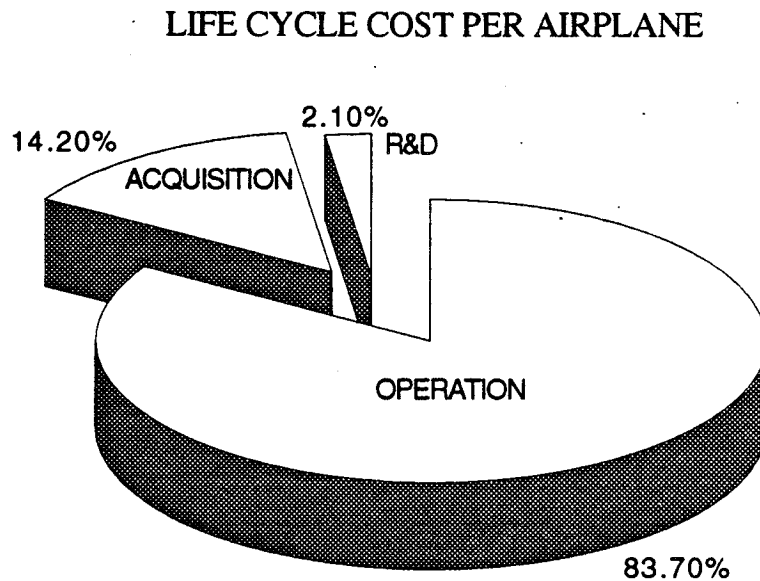


**Figure 14.1** Stingray LCC breakdown

The costs were based using the following assumptions:

- The material will be mostly titanium and aluminum alloys.
- Advanced technologies will be used in production.

- Advanced avionics systems will be included.
- Extra facilities and equipment will not be needed for production and maintenance.
- 500 airplanes will be built to production standards.
- The return on investment will be 10%.
- The aircraft has a depreciation period of 10 years.

The total LCC for the Stingray is calculated to be \$1.13 billion, and the estimated purchase price is \$202 million. For an airliner, the operating cost is very important in terms of obtaining the revenue per passenger mile. The DOC breakdown is shown in Figure 14.2.

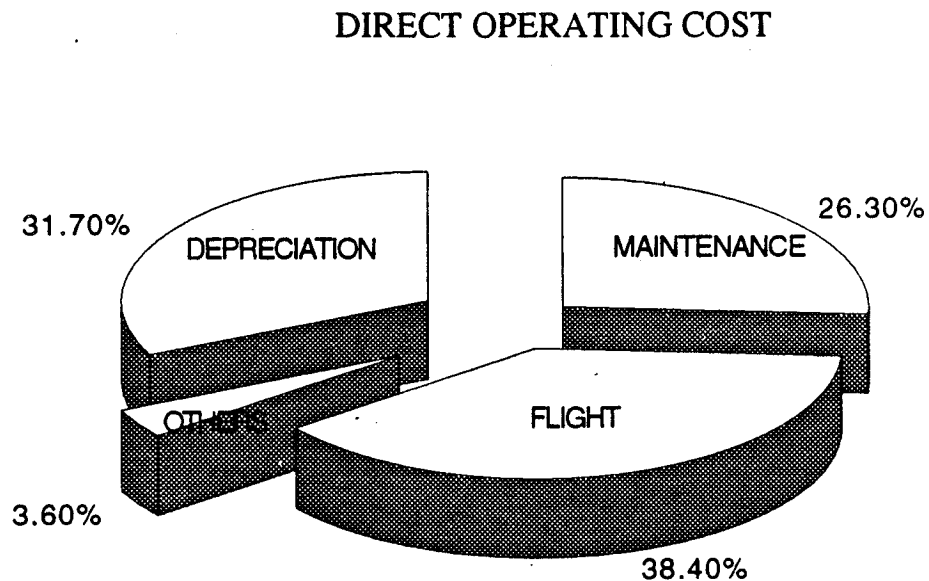


**Figure 14.2** Stingray Direct Operating Cost Breakdown

With a 10% return on investment and a direct operating cost (DOC) of \$0.07 per seat mile, the minimum ticket price is \$0.11 per passenger mile. This will represent a 21% increase over the current subsonic fleet ticket price.

However, the feasibility study (Ref. 16) shows that an increase of 20% in fare compared to conventional air carriers will be attractive in terms of time savings. Table 14.1 shows the comparison of revenue per passenger miles between the Stingray, the Concorde, and the Boeing 747-400.

	Concorde	Boeing 747-400	Stingray
Year	1971	1989	2005
Market	N. Atlantic	Atlantic & Pacific	Atlantic & Pacific
Range (nm)	3500	7300	5200
Pax	100	400	250
TOGW (lbs)	400000	870000	729000
Rev/pax mi require	\$0.87	\$0.10	\$0.11

**Table 14.1** Comparison of Revenue for Selected Existing Aircraft

By comparing these four planes in terms of market and revenue, it is very obvious that the Stingray is competitive with both existing subsonic and supersonic planes. The results from the cost analysis has proved that the Stingray will be an economically feasible aircraft by the year 2005.

## CONCLUSION AND RECOMMENDATIONS

The Stingray has been designed to be a realistic aircraft that can be built by the year 2005. There have been no major technological assumptions, with the exception of the 5% improvement in specific fuel consumption. The materials used in the design are all in existence and are currently being used on transports and military jets alike. This aircraft would represent only a 21% increase in ticket prices, which allows the Stingray to be economically feasible. The noise suppression and nitrous oxide modifications designed into the Stingray engine will make this aircraft environmentally sound. With technology improvements, the Stingray would be a lighter, more efficient aircraft, in terms of propulsion, structure, and aerodynamics.

Distinguishing features of the Stingray include an advanced cockpit visualization system, eliminating the requirement for a mechanically translating nosecone. Electrohydrostatic actuators are utilized in lieu of conventional bulky and heavy hydraulic systems throughout most of the aircraft. Widespread use of adhesives for bonding instead of rivets will be incorporated to help minimize weight, fatigue, and manufacturing costs.

Further detailed analysis includes a structural analysis using finite element methods, actual material performance data, and the development of a control system to enhance the handling qualities of the aircraft. These analyses will be required to complete the design of this supersonic transport.

## 16. REFERENCES

1. Roskam, J., Airplane Design: Part I. Preliminary Sizing of Airplanes, Roskam Aviation and Engineering Corporation, Kansas, 1989.
2. Roskam, J., Airplane Design: Part II. Preliminary Configuration Design and Integration of the Propulsion System, Roskam Aviation and Engineering Corporation, Kansas, 1989.
3. Roskam, J., Airplane Design: Part III. Layout Design of Cockpit, Fuselage, Wing and Empennage: Cutaways and Inboard Profiles, Roskam Aviation and Engineering Corporation, Kansas, 1989.
4. Roskam, J., Airplane Design: Part IV. Layout Design of Landing Gear and Systems, Roskam Aviation and Engineering Corporation, Kansas, 1989.
5. Roskam, J., Airplane Design: Part V. Component Weight Estimation, Roskam Aviation and Engineering Corporation, Kansas, 1989.
6. Roskam, J., Airplane Design: Part VI. Preliminary Calculation of Aerodynamic, Thrust and Power Characteristics, Roskam Aviation and Engineering Corporation, Kansas, 1989.
7. Roskam, J., Airplane Design: Part VII. Determination of Stability, Control and Performance Characteristics: FAR and Military Requirements, Roskam Aviation and Engineering Corporation, Kansas, 1989.
8. Roskam, J., Airplane Design: Part VIII. Airplane Cost Estimation: Design, Development, Manufacturing and Operating, Roskam Aviation and Engineering Corporation, Kansas, 1989.
9. Nicoli, L.M., Fundamentals of Aircraft Design, METS, Inc., Ca.
10. Hoak, D.E. and Ellison, D.E. et al; USAF Stability and Control Datcom, Flight Control Division, Air Force Flight Dynamics Lab, Wright Patterson A.F.B, Ohio, 1969 edition.
11. Raymer, D., Aircraft Design: A Conceptual Approach, AIAA Education Series, 1989.
12. Anderson, J., Introduction to Flight, McGraw-Hill Book Company, New York, 1989.
13. Metals Handbook, American Society for Metals, 1985
14. Corning, G., Supersonic and Subsonic, CTOL and VTOL and Airplane Design, Maryland, 1960.

15. Lambert, M., Jane's All the World's Aircraft, 1990-91 edition.
16. Mizuno, H. & Hagiwara, S., "Feasibility Study on Second Generation SST", AIAA-91-3104 paper, Sept 23-25, 1991
17. Seiner, J.M., "Supersonic Jet Noise and the HSCT", AIAA-89-2358 paper, July 1989.
18. Niu, M.C.Y., Airframe Structural Design, Technical Book Company, 1988.
19. Meriam, J.L. & Kraige, L.G., Engineering Mechanics II- Dynamics, Wiley and Sons, 1986.
20. Nelson, R.C., Flight Stability and Automatic Control, McGraw-Hill Book Co., New York, 1989.
21. Beer, Ferdinand & Johnston, E. Russell, Mechanics of Materials, McGraw-Hill Book Company, 1981.
22. "High-Speed Civil Transport Study" prepared by Boeing Commercial Airplanes, NASA Contractor Report 4234.
23. "Market and Feasibility Studies on the Future of the High Speed Commercial Transport," Economic Study Group, Aero 443 Design Class, December, 1991.
24. Stingray Design Team, "Appendix," December, 1991.
25. Stingray Design Team, "Request for Proposal," December, 1991.
26. Abbott, I., Von Doenhoff, A, Theory of Wing Sections, Dover, 1949.
27. NASA-Lewis Research Center, data for NASA Low Bypass Ratio Turbofan.
28. "Strong, Flexible Polyester HMs Bond Metal-To-Metal Systems." Adhesives Age Magazine, November, 1990.
29. "Structural Bonding Needs for Aerospace Vehicles." Adhesives Age Magazine, January, 1989.
30. Roskam, J, Airplane Flight Dynamics and Automatic Flight Controls, University of Kansas